Targeting Colorectal Cancer Stem Cells with Hemibodies

Eliminierung von Krebsstammzellen des kolorektalen Karzinoms mithilfe von Hemibodies

Doctoral thesis for a doctoral degree

at the

Julius-Maximilians-Universität Würzburg,

Section Biomedicine

submitted by

Hannes Gotthard

from

Bad Mergentheim

Würzburg, 2021

Submitted on: ……..……..

Members of the Thesis Committee

Chairperson:

Primary Supervisor: Prof. Dr. med. Gernot Stuhler (Med. Faculty)

Supervisor (Second): Priv.-Doz. Dr. Hannes Neuweiler (Biol. Faculty)

Supervisor (Third): Dr. Tim Schnyder

Date of Public Defence: ……..……

Date of Receipt of Certificates: ……

Table of contents

I List of tables

II List of figures

III Abbreviations

ACF	Aberrant crypt foci	CIN	chromosomal instability
AE	Adverse effect	DNA	Desoxyribonucleic acid
APC	Antigen presenting cell	5-FU	5-Fluoruracil
BiTE	Bispecific T-cell engager	SEC	Size exclusion chromatography
BLAST	basic local alignment search tool	TAE	tris-acetate-EDTA
BSA	Bovine serum albumin	RLU	Relative light unit
ca	circa	e.g.	For example
CAR	Chimeric antigen receptor	CAF	Cancer associated fibroblast
CD	Cluster of differentiation	MHC	major histocompatibility complex
CRC	Colorectal Cancer	FPLC	Fast protein liquid chromatography
CSC	Cancer Stem Cell	FDA	U.S. Food and Drug Administration
E.coli	Escherichia Coli	HIS	Histidine
EC_{50}	half maximal effective concentration	mAb	Monoclonal Antibody
F_C	Fragment crystallizable	pAb	Polyclonal antibody
HES	hairy and enhancer-of-split	EOMA	aorta derived endothelial cell line
IgG	Immunoglobulin G	v/v	volume by volume
IMAC	immobilized metal ion affinity chromatography	GBM	Glioblastoma multiforme
LRP	low density lipoprotein-related protein	HEY	Hes-related repressor Herp
MAPK	Mitogen-activated protein kinase	MFI	Mean fluorescence intensity
MAPK	Mitogen-activated protein kinase	TNBC	Triple negative breast cancer
MLH1	MutL homolog 1	BAX	Bcl-2-associated X protein
MSI	Microsatellite instability	BRAF	proto-oncogene B-Raf
NSCLC	Non-small-cell lung carcinoma	FACS	Fluorescent activated cell sorting
NTC	Notch transcription complex	NCID	Notch intracellular domain
OD	Optical density	PCR	Polymerase chain reaction
OS	Overall survival	TAA	Tumor associated antigen
OX	Oxaliplatin	PFS	Progression free survival

PAGE	Polyacrylamide gel electrophoresis	NTA	nitrilotriacetic acid
PBS	Phosphate buffered saline	SDS	sodium dodecyl sulfate
PDM	Patient derived micro-tumor		
PE	phycoerythrin	AF	
PEI	polyethylenimine	scFv	Single chain variable fragment
PI3K	phosphatidylinositol 3-kinase	TP53	Tumor Protein 53
SMAD4	Mothers Against Decapentaplegic Homolog 4	KRAS	Kirsten rat sarcoma virus
SSA	Sessile serrated adenoma	CIMP	CpG island methylator phenotype
TAF		RLU	Relative light unit
TGF	Transforming growth factor	APC	Adenomatous polyposis coli
TIC	Tumor initiating cell	NFκB	nuclear factor kappa-light-chain-enhancer of activated B cells
TIL	Tumor infiltrating lymphocyte	TAM	Tumor associated macrophages
TSA	Traditional serrated adenoma	CpG	Cytosin-Phosphat-Guanin
V_H	Variable domain of the heavy chain	V_L	Variable domain of the light chain
YT	Yeast tryptone	LB	Lysogeny broth

1. Abstract

The cancer stem cell hypothesis is a cancer development model which elicited great interest in the last decades stating that cancer heterogeneity arises from a stem cell through asymmetrical division. The Cancer Stem Cell subset is described as the only population to be tumorigenic and having the potential to renew. Conventional therapy often fails to eradicate CSC resulting in tumor relapse. Consequently, it is of great interest to eliminate this subset of cells to provide the best patient outcome. In the last years several approaches to target CSC were developed, one of them being immunotherapeutic targeting with antibodies. Since markers associated with CSC are also expressed on normal stem cells or healthy adjacent tissue in colorectal cancer, dual targeting strategies are preferred over targeting only a single antigen. Subsequently, the idea of dual targeting two CSC markers in parallel by a newly developed split T cell-engaging antibody format termed as Hemibodies emerged. In a preliminary single cell RNA sequencing analysis of colorectal cancer cells CD133, CD24, CD166 and CEA were identified as suitable targets for the combinatorial targeting strategy. Therefore, this study focused on trispecific and trivalent Hemibodies comprising a split binding moiety against CD3 and a binding moiety against either CD133, CD24, CD166 or CEA to overcome the occurrence of resistance and to efficiently eradicate all tumor cells including the CSC compartment. The study showed that the Hemibody combinations CD133xCD24, CD133xCD166 and CD133xCEA are able to eliminate double positive CHO cells with high efficacy while having a high specificity indicated by no killing of single antigen positive cells. A therapeutic window ranging between one to two log levels could be achieved for all combinations mentioned above. The combinations CD133xCD24 and CD133xCD166 furthermore proved its efficacy and specificity on established colorectal cancer cell lines. Besides the evaluation of specificity and efficacy the already introduced 1st generation of Hemibodies could be improved into a 2nd generation Hemibody format with increased half-life, stability and production yield. In future experiments the applicability of above-mentioned Hemibodies will be proven on patient-derived micro tumors to also include variables like tumor microenvironment and infiltration.

1. Zusammenfassung

In den letzten Jahrzenten wurde neben der klonalen Evolution ein weiteres Modell zur Krebsentstehung und dessen Heterogenität entwickelt: die Krebsstammzellhypothese. Diese Hypothese besagt, dass die Heterogenität eines Tumors durch asymmetrische Teilung von sogenannten Krebsstammzellen entsteht. Nur diese sind tumorigen und in der Lage Metastasen zu bilden. Außerdem werden Krebsstammzellen als resistent gegen konventionelle Therapien beschrieben, weshalb es nach einer anfänglichen Tumorregression oft zu einem Rezidiv durch erneutes Auswachsen von zurückbleibenden Krebsstammzellen kommt. Deshalb ist es von großem Interesse genau diese Population abzutöten, um eine erfolgreiche Therapie zu gewährleisten. In den letzten Jahren wurden zahlreiche Medikationen entwickelt, um Krebsstammzellen gezielt anzugreifen. Ein vielversprechender Ansatz ist hierbei die immuntherapeutische Adressierung mittels Antikörpern gegen Krebsstammzellmarkern. Einzelne Marker sind allerdings auch auf normalen Stammzellen und gesundem Gewebe exprimiert, weshalb Therapien, die auf mindestens zwei verschiedene Oberflächenproteine abzielen, erfolgsversprechender sind. In dieser Arbeit wurde ein neues T-Zell rekrutierendes Antikörperformat entwickelt, sogenannte Hemibodies. Hierbei handelt es sich um ein trispezifisches und trivalentes Format, bestehend aus jeweils zwei Fragmenten. Jedes Fragment besteht aus einer Bindedomäne gegen ein Krebsstammzellmarker und einer geteilten Bindedomäne gegen CD3. Durch Bindung beider Fragmente an einen Stammzellmarker kommt es zur Komplementierung der geteilten anti-CD3 Domäne und zur T-Zellrekrutierung. Der erste Teil der Arbeit befasst sich mit der bioinformatischen Analyse von Einzelzell-RNA-Daten des kolorektalen Karzinoms (KRK) zur Identifizierung von potentiellen Krebsstammzellmarkern. Dabei konnten die Oberflächenproteine CD24, CD133, CD166 und CEA und besonders deren Kombination als geeignete Zielstrukturen identifiziert werden. Die gegen oben genannte Antigene gerichteten Hemibodies zeigten in den Kombinationen CD133xCD24, CD133xCD166 und CD133xCEA auf doppelt positiven CHO-Zellen eine hohe Effektivität. Außerdem konnte die Spezifität durch ein Ausbleiben von Zelltod auf einzel-positiven CHO Zellen bewiesen werden. Die Kombinationen CD133xCD24 und CD133xCD166 konnten Effektivität und Spezifität auch auf etablierten Krebszellen zeigen. Die oben genannten Kombinationen waren in einem therapeutischen Fenster von ein bis zwei Logstufen funktional. Neben der Testung verschiedener Hemibody-Kombinationen konnten die bereits publizierten Hemibodies der ersten Generation in ein neues Format der zweiten Generation weiterentwickelt werden. Das neue Format zeigte eine verbesserte Halbwertszeit, Stabilität und Produzierbarkeit. In zukünftigen Experimenten

werden die in der Thesis benutzten Hemibodies auf Mikrotumoren getestet, um weitere Variablen, die die Effektivität und Spezifität beeinflussen zu ermitteln.

2. Introduction

2.1. Colorectal Cancer

2.1.1. Epidemiology

After cardiovascular diseases, cancer ranks as the second leading cause of death worldwide. In 2020, 19,3 million new cases and almost 10 million cancer deaths were registered (Sung et al. 2021). In Europe alone, 4,4 million people were diagnosed with cancer, of which 1,9 million died because of the disease. With approximately 520.000 new cases and 240.000 related deaths, colorectal cancer is the second most frequently diagnosed malignant tumor disease and the second most frequent cause of death across genders (Sung et al. 2021).

In addition to genetic and endogenous predisposition factors, colorectal cancer is primarily a lifestyle disease that occurs more frequently in countries with a high development index [Figure 1]. Physical inactivity, obesity, alcohol intake and a poor diet characterized by higher intake of red and processed meat favor inflammatory bowel diseases and thus the development of colorectal cancer (Vazzana et al. 2012; Devkota et al. 2012). This widespread lifestyle together with the ongoing ageing of the population will further increase annual new cases of colorectal cancer in western societies (Bray et al. 2018).

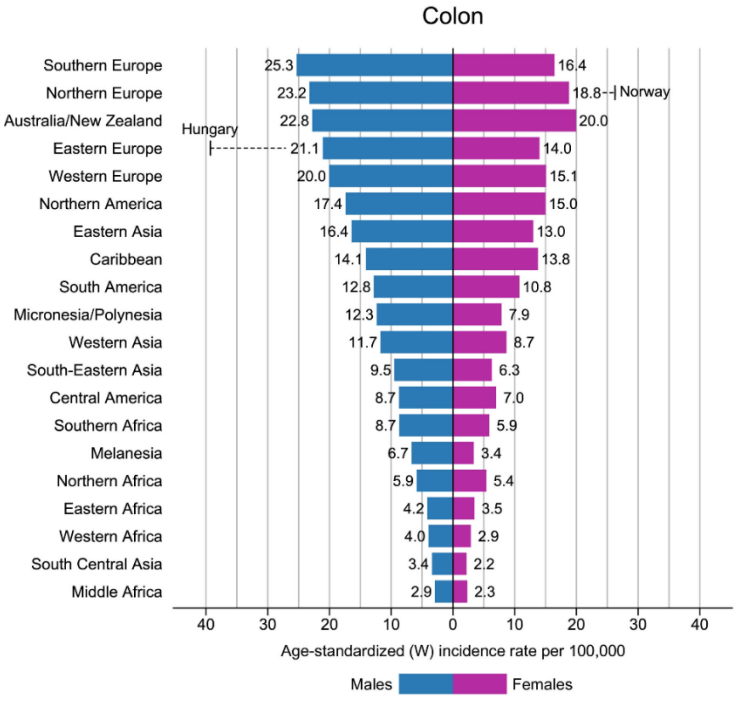

Figure 1: Region-Specific Incidence Age-Standardized Rates by Sex for Colorectal cancer in 2020 Disease occurs mainly in countries with a high level of development and increasingly in men. Adopted from (Sung et al. 2021).

2.1.2. Pathogenesis

CRC is a genetic disease caused by the accumulation of genetic mutations leading to either an activation of oncogenes (gain of function) or in the inactivation of tumor suppressor genes (loss of function). These genetic alterations are associated with specific pathological/ anatomical changes of the colonic mucosa, which can be described by two distinct morphological pathways, namely the conventional adenoma to carcinoma sequence (Vogelstein et al. 1988) and the serrated neoplasia pathway (Leggett und Whitehall 2010).

The conventional adenoma to carcinoma sequence is histologically homogeneous, starting with the development of aberrant crypt foci (ACF). Their progressive accumulation results in a benign polyp or adenoma, including tubular or tubulovillous adenoma, which can further develop into a carcinoma over years or even decades (Simon 2016). On the molecular level of the adenoma-to carcinoma- sequence, each developmental stage is characterized by defined mutations induced by two mechanisms of tumorigenesis, namely chromosomal instability (CIN) and microsatellite instability (MSI).

CIN results in gains or losses of large portions or whole chromosomes leading to chromosomal and karyotypic abnormalities. Typically, CIN initiates mutations in the tumor suppressor APC. Loss of APC leads to an activation of β-catenin, an effector of the WNT-signaling pathway, which is a critical pathway for cell proliferation and migration. Subsequently mutations in the protooncogenes KRAS and SMAD4 with consequent dysregulation of the MAPK, PI3K and TGF-β signaling pathways drive tumor progression from an early adenoma to a late adenoma (Figure 2). Transformation from late adenoma into an adenocarcinoma is ultimately caused by a mutation and loss of the tumor suppressor TP53 (Pino und Chung 2010).

Whereas CIN accounts for approximately 85%, MSI occurs in about 15% of CRCs and can also be detected in the serrated pathway (Gupta et al. 2018; O'Brien et al. 2006). Malignant transformation is triggered by germline mutations of mismatch repair genes, e.g. *hMLH1, hMSH2, hMSH6, hPMS1, hPMS2*, causing an impaired DNA repair system (Yamagishi et al. 2016). Subsequently DNA errors accumulate in short nucleotide repeats (microsatellites) leading to an initial alteration of the WNT signaling pathway and the formation of an early adenoma. Progression towards the intermediate and late stages of carcinogenesis is then caused by BRAF mutation followed by alterations of the genes TGFBR2, IGF2R and BAX, activating proliferative pathways such as the MAPK-pathway, and inactivating apoptotic signals (Palma et al. 2019).

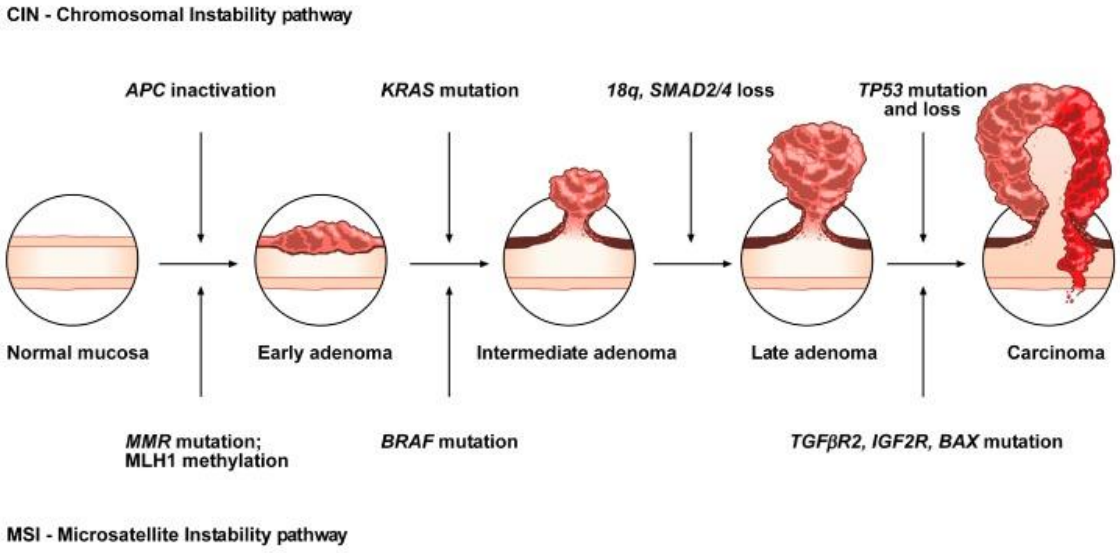

Figure 2: adenoma to carcinoma sequence. The chromosomal instability pathway is initiated by APC (tumor suppressor) inactivation, followed by mutations in the genes KRAS, SMAD4 and TP53 leading to tumor progression from early adenomas to carcinomas. The MSI pathway starts with alterations in the WNT signaling with subsequent mutations in the genes BRAF, TGFBR2, IGF2R and BAX, stepwise developing a carcinoma. Adopted from (Palma et al. 2019).

The alternative serrated pathway is characterized by serrated (saw-toothed) precursor lesion, present as hyperplastic polyps (HPs), sessile serrated adenomas (SSA), traditional serrated adenomas (TSA) and mixed polyps. On a molecular level MSI and the CpG island methylator phenotype (CIMP) are the major tumorigenic mechanisms leading to genomic instability (Palma et al. 2019). By hypermethylation of CpG islands (Cytosin-Guanine dinucleotide group) in gene promoter regions target genes are silenced. Typically, mutations in the MAPK-pathway activating genes BRAF or KRAS initiate the lesions of the serrated pathway, further silencing of tumor suppressors and DNA repair genes via CIMP boost neoplastic progression.

2.2. Clonal evolution and cancer stem cell model

The dominating model of cancer development is the model of clonal evolution (Nowell 1976). It proposes that a neoplasm arises from a single cell of origin. Through stepwise acquisition of somatic mutations in individual cancer cells, new subclones arise and if these mutations confer a selective advantage, they will outgrow other cancer cells by clonal expansion. In this way new subpopulations are generated during tumor progression producing a heterogeneous tumor.

According to this model, any cancer cell bears a tumorigenic potential, can develop treatment resistance, and thus lead to recurrence. For successful cancer treatment it is therefore important that all cells are eradicated to eliminate the tumorigenic potential of the tumor.

The cancer stem cell model, however, proposes that cancer is a hierarchical disease, where every tumor comprises a rare population of cells termed as cancer stem cells (CSCs) or tumor-initiating cells (TICs). Only CSCs or TICs have self-renewing and tumorigenic properties and are responsible for the generation of cancer cells and their hierarchical organization. Via symmetrical division, pluripotent daughter cells are produced which maintain the cancer stem cell pool. Asymmetrical division results in more differentiated cancer cells or progenitor cells up to terminally differentiated cancer cells.

CSCs are generally slow cycling cells close to quiescence and often show an increased expression of drug efflux pumps (ABC transporter), resulting in drug resistance against chemotherapeutics. Only the tumor bulk consisting of proliferating progenitor cells and terminally differentiated cancer cells can be eradicated leading to a recurrence of the tumor via surviving CSCs. Taken together, therapies against tumors following the cancer stem cell model should concentrate on targeting CSCs which are important for tumor progression instead of the daughter cells which play a subordinate role in the course of the disease (Figure 3).

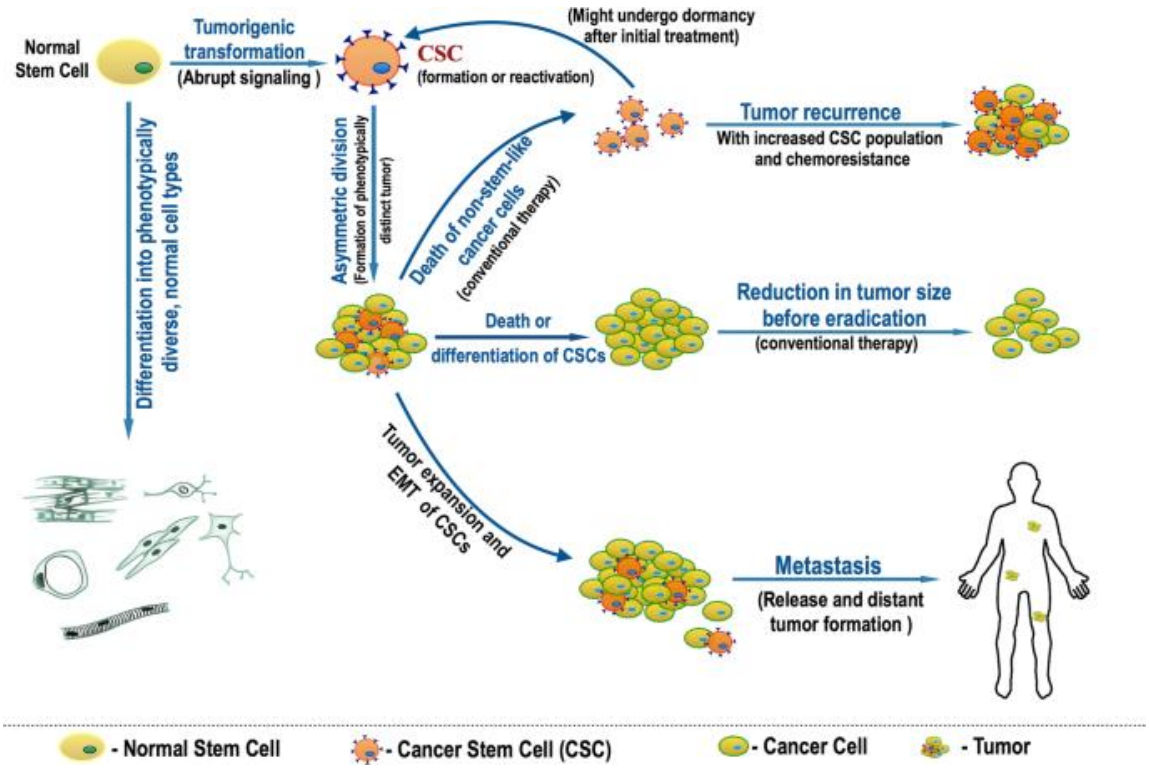

Figure 3: schematic representation of cancer stem cell model: CSCs arise either through the stepwise accumulation of mutations in normal stem cells or by dedifferentiation of cancer cells. CSCs have the ability to form metastasis in distant organs. Conventional therapy eradicates the tumor bulk while sparing the CSCs. Consequently, the tumor recurs. Eradicating the CSCs instead leads to a reduction in tumor size. Combined with conventional therapy the tumor can be destroyed without the risk of a relapse. Adapted from (A. Yadav und N. Desai 2019).

The cell of origin of CSCs varies between tumors. Barker et al. could show that somatic alterations in normal tissue stem cells can give rise to CSCs and a rapid adenoma formation (Barker et al. 2009). More recent studies also demonstrated that as a consequence of constitutive nuclear factor kB (NF-kB) activation, or APC depletion and chemically induced inflammation in colorectal cancer transit amplifying cells and more differentiated cells can dedifferentiate into less developed stages and thereby sustain the CSC pool (Chaffer et al. 2013; Schwitalla et al. 2013). This dynamic process transitioning between stem and differentiated states in response to therapeutic agents or stimuli from the microenvironment is mediated by epigenetic alterations and presents a challenge against tumor eradication.

2.2.1. Identification and characteristics of cancer stem cells

Cancer stem cells share a set of basic characteristics including: 1) a small number of CSCs can initiate new tumors; 2) self-renewal and differentiation properties; 3) expression of specific surface markers; 4) resistance to conventional chemotherapy and radiotherapy; 5) ability to be serially transplanted (Deonarain et al. 2009; Chen et al. 2012; Pan et al. 2018). Based on these characteristics, several assays were developed to identify and enrich for CSCs. The serial transplantation assay utilizes 1) and 5). Cancer cells are divided into subpopulations and transplanted into mice, subpopulations which are able to generate new tumors are termed cancer stem cells. Another often used test is the side population assay. Cancer cells are treated with a dye called Hoechst 33342, as cancer stem cells are equipped with ABC-efflux pumps and thus show resistance to several chemotherapeutics. Consequently, CSCs can be distinguished from differentiated cancer cells as an unstained side population. Finally, CSC can be enriched by growing cancer cells as spheres in a special stem cell medium on ultra-low attachment plates. It is reported that under these conditions, only CSCs can survive and build spheres. Harnessing the listed techniques among others, several core regulatory pathways, surface biomarkers and transcription factors specific for CSCs could be identified, which are explained in more detail in the following section.

Key Signaling Pathways

As stated earlier, two key properties of CSC are self-renewal and quiescence. In normal stem cells, these processes are highly regulated by transcription factor mediated pathways responding to extrinsic growth factors. These pathways, namely the WNT-, Notch - and Hedgehog-Signaling-Pathway, are dysregulated in CSC resulting in tumorigenic cells which are able to differentiate into highly proliferative tumor cells.

WNT pathway: The WNT-Pathway is usually involved in embryonic development and homeostasis and is divided in a canonical and non-canonical pathway. In the canonical signaling, Wnt binds to its receptor Frizzled and/or low-density lipoprotein-related protein (LRP) 5 and 6 coreceptors. Subsequently, Dishevelled is activated and inhibits a protein complex consisting of GSK3-beta, APC and Axin-1, which normally degrades beta-catenin. Beta-catenin accumulates in the cytoplasm and translocates to the nucleus where it activates specific target genes together with the TCF/LEF protein complex. In the non-canonical pathway, signal transduction proceeds through a signaling cascade resulting in activation of the calmodulin-dependent protein kinase II which suppresses the canonical pathway and increases differentiation of cells in the neuronal system. During the development of CSC, the most common alteration is the hyperactivation of WNT signaling. Malanchi et al. for example observed that genetic depletion of beta-catenin induced tumor regression in chemically induced skin tumors through a decrease of CD34+ stem cells (Malanchi et al. 2008). Further publications highlighted the importance of the WNT signaling in CSC of different cancer types including human acute leukemia (Heidel et al. 2012), non small cell lung cancer (Fang et al. 2015) and colorectal cancer (Prieur et al. 2017).

Notch pathway: Developmental and homeostatic processes like proliferation, stem cell maintenance, cell fate specification, differentiation or angiogenesis are strictly regulated by Notch signaling. There are four different Notch receptors (Notch 1-4) and four Notch Ligands (Dll1, Dll4, Jag1 and Jag2). Binding of a Notch ligand to its receptor induces a conformational change in the receptor, exposing cleavage sites for ADAM metalloproteinases. Once the extracellular domain is cleaved, gamma-secretase cleaves the transmembrane domain releasing the Notch intracellular domain (NCID) that translocates to the nucleus forming the Notch transcription complex (NTC) together with Recombination Signal Binding Protein for Immunoglobulin Kappa J (RBPJ) and Mastermind-like (MAML) transcriptional coactivators. The NTC binds to regulatory elements and transcriptional coregulators are recruited, which activate the transcription of Notch target genes like hairy and enhancer-of-split (HES) and Hes-related repressor Herp (HEY). Notch signaling is reported to be dysregulated in a variety of tumors including lymphoma, breast cancer, lung cancer, head and neck cancer, pancreatic cancer, colon cancer osteosarcoma and glioblastoma (Wang et al. 2009; Katoh und Katoh 2020). As several studies revealed, Notch signaling also plays a major role in cancer stem cells. Fan and Eberhart e.g. reported that inhibition of gamma-secretase (GSI-18) leads to a depletion of CD133+ stem-like subpopulation of medulloblastoma cell lines. GSI-18 was able to induce apoptosis 10 fold stronger in stem cell marker Nestin positive cells compared to the Nestin

negative compartment, indicating Notch dependence of the cancer stem cell population (Fan et al. 2006). Similar results were obtained in CD133+ cancer stem cells derived from glioblastoma (Fan et al. 2010). In renal cancer, Xiao et al. could show that CD133+/CD24+ cancer stem cells showed increased Notch signaling and subsequently enhanced self-renewable ability and less response to cisplatin and sorafenib. Blockage of Notch1 or Notch2 resulted in loss of stemness features including self-renewal, chemo-resistance, invasive and migratory potential and tumorigenesis in vivo (Xiao et al. 2017a).

Hedgehog pathway: The Hedgehog (Hh) signaling pathway is a key regulator of stem cell maintenance, polarity, migration and differentiation during embryonic development. Hedgehog signaling is activated by a Hh ligand binding to its receptor Protein patched homolog 1 (PTCH). Consequently PTCH, which normally inhibits Smoothened (Smo), relieves repression of Smo triggering interaction with the Mammalian Cos2 Homolog Kif7. Glioma-associated oncogene (Gli1) is then released from its Suppressor of fused homolog (SuFu/Fu) repressor complex, bypassing proteolytic cleavage, and can translocate into the nucleus where it activates Hh target genes. The non-canonical signaling pathway is independent of Gli proteins and not yet fully understood. There are hints that the Hh signaling pathway is involved in the maintenance of CSCs. Eli et al. for example showed that glioblastoma derived neurospheres lacked sphere formation after treatment with the hedgehog inhibitor cyclopamine, indicating the depletion of clonogenic cancer stem cells. This was further validated by an ALDH-Assay and side population assay. Cancer stem like fractions identified by these assays were significantly reduced or eliminated by cyclopamine (Bar et al. 2007). Similar results were obtained in breast cancer where the CD44+/CD24- cancer stem cell fraction could be eliminated with cyclopamine (Cochrane et al. 2015). Inhibition of Hh signaling in colorectal cancer led to decreased capacity of cancer stem cells to form tumorspheres but had no effect on adherent cells. Furthermore studies investigating several leukemias, prostate and lung cancers emphasized the importance of the Hh signaling pathway in the maintenance of CSC (Cochrane et al. 2015).

NFkB- pathway: The nuclear factor 'kappa-light-chain-enhancer' of activated B-cells (NFκB)-pathway is a well-studied pathway involved in many cellular processes including inflammation and immune control but also cellular proliferation, survival and differentiation. NFκB/ Rel proteins are inhibited in a complex with IκB proteins. Once growth factors, proinflammatory cytokines, chemotherapy or antigen receptors activate the so called IkappaB kinase (IKK) complex, IKK phosphorylates IκB. IκB subsequently is ubiquitinated and degraded in the proteasome. The thereby release NFκB acts as a transcription factor and promotes the expression of cytokines, cell adhesion proteins and

antiapoptotic proteins, but also influences biological processes like innate and adaptive immunity, inflammation, stress responses, B-cell development and lymphoid organogenesis. Besides the canonical pathway which relies on activation through inflammatory reactions (interleukins, TNF-α or LPS) there is a non-canonical pathway which is p100 mediated.

The linkage between the NFκB and cancer stem cells was first discovered in AML, where Guzman et al. showed that CD34+ cancer stem cells bound with NFκB, whereas normal hematopoietic stem cells did not (Guzman et al. 2001). Later in colon cancer, increased NFκB levels were discovered because of chronic inflammation and the accumulation of proinflammatory cytokines (Terzić et al. 2010). Increased NFκB promotes a tumorigenic microenvironment. In the last decade, several drugs targeting these pathways including thalidomide or bortezomib were reported. BMS-345541 is another therapeutic drug that inhibits IKKβ and IκB. Treatment with this inhibitor lead to a reduction of stemness, self-renewal and migration capacity in lung cancer, highlighting the importance of the NFκB-pathway in CSC (Zakaria et al. 2018).

Besides the above mentioned other pathways such as the Hippo-Yap-, TGFbeta and the MAPK-pathway seem to be of relevance in the course of CSC formation and maintenance (Espinosa-Sánchez et al. 2020).

CSC transcription factors

Accompanied by dysregulated signaling pathways, several transcription factors promoting stemness of cancer cells are upregulated in CSC. Key stem cell TFs like SOX2, OCT4, and Nanog have been proven to be overexpressed. SOX2 plays many roles during embryogenesis and cell differentiation of normal tissues including the morphogenesis and homeostasis of the esophagus, lung and trachea (Sarkar und Hochedlinger 2013). In the last decade it could be shown that SOX2 is also expressed in a variety of cancers linked to poor prognosis and a high tumor grade (Talebi et al. 2015; Wuebben und Rizzino 2017; Takeda et al. 2018). After initial findings that SOX2 is involved in the maintanence of cancer stem cells in skin and bladder cancers, Takeda et al. also found a correlation of SOX2 and cancer cell stemness in colorectal cancer (Takeda et al. 2018). Similar results were obtained for transcription factor OCT4 which is normally expressed in embryonic or adult stem cells, maintaining stem cell like properties or being involved in proliferation and differentiation (Han et al. 2014). Overexpression of OCT4 in gastric cancer for example dedifferentiated cancer cells into CSC acquiring self-renewal capacity, downregulation of OCT4 on the other hand induced differentiation of gastric cancer cells (Chen et al. 2009; Tai et al. 2005). Nanog is a TF regulating self-renewal

and multipotency. Consequently in normal somatic tissues it is not expressed. Nevertheless its expression could be detected in several cancers including GC and CRC where it correlated with tumor grade and a decreased overall survival. Furthermore, colony formation studies revealed more stem cell properties in Nanog overexpressing cells (Santaliz-Ruiz, IV et al. 2014; Hadjimichael et al. 2015). With respect to colorectal cancer stem cells, KLF4, c-Myc, SOX9, Gli1, STAT3, SALL4 and beta-catenin are also often discussed TFs linked to stemness properties (Pádua et al. 2020).

Specific CSC surface antigens

Bonnet and Dick were the first to identify certain surface markers on CSCs. They performed a serial transplantation assay in acute leukemia, where several subpopulations of tumor cells are transplanted into mice and evaluated for tumor formation. Based on this study Bonnet et al. could show that only a small population of CD34+/CD38- cells was able to establish a tumor in immunocompromised mice which showed a similar hierarchy as the initial disease (Bonnet und Dick 1997). Serial transplantation assays became the gold standard for defining CSCs, identifying them in several solid tumors including glioblastomas (Singh et al. 2003), breast (Al-Hajj et al. 2003), pancreatic (Li et al. 2007), prostate (Collins et al. 2005) and colorectal cancer (Fanali et al. 2014). For colorectal carcinomas the following surface markers could be identified: CD133, CD24, CD166, LGR5, ALDH1, EpCAM and CD44 (Fedyanin et al. 2017). However, none of these markers are restricted to cancer stem cells but can also be identified in other compartments of the tumor or healthy tissue (Kim und Ryu 2017). This indicates the need to use a combination of multiple surface markers for specific targeting of the CSC compartment.

2.2.2. Colorectal cancer stem cell marker

As stated in 2.1.3.1 several surface markers for colorectal cancer stem cells were identified via serial transplantation assays. In this section, selected surface markers will be discussed in more detail.

2.2.2.1. CD24

In 1978, cluster of differentiation 24 (CD24) was first recognized as a heat-stable antigen (HSA), predominantly expressed in the early stage of pre-mature B-lymphocytes (Springer et al. 1978; Abramson et al. 1981). It is a highly glycolysated single chain sialic acid protein with a molecular mass between 35kDa and 70 kDa, depending on the degree of glycolysation in different cell types (Kay et al. 1990; Pirruccello und LeBien 1986). Since it is a glycosylphosphatidylinositol (GPI)-anchored protein lacking an intracellular

domain, it cannot directly activate intracellular signaling pathways but does so via interactions with signaling proteins and receptors. It is resident in cholesterol-rich microdomains/ lipid rafts (Lingwood und Simons 2010), showing a broad expression on hematopoetic cells, including B-cells, T-cells, neutrophils, eosinophils, dendritic cells and macrophages, as well as non hematopoetic cells, including neural cells, ganglion cells, epithelia cells, keratinocytes, muscle cells, pancreas, epithelial stem cells and many types of cancers (Fang et al. 2010b). Furthermore, its expression tends to be more prominent on progenitor cells compared to terminally differentiated cells. As an example, CD24 is present on early-stage B-cells and mature B-cells. It disappears after antigen stimulation and transformation into plasma cells (Suzuki et al. 2001). On activated B-cells, CD24 is a T-cell costimulatory signal for the clonal expansion of CD4+ T-cells and is required for homeostatic proliferation of T-cells. For other cell types, the role of CD24 remains unclear. However, under pathological conditions its expression is linked to autoimmune, inflammatory as well as malignant diseases (Fang et al. 2010a). In breast cancer, CD24 is expressed higher in invasive ductal carcinomas and ductal carcinomas compared to normal tissue with a correlation to an unfavorable overall survival (OS) and adverse disease free survival (DFS) (Kwon et al. 2015; Bircan et al. 2006). Moreover, membranous staining of CD24 is associated with lymph node metastasis and poor OS in NSCLC (Majores et al. 2015). Its high abundance in pancreatic cancers (71,6% in primary pancreatic carcinomas) and colorectal cancers (86,3% of adenocarcinomas and 90,7% of adenomas) further emphasizes the importance of HSA in the early process of carcinogenesis (Jacob et al. 2004; Sagiv et al. 2006). Suggested mechanisms for the aggressive characteristics of CD24 expressing tumors involve enhanced tumor cell migration by binding with its ligands P-selectin, E-selectin and L1CAM and the regulation of multiple signaling pathways including EGFR, WNT, STAT3, Src kinase, MAPK, CXCR4 and Hedgehog, which are influencing proliferation, angiogenesis, invasion and metastasis of cancer cells (Ni et al. 2020).

The role of CD24 in cancer stem cells remains controversial. In breast cancer, for several studies reported a CD44+/CD24^{low} phenotype to be more tumorigenic and has the ability to form mammospheres in vitro compared to CD44+/CD24+ phenotypes. In contrast to breast cancer, in pancreatic cancer, cervical cancer, gastric cancer and colorectal cancer the CD24+ subset of cells proved to be the putative CSC population. Yeung et al. e.g. showed that CD44+/CD24+ cells are enriched for colorectal CSCs in HT29 and SW1222 cell lines with a high self-renewing capacity being most clonogenic in vitro and can initiate tumors in vivo (Yeung et al. 2010). Ke et al. further validated these findings by demonstrating that CD24+ cells of the colorectal cancer cell lines HCT116, SW480 and HT29

exhibited enhanced chemotherapy-resistance, self-renewal and tumorigenic capacity in vitro and in vivo (Ke et al. 2012). The underlying mechanism for CD24 association with stemness could be linked to an CD24-dependent activation of STAT3, which subsequently initiates the expression of stemness related genes including Nanog2, Sox2, Oct4 and c-myc. (Liu et al. 2014).

2.2.2.2. CD133

CD133 or prominin-1 is a 97 kDa – 120 kDa transmembrane glycoprotein depending on its glycolysation status. It contains an extracellular N-terminal domain, five transmembrane domains separating two large extracellular loops, two small intracellular loops and the intracellular C-terminal domain. Under physiological conditions, CD133 is expressed on a variety of cells including hematopoetic stem cells, endothelial progenitors, embryonic neural stem cells (NSCs) and in ependymal NSC in the early postnatal stage and in the adult brain. Because of its localization in membrane protrusions and microvilli, it was proposed that it acts as an organizer of cell membrane topology by binding cholesterol in cholesterol-containing plasma membrane microdomains. The exact molecular functions still remain unclear. Because of its localization, it was proposed that CD133 may be involved in various signaling cascades including the WNT-signaling pathway. Suppression of CD133 led to a loss of nuclear localization of beta-catenin leading in a reduction in canonical WNT-signaling (Bisson und Prowse 2009; Rappa et al. 2013). Mak et al. could also show that CD133 interacts with the deacetylase HDAC6, stabilizing beta-catenin. Inhibition of either CD133 or HDAC6 consequently led to beta-catenin degradation and decreased proliferation and tumorigenesis (Mak et al. 2012). Studies in colorectal carcinoma cell lines furthermore revealed its involvement in the PI3K-Pathway. $CD133^{high}$ cells substantially expressed more Akt compared to $CD133^{low}$ cells (Sahlberg et al. 2014).

With respect to its expression in hematopoetic, neural and prostate stem cells together with its participation in the above mentioned stem cell related pathways, CD133 was found to be expressed in a variety of CSCs serving as an important regulator of stemness (Glumac und LeBeau 2018). In a variety of cancers, CD133 is associated with recurrence, metastasis, chemotherapy resistance and poor prognosis. In glioblastoma PROM1 was found to be overexpressed in a subset of cells which were resistant to chemotherapeutic agents and formed spheres in vitro (Liu et al. 2006). Furthermore, CD133 suppression in GBM cells led to a reduced neurosphere formation and displayed lack of self-renewal (Ahmed et al. 2018). Another extensively studied cancer in the context of CD133 as a CSC marker is the colorectal carcinoma. Already in 2007, O´Brien et

al. found out that a small subset of PROM1 expressing colorectal cancer cells was able to maintain themself, differentiate and to re-establish tumor heterogeneity in serial transplantation assays in immunocompromised mice. The majority of cells not expressing CD133 was unable to initiate tumor growth (O'Brien et al. 2007; Ricci-Vitiani et al. 2007). According to CSC theory, CSCs are the main drivers of tumor progression and subsequently correlate with low patient survival. Horst et al. therefore analyzed 110 cases of patients with colorectal adenocarcinoma for expression of the cancer stem cell marker CD133 and its contribution to patient survival. Kaplan-Meier analyses showed a strong correlation with low survival, underpinning CD133 as a robust cancer stem cell marker in colorectal cancer. Additionally they could show a correlation between high CD133 expression with CD166 expression raising the assumption that CD166 could be a good co-CSC-marker for CRC (Horst et al. 2009a). Stemness of CD133 expressing CRC-SC was later linked to enhanced WNT-signaling activity (Vermeulen et al. 2010). Even CD133 overexpressing HEK293 cells transplanted to xenograft mouse models resulted in significantly larger tumors compared to $CD133^{low}$HEK293 cells, suggesting its important role as a CSC marker (Canis et al. 2013). However, PROM1s character as a CSC in colorectal cancer remains controversial. Shmelkov et al. demonstrated that CD133 is also expressed on differentiated tumor cells and that $CD133^{-}$ cells were able to form tumorspheres in vitro and tumors in vivo (Shmelkov et al. 2008). In 2010, a Dutch group could solve this controversy by using a specific glycosylated epitope termed AC133 for detection of PROM1. They demonstrated that the AC133 epitope is lost upon differentiation of CSC in parallel with a loss of clonogenicity. While CD133 was still expressed on the differentiated cancer cells, AC133 expression was restricted to the CSC subset of cells (Kemper et al. 2010).

Several other studies also identified CD133 as a CSC marker in ovarian cancer (Cioffi et al. 2015), pancreatic cancer (Gzil et al. 2019), prostate cancer (Vander Griend et al. 2008) and lung cancer (Bertolini et al. 2009) among others. Combinatorial identification of CSC using two antigens allows for a more precise prediction and targeting. Especially the combination CD133-CD24 proved to be interesting in some cancer types. In urinary bladder carcinoma $CD133^{+}CD24^{+}$ cells exhibited the most aggressive phenotype (Farid et al. 2019), in colorectal cancer they showed high invasiveness and differentiation which are clinicopathological factors related to cancer stem cells (Choi et al. 2009) and in hepatocellular carcinomas, these cells possessed a greater colony-forming efficacy, higher proliferative output and a greater ability to form tumor identical to the original in vivo compared to other cell subsets (Feng et al. 2015).

In summary, it can be said that CD133 turns out to be the most universal marker for CSC in a variety of cancers.

2.2.2.3. CD166

CD166 or the activated leukocyte cell adhesion molecule (ALCAM) is a 100 to 105 kDa cell adhesion molecule belonging to the transmembrane immunoglobulins. As indicated by the name, ALCAM was first identified in activated leukocytes playing a major role in optimal activation of T-Cells together with its ligand CD6 (Gimferrer et al. 2004). Throughout the activation process of T-cells via forming an immunological synapse with an antigen-presenting cell (APC), the heterotypic interaction with CD6 is required. In this context Caryol et al. could show that ALCAM is also involved in mediating the transmigration of T-Cells and monocytes across the blood-brain barrier (Cayrol et al. 2008). Besides its role in hematopoietic cells, ALCAM is crucial in development where it is expressed on human blastocytes and most developing tissues, mediating cell adhesion either through heterotypic (ALCAM-CD6) or homotypic (ALCAM-ALCAM) interactions (Diekmann und Stuermer 2009; Hirata et al. 2006). In embryonic hematopoiesis for example, CD166 was specifically expressed on a stromal cell line derived from yolk sac but not in an aorta derived endothelial cell line (EOMA). Transfection of the EOMA cell line with ALCAM conferred them the ability to develop hematopoietic progenitor cells, suggesting CD166s crucial role for hematopoiesis (Ohneda et al. 2001).

Besides its expression on hematopoietic stem cells, further multipotent cells from a variety of tissues including umbilical cord blood (Prat-Vidal et al. 2007), bone marrow (Liu et al. 2008), testes (Gonzalez et al. 2009), fetal lung (Hua et al. 2009) and dental pulp (Karaöz et al. 2010) were found to express CD166.

In the last decade, CD166 was placed in the limelight as a cancer stem cell marker. As cancer stem cells are substantial for tumor relapse and progression, its amount should be relevant for patient´s outcome. Consistent with this hypothesis, CD166 expression was correlated with shortened patient survival in colorectal cancer (Weichert et al. 2004). Horst et al. further underlined ALCAMs role as a cancer stem cell marker by analyzing 110 stage I and II colorectal adenocarcinomas for CD166 expression together with the proposed CSC markers CD133 and CD44 and compared them for their correlation with patient outcome. The research group highlighted CD133 to be the most robust CSC marker but emphasized that the combined evaluation of CD133 together with CD166 and CD44 is even more valuable to separate high-risk from low-risk colorectal cancer cases (Horst et al. 2009b). Apart from Horst et al., also researchers from Romania confirmed the coexpression of CD133 and CD166 which correlated with higher grade

dysplasias in colon carcinoma (Mărgaritescu et al. 2014). ALCAM was then also found to be a CSC marker in several other cancer types including head and neck cancer (Yan et al. 2013), prostate cancer (Jiao et al. 2012), pancreatic cancer (Fujiwara et al. 2014) and ovarian cancer (Kim et al. 2020). Its function as a CSC marker was confirmed by sphere-forming ability, tumorigenicity in mice, migration abilities and resistance to conventional chemotherapy.

Besides many evidences of CD166 being a robust CSC marker, there are still controversial views on this topic with research groups having contradictory opinions (Hatano et al. 2017; Tachezy et al. 2014; Muraro et al. 2012).

The exact mechanism of ALCAM conferring tumorigenicity, invasiveness and stemness are still elusive, but the involvement of CSC related pathways like WNT, NFKB- and Hippo-YAP pathway was already proposed in several reports (King et al. 2010; Cizelsky et al. 2014). Ma et al. for example found out that ALCAM can promote YAP, a downstream effector of the Hippo-Yap pathway, to bind to TEAD, which consequently promotes cell proliferation, migration and invasion (Xia et al. 2014).

CD166 is also highly expressed in the colon and small intestine´s stem cell niche. As an important cell adhesion molecule, it is proposed to be involved in stem cell´s anchorage in intestinal stem cell niche and dictating stem cell´s behavior (Levin et al. 2010). On the one hand this emphasizes CD166´s role as a CSC/ stem cell marker but on the other hand also highlights the importance for combining CD166 with the expression of other CSC marker like CD133 for efficient targeting with anti-cancer drugs to enhance specificity and reduce off-target effects.

2.2.2.4. CEACAM5

CEA or the carcinoembryonic antigen was one of the first markers for colorectal cancers already identified 50 years ago. Further investigations lead to the discovery of a much larger family of 12 carcinoembryonic antigen-related cell adhesion molecules (CEACAMs) with diverse functions including cell adhesion, intracellular and intercellular signaling in many biological processes like cancer progression, inflammation, angiogenesis and metastasis (Beauchemin und Arabzadeh 2013).

CEACAM5 is a member of the immunoglobulin (Ig) supergene family and consists of one variable domain (N-domain) followed by seven Ig domains yielding to a molecular weight of 71 kDA. The protein is anchored to the cell membrane by a GPI-anchor (Beauchemin und Arabzadeh 2013). CEACAM5 has a broad expression in colorectal cancers being detectable in human serum from nearly 85% of colon carcinoma patients and can be

used as a sensitive and highly specific biomarker for colorectal cancer. Besides its expression on colorectal cancer cells, its expression is restricted to epithelial cells and most abundantly found on the apical surface of the gastrointestinal epithelium, but also on other mucosal epithelia including nasopharynx, the lung, the urogenital tract and sweat glands (Kuespert et al. 2006). Via homotypic binding to itself or heterotypic binding to other CEACAM members, CEACAM5 mainly mediates cell-cell adhesions (Kuespert et al. 2006). Signaling of CEACAMs is initiated by ligand binding. CEACAM1 then forms oligomers in cis between extracellular and transmembrane domains and is recruited to microdomains. In these microdomains, CEACAMs, including CEACAM5, connect to co-receptors and trigger intracellular signaling through the PI3K-pathway (Tchoupa et al. 2014). Via this signaling and cell-adhesion to different immune and non-immune cell types, CEACAMs are implicated in morphogenesis, angiogenesis, cell proliferation, cell motility, apoptosis, regulation of cell matrix attachment epithelial cell-cell interactions and cell polarization, but knowledge about its function and signaling remains limited (Tchoupa et al. 2014).

In the context of cancer, CEACAMs role is contradictory. Some reports stated that CEA expression does not have influence on tumorigenesis by employing mouse models with CEA-positive and CEA-negative compound mice. None of the CEA-positve mice demonstrated a higher tumor burden relative to the CEA-negative ones (Thompson et al. 1997). In another experimental setting where colon cancer was induced in mice via the colon-specific carcinogen azoxymethane, CEACAM5, CEACAM6 and CEACAM7 positive mice had twice the amount of colonic adenomas and adenocarcinomas compared to their wildtype counterparts (Chan et al. 2006). Furthermore, CEA is known as a modulator of anticancer immunity. The heterophilic binding of CEACAM5-CEACAM1 results in MHC-independent inhibition of NK cell killing. When the heterophilic binding is blocked, NK cells could efficiently eliminate human CRC expressing CEA by an CEA-binding antibody through ADCC (Conaghan et al. 2008). Via heterophilic adhesion or in association with signaling receptors like DR5 and TGF-bR1, CEACAM5 is reported to support metastasis (Beauchemin und Arabzadeh 2013).

The involvement of CEA in the metastasis process raised interest in it to probably be a cancer stem cell marker. In breast cancer, serially passaged lung metastases from mice were implanted in mammary fat pads of recipient mice to enrich for gene expression changes that drive metastasis. Transcriptomic analysis revealed CEACAM5 as a metastatic driver, facilitating tumor outgrowth at metastatic sites (Powell et al. 2018). Furthermore, CSCs were isolated from colorectal cancer using the CSC marker CD133 and the proteome of these cells was analyzed. LC-MS/MS and Flow cytometry could identify

CEACAM5 overexpression in all thirty CD133+ colorectal tumor samples (Gisina et al. 2021). Combining this finding with the fact that CEACAM5 is broadly expressed on epithelial cancer cells and normal cells, simultaneous targeting of CD133 and CEACAM5 could be a promising strategy to eradicate colorectal cancer stem cells specifically.

2.3. Current therapies against colorectal cancer

Many treatments against colorectal cancers are currently available.

The most common untargeted therapy is the surgical removal of the tumor and metastases, which is still the most effective intervention. For unresectable lesions, other strategies must be employed to achieve maximum shrinkage of the tumor and suppression of further tumor spread and growth. Mostly radiotherapy and chemotherapies are the medium of choice. More precise, fluoropyrimidine (5-FU) and multiple-agent regimens containing one or several drugs like oxaliplatin (OX), irinotecan (IRI) and capecitabine (CAP/ XELODA/ XEL) (Xie et al. 2020).

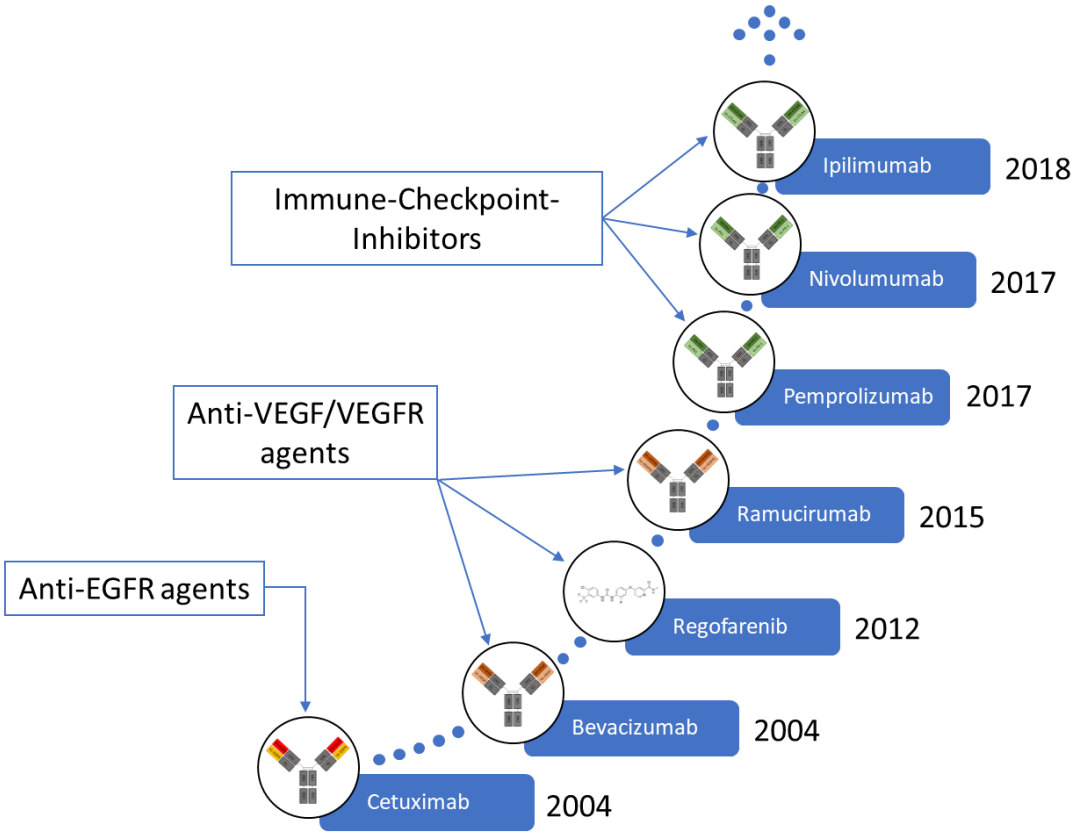

Figure 4: FDA-approved targeted therapies against CRC: approved drugs from the FDA targeting EGFR, VEGF/ VEGFR and the immune checkpoints PD-1 and CTLA-4. Targeted Therapies comprise of either antibodies or small molecule inhibitors.

As seen in Figure 4, which shows a list of selected drugs approved by the FDA, in the last decades several targeted therapies were developed to overcome resistance and

toxic side effects of common chemotherapy. In 2004, the first targeted agent approved by the FDA was cetuximab, a fully monoclonal antibody targeting EGFR, which is over-expressed in 25-80% of colorectal cancers (Reynolds und Wagstaff 2004). Through binding to EGFR, it induces/ inhibits a broad range of cellular responses in tumors and confers ADCC with its Fc-portion. After initial promising results, another EGFR-targeted antibody, Panitumumab, binding to a different epitope and thereby hindering EGFR from dimerizing and blocking downstream signaling pathways was approved in 2006 (Xie et al. 2020). Important to mention here is, that only RAS wild-type tumors can be efficiently eliminated with these antibodies. Another often-used signaling pathway that is involved in angiogenesis is the VEGF/ VEGFR pathway. As angiogenesis is pivotal for tumor initiation, growth and metastasis, blocking this pathway promises to prevent vascularization of tumors which “starves” the tumors to death. Consequently, Bevacizumab and Ramucirumab, respectively targeting VEGF and VEGFR2, were approved by the FDA in 2004 and 2015. Together with the small molecule kinase inhibitor Regorafenib, which inhibits several kinases including VEGFR, these three drugs build the class of anti-VEGF/VEGFR agents. All these antibodies and drugs conferred an enhanced OS and PFS when combined with chemotherapy. In the last years a new milestone in tumor therapy arose with promising outcome for cancer patients, the immune checkpoint inhibitor therapy. Instead of blocking pathways that contribute to tumor growth and spread, these therapies are aiming at enhancing immunorecognition and response of cancer cells against the human immune system. Cancer cells often acquire immune escape by two major mechanisms: downregulation of MHC-I molecules, which are required for recognition of malignant cells by T-cells, and the inactivation or exhaustion of T-lymphocytes via the activation of co-inhibitory receptor including PD-1. By administering immune-checkpoint inhibitors, namely Pembrolizumab and Nivolumumab, antibodies binding to PD-1 and blocking its interaction, and Ipilimumab, an antibody binding and blocking CTLA-4, inactivation of T-lymphocytes can be circumvented. In colorectal cancer, immune checkpoint inhibitors and its combinations showed good responses in patients, reaching a PFS of 71% and OS of 85% at one year (Xie et al. 2020).

In summary, it can be said that with the field of cancer immunotherapy, a huge step forward in cancer curation was made.

Table 1 shows a list of therapeutics based on the killing of cancer stem cells especially in the context of colorectal cancer. Above mentioned treatments are more or less targeting the tumor bulk in colorectal carcinomas. Targeting the subset of CSC is an emerging field of research yielding promising results. The first agent targeting CRC-SC via EpCAM is Catumaxomab. In a phase II/III study, Catumaxomab was able to eliminate CD133+/

EpCAM+ CSC in 9 of 14 patients after the first injection, after 4 i.p. catumaxomab infusions these cells were completely eliminated from the peritoneal fluids of all 14 patients (Lindhofer et al. 2009). Since EpCAM is also broadly expressed on other tissues in the colon, severe adverse effects including cytokine release syndrome, headache, infection and anaemia are common. Generally, therapeutics against CRC-SC can be divided in monoclonal antibodies (mAbs), bispecific antibodies (bsAb) and drug conjugates targeting CSC marker and inhibitors of CSC related pathways consisting of mAbs and small molecule inhibitors. In recent years CAR T-cell based therapies were clinically tested against e.g CD133.

Table 1: CSC targeting therapeutics in clinical development

Drug	**Format**	**Target**	**disease**	**Most advanced clinical stage**	**Reference**
Bivatuzumab	mAb	CD44v6	colorectal cancer	III	NCT00700102
MCLA-158	bispecific antibody	LGR5, EGFR	colorectal cancer	I	NCT03526835
Adecatumumab	mAb	EpCAM	colorectal cancer	II	NCT00866944
Catumaxomab	bsAb	EpCAM, CD3	colorectal cancer	approved	approved
RO5429083	mAb	CD44	gastric cancer	I	NCT01358903
hG7-BM3-VcMMAE	mAb	CD24	hepatocellular carcinoma	-	preclinical
Pralu-zatamab Ravtansine	probody drug conjugate	CD166	breast cancer	II	NCT04596150
CAR-CD133 T-cell	CAR T-cell	CD133	colorectal cancer	II	NCT02541370
Vismodegib	small molecule inhibitor	Hedgehog inhibitor	colorectal cancer	II	NCT00636610
RO4929097	small molecule inhibitor	Notch inhibitors	colorectal cancer	II	NCT01116687
Ipafricept	fusion protein	WNT inhibitors	colorectal cancer	I	NCT01608867
Vantictumab	mAb	WNT inhibitors	colorectal cancer	I	NCT01345201

2.4. Bispecific T-cell recruiting antibody formats

Besides above-mentioned full antibodies, there are several other antibody formats available, partly approved, partly in preclinical development. These formats vary in valency and specificity. Bispecific formats are one of the most extensively studied molecules. Figure 5 shows the huge variety of bispecifics developed in labs around the world. They are ranging from over 150 kDa proteins having a Fc-portion to small fragments with a size of around 25 kDa. The bigger the molecule and having a Fc portion greatly enhances in vivo half-lifes but interfere with tissue penetration. Smaller sizes on the other hand facilitate tumor penetration but greatly decrease in vivo half-lifes.

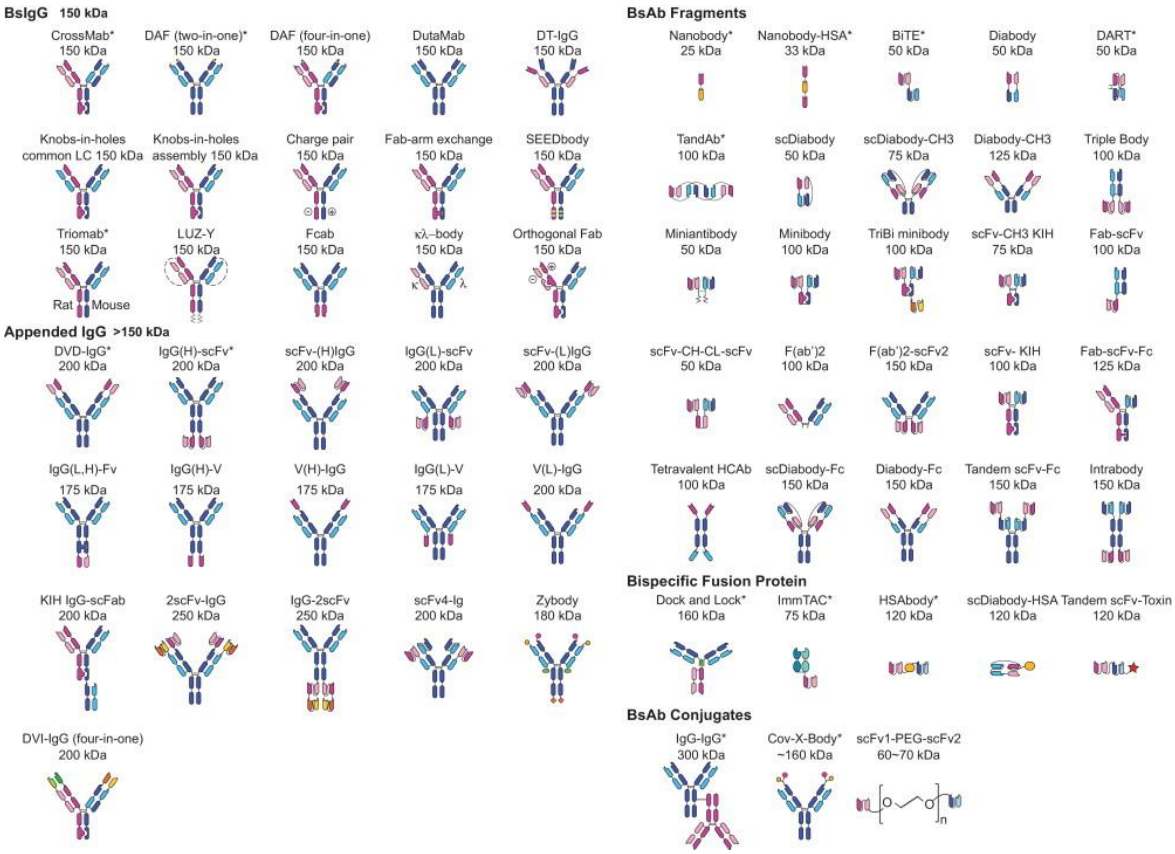

Figure 5: Bispecific antibody formats: bispecific antibodies or antibody fragments can be divided in 5 major classes: BsIgG, appended IgG, BsAb fragments, bispecific fusion proteins and BsAb conjugates. Heavy chains are depicted in dark blue, dark pink and dark green, corresponding light chains in lighter shades of the same colour. (adapted from (Spiess et al. 2015)

Antibodies having only entities against tumor antigens and a Fc portion, mainly demonstrate anti-tumor effects via ADCC, CDC and via blocking of the targeted receptors. With the approval of Blinatumomab in 2009, a major breakthrough in immunotherapy was made. Blinatumomab (Blincyto ®) is a bispecifc and bivalent BsAb fragment consisting of an scFv against CD3 and a scFv against CD19, connected by a glycine serine linker. After binding of the scFv against CD19 on acute lymphatic leukemia cells immune cells,

namely CD8+ cytotoxic T-cells are recruited to the tumor cells by binding of CD3 with the second scFv entity. Consequently, through the close proximity of T-cell and cancer cell an immunological synapse is formed resulting in cancer cell killing. Thus, the so-called bispecific T-cell engagers (BiTEs) bridge endogenous T-cells to tumor-associated antigens, using the cytotoxic potential of a patient´s own immune cells. In comparison to CAR T-cell therapy, there is no need for genetic alteration of T-cells and its ex vivo expansion/ manipulation. Currently there are several BiTEs tested in clinical studies. For solid tumors, T-cell engagers against prostate (NCT03792841), glioblastoma (NCT03296696), small-cell lung cancer (NCT03319940) and gastric cancer (NCT04117958, NCT04260191) are under clinical evaluation (Einsele et al. 2020). Despite showing a great killing efficacy against tumor cells, BiTE molecules suffer from substantial adverse effects of grade ≥ 3 (Hummel et al. 2019). Because of that high grade toxicities, many molecules were discontinued during early clinical studies (Another clinical trial of Amgen's BiTE therapy has been suspended - iNEWS 2021). This can be explained by the fact that BiTEs target only one tumor associated antigen. As tumor associated antigens are also expressed on normal tissue, killing of healthy cells leads to severe adverse effects including cytokine release syndrome.

2.5. Hemibodies

In this study, two new different trispecific antibodies with the same mode of action (MoA) were used: 1st gen Hemibodies and 2nd gen Hemibodies. 1st gen Hemibodies consist of one scFv against a TAA connected to a split scFv against CD3. Thereby, two split T-cell engaging fragments arise, one Hemibody carrying the VH domain of a scFv against CD3 and one the VL domain (Figure 6A). The 2nd generation of Hemibodies incorporates a Fc-portion for half-life extension and increased stability. The targeting scFv domain and the VH/VL domain against CD3 are N-terminally fused to Fc-knob and Fc-hole respectively. Combination of Fc-knob and Fc-hole resembles a Hemibody-fragment (Figure 6A).

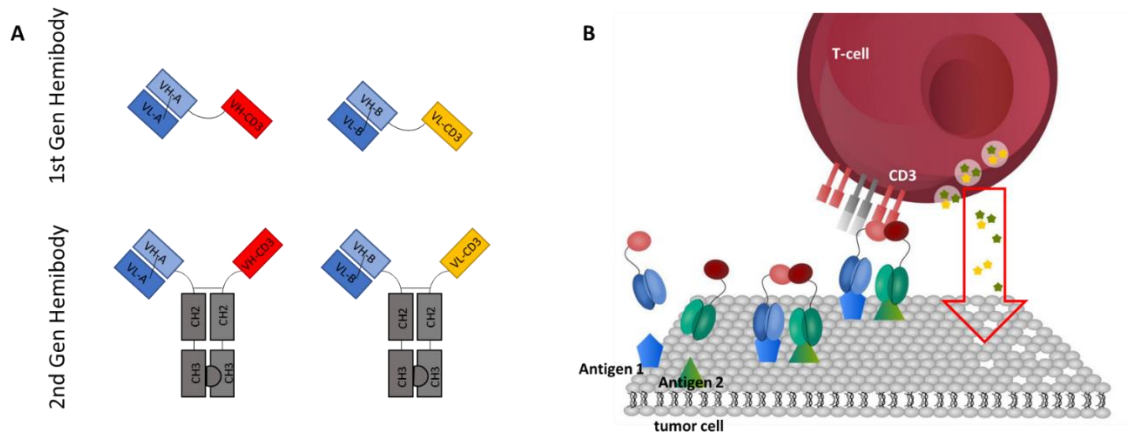

Figure 6: Schematic representation and mode of action (MoA) of different Hemibody generations (A) Schematic representation of the bispecific split antibody formats Hemibody and Hemibody-Fc including variable domains (VH-A, VL-A, VH-B, VL-B, VH-CD3, VL-CD3) and the Fc region of the Hemibody-Fc (hinge plus CH2 and CH3) (B) MoA of Hemibodies: once both hemibodies are bound to the tumor cell, the split CD3 scFv rejoins and recruits a T-cell via CD3 binding. Consequently, the T-cell is activated and kills the tumor cell (adapted from (Maria Geis 2019)

A functional Hemibody drug consists of two Hemibody fragments: one harboring the VH domain against CD3 and one harboring the VL domain against CD3. As seen in Figure 6B, both fragments have to be bound on the surface of the tumor cell. Being in close proximity to each other together with CD3 on the T-cell leads to complementation of the VH and VL domain to a functional Fv domain. When only one Hemibody is bound, no complementation can occur. The anti CD3 Fv domain then recruits a T-cell to the tumor by binding of CD3 on the T-cell. Consequently, an immunological synapse is formed, the T-cell is activated and the tumor cell lysed via secretion of granzyme and perforin. As seen in BiTE therapy, T-cell activation is independent from MHC- and costimulatory molecules.

The main advantage of Hemibodies over BiTEs is the highly specific targeting of tumor cells. While BiTE molecules only bind one TAA, Hemibodies are only functional when two different TAAs are bound on the tumor cell. Adverse effects (AEs) are expected to be significantly lower compared to BiTEs. Another advantage of Hemibodies is the possibility to target antigens that are currently “undruggable” because of broad expression throughout the body. Combining these antigens together with other TAAs enables efficient lysis of target cells without harming healthy tissue. A good example for this was published in 2019 (Banaszek et al. 2019). In an allogeneic mismatch transplantation model for leukemia, the patient is HLA-A2 positive, the donor HLA-A2 negative. After stem cell transplantation, tumor recurrence often occurs due to remaining cancerous leukemia cells. Applying the Hemibody technology, a combinatorial targeting of HLA-A2 and CD45, a pan hematopoietic lineage marker, enables the elimination of HLA-A2 and

CD45 dual positive remaining leukemia cells while sparing the HLA-A2 positive healthy tissue and the CD45 positive donor blood stem cells (Banaszek et al. 2019). With the BiTE technology, this approach would not be possible. Hemibody technology was further validated for multiple myeloma therapy (Geis et al. 2021).

2.6. Objective of this study

As stated in 2.2, CSC are highly tumorigenic, slowly cycling cancer cells, which are responsible for therapy resistance, failure and recurrence after therapy. Eliminating this subset of cancer cells holds great potential for patient outcome and cancer therapy.

In a first step this study focuses on the characterization of colorectal tumors. With the analysis of single-cell RNAseq-datasets mentioned above, CSC markers should be validated for co-expression and if they can be really considered as CSC markers.

Afterwards, Hemibodies, were constructed against the validated CSC markers, produced and tested in vitro by binding studies and killing-assays on CHO cells and different cancer cell lines. Construction and production further should be optimized for yield, stability and in vivo-half life.

3. Materials and Methods

3.1. Material

3.1.1. Instruments

Balances	All used balances were purchased from Kern [KERN & SOHN GmbH, Balingen-Frommern, Germany]
Cell counter	Countess II [Thermo Fisher Scientific Inc., Waltham, MA, USA]
Centrifuges	Centrifuge 5424 [Eppendorf, Hamburg, Germany], Avanti JXN-26 [Beckman Coulter GmbH, Krefeld, Germany], Beckman J6-MI [Beckman Coulter GmbH, Krefeld, Germany]
Electrophoresis systems	Mini-PROTEAN Tetra Electrophoresis System [Bio-Rad Laboratories, CA, USA], Electrophoresis Unit ROTIPHORESE® PROfessional I [Carl Roth GmbH + Co. KG, Karlsruhe, Germany]
Plate reader	Tecan Spark ® [Tecan Group Ltd., Männedorf, Zürich, Switzerland]
Flow cytometers	FACSCaliburTM [Becton Dickinson, Franklin Lakes, NJ, USA], MACSQuant Analyzer 10 [Miltenyi Biotec, Bergisch Gladbach, Germany]
Heat block	Thermoschüttler pro [CellMedia GmbH & Co. KG, Zeitz, Germany]
FPLC systems	Äkta Pure Chromatography System [GE-Healthcare Life Sciences, Chicago, Illinois, USA]
Incubator for bacteria	BE 200 Incubator [Memmert GmbH + Co. KG, Schwabach, Germany], Innova ® 44 [New Brunswick/ Eppendorf, Hamburg, Germany]
Incubator for cell culture	HERAcell 240i [Thermo Fisher Scientific Inc., Waltham, MA, USA], Multitron Pro [Infors HT, Bottmingen, Switzerland]
Microscope	Leica DMi1 [Leica Mikrosysteme Vertrieb GmbH, Wetzlar, Germany], Motic BA210 Series + Moticam Serie, Moticam 5+ [Moticeurope S.L.U., Barcelona, Spain]
PCR cycler	C1000 Touch Thermal Cycler [Bio-Rad Laboratories, CA, USA]
Spectrophotometer	NanoDrop TM 2000 [Thermo Fisher Scientific Inc., Waltham, MA, USA], OD600 DiluPhotometerTM [Implen GmbH, München, Deutschland]
Homogenizer	EmulsiFlex-C3 [Avestin Europe GmbH, Mannheim, Germany]
Electroporation system	Neon Transfection System [Thermo Fisher Scientific Inc., Waltham, MA, USA]
Imaging System	Gel Doc ™ XR [Bio-Rad Laboratories, CA, USA]

3.1.2. Special implements

Chromatography columns	Cytiva Superdex™ 200 Increase 10/300 GL [Global Life Sciences Solutions USA LLC, Marlborough, MA, USA]
Counting Chambers	Hemacytometer [Marienfeld, Lauda-Königshofen, Germany]
Dialysis membranes	MEMBRA-CEL® DIALYSIS MEMBRANES 14 kDa cutoff [Viskase ®, Lombard, Illinois, USA]
IMAC affinity beads	High Density Cobalt resin [Agarose Bead Technologies, Madrid, Spain]
Centrifugal filters	Amicon® Ultra-4 centrifugal filter units [Merck KGaA, Darmstadt, Germany]

3.1.3. Chemicals and consumables

All chemicals were obtained from Carl Roth GmbH + Co. KG [Karlsruhe, Germany]. It is stated if chemicals were obtained from other companies. Plastic ware for laboratory was purchased from Eppendorf [Hamburg, Germany], Greiner Bio-One [Kremsmünster,Austria] and Sarstedt AG & Co. KG [Nümbrecht, Germany]. Laboratory glassware was purchased from Schott AG [Mitterteich, Germany].

3.1.4. Buffers and solutions

Bradford reagent	ROTI®Nanoquant [Carl Roth GmbH + Co. KG, Karlsruhe, Germany]
Coomassie staining solution	0,25% Coomassie Brilliant Blue + 45% Methanol (v/v) + 10% glacial acetic acid (v/v) + 45% H_2O
DNA loading dye, 5x	GelPilot DNA Loading Dye [Qiagen, Hilden, Germany]
Freezing solution	90% complete growth medium + 10% DMSO (v/v)
IMAC loading buffer	50 mM Na-Phosphatpuffer (pH 7,5) 300 mM NaCl 10 mM Imidazol (pH 8,0)
IMAC wash buffer	50 mM Na-Phosphatpuffer (pH 7,5) 300 mM NaCl 1 mM Imidazol (pH 8,0) 0,2 % v/v Triton x 114
IMAC elution buffer	50 mM Na-Phosphatpuffer (pH 7,5) 300 mM NaCl 150 mM Imidazol (pH 8,0)
IMAC regeneration buffer	50 mM Na-Phosphatpuffer (pH 7,5) 300 mM NaCl 300 mM Imidazol (pH 8,0)
Laemmli sample buffer (4x)	Tris (1.0 m, pH 6.8) 10 mL SDS 4.0 g Glycerol 20 mL ± β-Mercaptoethanol 10 mL Bromophenol blue 0.1 g dH2O to 50 mL
DPBS	D8537-500ML [Sigma-Aldrich, Merck KGaA, Darmstadt, Deutschland]
10x SDS running buffer	1,92 M Glycin 250 mM Tris ultrapure 1 % SDS
TAE buffer, 50x	ROTIPHORESE®50x TAE Puffer [Carl Roth GmbH + Co. KG, Karlsruhe, Germany]
TBE buffer, 10x	890 mM Tris Ultrapure 890 nM Borsäure 290 mM EDTA
FACS Buffer	PBS + 0,5% BSA
Agarose Gel 1%	1% w/v Universal Agarose in 1 x TBE/TAE Buffer 200 ng/ml Nancy-520
Polyacrylamidgels	See 3.2.7.2
Coomassie destaining solution	45 % v/v Methanol absolut 10 % v/v Essigsäure absolut 45% v/v H_2O
SEC-Buffer	50 mM Na-Phosphatpuffer (pH 7,5) 300 mM NaCl
Glycerolstock-Buffer	65 % v/v Glycerol (100 %) 25 mM Tris-HCl (pH 8,0) 0,1 M MgSO4

3.1.5. Media and supplements

3.1.5.1. Bacterial culture

Carbenicilin-Stock	100 mg/ml Carbenicillin in dH2O
LB-medium	1 % v/v NaCl 1 % v/v Trypton 0,5 % w/v yeast extract pH 7,0
2xYT medium	1,6 % w/v Tryptone 1 % w/v Yeast extract 0,5 % w/v NaCl pH 7,0
Kanamycin-Stock	50 mg/ml Kanamycin in dH2O
LB agar plates	1 % v/v NaCl 1 % w/v Trypton 0,5 % w/v Hefe 2 % w/v Agar-Agar pH 7,0, autoklaviert
IPTG	1 M IPTG in dH2O
Glucose stock solution	20% Glucose (w/v) in dH_2O
Glycerol Stock Buffer	65% v/v Glycerol + 25 mM Tris-HCl pH 8 + 0,1 M $MgSO_4$ in ddH_2O

3.1.5.2. Eukaryotic cell culture

Trypan Blue Stain	Trypan Blue Solution 0,4% [Sigma-Aldrich, Merck KGaA, Darmstadt, Deutschland]
Advanced DMEM	[Thermo Fisher Scientific Inc., Waltham, MA, USA]
Advanced RPMI	[Thermo Fisher Scientific Inc., Waltham, MA, USA]
F-12K (Kaighn's) Medium	[Thermo Fisher Scientific Inc., Waltham, MA, USA]
Opti-MEM	[Thermo Fisher Scientific Inc., Waltham, MA, USA]
Freestyle 293 Medium	[Thermo Fisher Scientific Inc., Waltham, MA, USA]
HyClone™ ActiPro	[Global Life Sciences Solutions USA LLC, Marlborough, MA, USA]
McCoy´s 5A Medium	[Thermo Fisher Scientific Inc., Waltham, MA, USA]
Fetal bovine serum (FBS)	[Thermo Fisher Scientific Inc., Waltham, MA, USA]
Polyethylenimine (PEI)	1mg/ml Polyethylenimine, Linear, MW 25000, Transfection Grade in ddH_2O [Polysciences Inc., Warrington, PA, USA]
Penicilin/ Streptomycin/ Neomycin (100x)	[Thermo Fisher Scientific Inc., Waltham, MA, USA]
Trypsin	[Thermo Fisher Scientific Inc., Waltham, MA, USA]
TrypLE Express	[Thermo Fisher Scientific Inc., Waltham, MA, USA]
Trypon N1 (TN1)	
Lipofectamine 3000	[Thermo Fisher Scientific Inc., Waltham, MA, USA]
Hygromycin	50 mg/ml Hygromycin B [Invitrogen, Thermo Fisher Scientific Inc., Waltham, MA, USA]
Puromycin	[InvivoGen, Toulouse, France]
Luciferin	0,1 M in 1x PBS [Biosynth AG, Staad, Switzerland]
MEM-NEA	[Thermo Fisher Scientific Inc., Waltham, MA, USA]
Sodium Pyruvate 100 mM	[Thermo Fisher Scientific Inc., Waltham, MA, USA]
B-Mercaptoethanol 55 mM	[Thermo Fisher Scientific Inc., Waltham, MA, USA]
Lentivirus Fluc GFP	Kind gift from AG Hudecek [Würzburg, Germany]
Tumorsphere Medium	DMEM/F12 [Thermo Fisher Scientific Inc., Waltham, MA, USA] 1xB27 Supplement [Thermo Fisher Scientific Inc., Waltham, MA, USA] EGF (20ng/ml) [Peprotech, Cranbury, New Jersey, USA] FGF2 (10ng/ml) [R&D Systems, Minneapolis, MN, USA]

3.1.6. Antibodies and FACS stains

Name	Origin	Dilution
Anti-CD24	Mouse mAb, IgG1, PE conjugated [Thermo Fisher Scientific Inc., Waltham, MA, USA] – Cat: MA1-10154	1:20
Anti-CD24	Mouse mAb, IgG1, FITC conjugated [Thermo Fisher Scientific Inc., Waltham, MA, USA] – Cat: 11-0247-42	1:20
Anti-CEA	Mouse mAb, IgG2bk, FITC conjugated [Miltenyi Biotec, Bergisch-Gladbach, Germany] – Cat: 130-116-668	1:50
Anti-CD133	Mouse mAB, IgG2a, AF488 conjugated [R&D Systems, Minneapolis, MN, USA] – Cat: FAB11331G-100	1:20
Anti-AC133	Mouse mAb, IgG1k, APC conjugated [Miltenyi Biotec, Bergisch-Gladbach, Germany] – Cat: 130-113-668	1:20
Anti-CD166	Mouse mAb, IgG1, AF488 conjugated [Bio-Rad Laboratories, CA, USA] – Cat: MCA1926A488	1:20
Anti-CD166	Mouse mAb, IgG1, PE conjugated [Biolegend, San Diego, CA, USA] – Cat: 343904	1:20
Anti-human IgG	Goat pAb, AF488 conjugated [Thermo Fisher Scientific Inc., Waltham, MA, USA] – Cat: A-11013	1:400
Anti-Strep-Tag	Mouse mAb, IgG1, AF488 coupled [IBA Lifesciences GmbH, Göttingen, Germany] – Cat: 2-1564-050	1:100
Anti-mouse IgG1, κ Isotype Ctrl	Mouse mAb, IgG1k, AF488 coupled [Biolegend, San Diego, CA, USA] – Cat: 400129	1:20
Anti-mouse IgG1, κ Isotype Ctrl	Mouse mAb, IgG1k, FITC coupled [Biolegend, San Diego, CA, USA] – Cat: 400108	1:20
Anti-mouse IgG1, κ Isotype Ctrl	Mouse mAb, IgG1k, PE coupled [Biolegend, San Diego, CA, USA] – Cat: 400111	1:20

Anti-Mouse IgG2a, κ Isotype Ctrl	Mouse mAb, IgG2a, AF488 coupled [Biolegend, San Diego, CA, USA] – Cat: 400233	1:20
Anti-Mouse IgG2b, κ Isotype Ctrl	Mouse mAb, IgG2b, FITC coupled [Biolegend, San Diego, CA, USA] – Cat: 400310	1:20
CSFE	CFSE Cell Division Tracker Kit [Biolegend, San Diego, CA, USA] – Cat: 423801	As specified in manufacturer's protocol
Cell Trace Violet	CellTrace™ Violet Cell Proliferation Kit [Thermo Fisher Scientific Inc., Waltham, MA, USA] – Cat: C34557	As specified in manufacturer's protocol
7-AAD	[BD Biosciences, Franklin Lakes, NJ, USA]	1:1000

3.1.7. Enzymes

FastDigest EcoRI	[Thermo Fisher Scientific Inc., Waltham, MA, USA]
FastDigest NotI	[Thermo Fisher Scientific Inc., Waltham, MA, USA]
FastDigest KpnI	[Thermo Fisher Scientific Inc., Waltham, MA, USA]
FastDigest Kpn2I	[Thermo Fisher Scientific Inc., Waltham, MA, USA]
FastDigest SalI	[Thermo Fisher Scientific Inc., Waltham, MA, USA]
FastDigest NcoI	[Thermo Fisher Scientific Inc., Waltham, MA, USA]
NgoMIV	[New England Biolabs, Ipswich, MA, USA]
FastDigest SwaI	[Thermo Fisher Scientific Inc., Waltham, MA, USA]
FastDigest BstBI	[Thermo Fisher Scientific Inc., Waltham, MA, USA]
FastDigest NheI	[Thermo Fisher Scientific Inc., Waltham, MA, USA]
FastDigest BmtI	[Thermo Fisher Scientific Inc., Waltham, MA, USA]
Fast alkaline phosphatase	[Thermo Fisher Scientific Inc., Waltham, MA, USA]
Taq DNA polymerase	[Thermo Fisher Scientific Inc., Waltham, MA, USA]
Q5 Hot Start polymerase	[New England Biolabs, Ipswich, MA, USA]
T4 DNA ligase	[Thermo Fisher Scientific Inc., Waltham, MA, USA]

3.1.8. Marker

GeneRuler™ 1kb Plus ladder	[Thermo Fisher Scientific Inc., Waltham, MA, USA]
PageRuler™ unstained	[Thermo Fisher Scientific Inc., Waltham, MA, USA]

3.1.9. Kits

NucleoBond® Xtra Midi	[Qiagen, Hilden, Germany]
REDTaq ReadyMix PCR Reaction Mix (1 U/ml)	[Sigma-Aldrich, Merck KGaA, Darmstadt, Deutschland]
MiniElute Gel Extraction Kit	[Qiagen, Hilden, Germany]
MiniElute PCR Purification Kit	[Qiagen, Hilden, Germany]
QIAprep® Spin Miniprep Kit	[Qiagen, Hilden, Germany]
Caspase-Glo® 3/7 Assay System	[Promega, Madison, Wisconsin, USA]

3.1.10. Bacterial strains

For cloning experiments, *Escherichia coli* MACH1 strain (Genotype: F- φ80(lacZ)ΔM15 ΔlacX74 hsdR(rK-mK+) ΔrecA1398 endA1 tonA; ThermoFisher Scientific, Waltham, USA) was used. Production of Hemibody constructs was conducted with SHuffle® T7 Competent E. coli (Genotype: F´ lac, pro, lacIq / Δ(ara-leu)7697 araD139 fhuA2 lacZ::T7 gene1 Δ(phoA)PvuII phoR ahpC* galE (or U) galK λatt::pNEB3-r1-cDsbC (SpecR, lacIq) ΔtrxB rpsL150(StrR) Δgor Δ(malF)3; New England Biolabs, Ipswich, USA).

3.1.11. Eukaryotic cell lines

All cell lines were purchased from the DSMZ (Braunschweig, Germany). HCT116 Fluc+ GFP+ was a kind gift from AG Otto (University Hospital Würzburg, Germany). CHO-K1 cell lines were transfected in-house using the PiggyBac Transposon System.

Cell line	Origin	Culture Medium
HCT116	Human colorectal carcinoma	McCoy´s 5A + 10% FBS + 1x PSN + 1x MEM-NEA + 1mM Sodium Pyruvate + 55µM B-Mercaptoethanol
HCT116 Fluc+ GFP+	Human colorectal carcinoma	McCoy´s 5A + 10% FBS + 1x PSN + 1x MEM-NEA + 1mM Sodium Pyruvate + 55µM B-Mercaptoethanol
HT29	Human colorectal adenocarcinoma	McCoy´s 5A + 10% FBS + 1x PSN + 1x MEM-NEA + 1mM Sodium Pyruvate + 55µM B-Mercaptoethanol
HT29 Fluc+ GFP+	Human colorectal adenocarcinoma	McCoy´s 5A + 10% FBS + 1x PSN + 1x MEM-NEA + 1mM Sodium Pyruvate + 55µM B-Mercaptoethanol
Caco2 Fluc+ GFP+	Human colorectal adenocarcinoma	Advanced DMEM + 10% FBS + 1x PSN
Caco2	Human colorectal adenocarcinoma	Advanced DMEM + 10% FBS + 1x PSN
A549	Human lung carcinoma	F12K + 10% FBS + 1x PSN

A549 Fluc+ GFP+	Human lung carcinoma	F12K + 10% FBS + 1x PSN
CHO-K1	Hamster ovary cell line	F12K + 10% FBS + 1x PSN
CHO-K1 CD24+ CD133+ Fluc+ RFP+	Hamster ovary cell line	F12K + 10% FBS + 1x PSN
CHO-K1 CD166+ CD133+ Fluc+ RFP+	Hamster ovary cell line	F12K + 10% FBS + 1x PSN
CHO-K1 CD166+ CD24+ Fluc+ RFP+	Hamster ovary cell line	F12K + 10% FBS + 1x PSN
CHO-K1 CD24+ CEACAM5+ Fluc+ RFP+	Hamster ovary cell line	F12K + 10% FBS + 1x PSN
CHO-K1 CD133+ CEACAM5+ Fluc+ RFP+	Hamster ovary cell line	F12K + 10% FBS + 1x PSN

3.1.12. Primer

#	**Primer**	**Sequence**
7	NheI_CD24_fw	5' GGTGGTGCTAGCATGGGCAGAGCAATGGTG
8	SwaI_CD24_rev	5' GGTGGTATTTAAATTTAAGAGTAGAGATGCAGAAGAGAGAG
13	NheI_CD133_fw	5' GGTGGTGCTAGCATGGCCCTCGTACTCGG
14	SwaI_CD133_rev	5' GGTGGTATTTAAATTTAATGTTGTGATGGGCTTGTCAT
17	NheI_CD166_fw	5' GGTGGTGCTAGCATGGAATCCAAGGGGGCCAGT
18	SwaI_CD166_rev	5' GGTGGTATTTAAATTTAGGCTTCAGTTTTGTGATTGTTTTCTTCTA
19	NheI_CEA_fw	5' GGTGGTGCTAGCATGGAGTCTCCCTCGGC
20	SwaI_CEA_rev	5' GGTGGTATTTAAATTTATATCAGAGCAACCCCAACCAG
47	Kpn2I_PrimerfwTargetscFvs	5' GGTGGTCCGGAGGCGGAGGATC
50	SalI_CD133_rev	5' GCCACCGTCGACCTTGATTTCCAGCTTGGTGC
51	SalI_CEA_rev	5' GCCACCGTCGACCTTGATTCCCACTTTGGTGC
52	Kpn2I_scFv-CD166_fw	5' GCTCCGGAGGCGGA
85	NotI_StopHIS_rev	5' GGTGGTGCGGCCGCTTATCAATGATGGTGATGGTG
86	EcoRI_scFvCD24_fw	5' GGTGGTGAATTCGATGTGCATCTGCAAGAGT

87	Kpn2I_scFvCD24_rev	5' GGTGGTTCCGGACTTCAGGCCCAGCTT-TGT
90	EcoRI_scFvCD133_fw	5' GGTGGTGAATTCCAGGTTCAGTT-GCAGCAG
91	Kpn2I_scFvCD133_rev	5' GGTGGTTCCGGACTTGATTTCCAGCTT-GGTGC
92	EcoRI_scFvCD166_fw	5' GGTGGTGAATTCCAGATCACCCT-GAAAGAGTCTG
93	Kpn2I_scFvCD166_rev	5' GGTGGTTCCGGACCTTGATTTCCAGCTT-GGTGC
94	EcoRI_scFvCEA_fw	5' GGTGGTGAATTCGAGGTCCAGCTGGTG-GAA
95	Kpn2I_scFvCEA_rev	5' GGTGGTTCCGGACTTGATTCCCACTTT-GGTGC
96	KpnI_fcHole_knob_fw	5' GGTGGTGGTACCGCCACCATGGAAAC-CGACACACTGC
97	NotI_FcHole_rev	5' GGTGGTGCGGCCGCTCATCACTT-GCCTGGAGACA
98	NotI_Fcknob_rev	5' GGTGGTGCGGCCGCTCATCAGTGGT-GATGGTGG
126	NotI_Blo-ckingscFvs_rev	5' GGTGGTGCGGCCGCTCATTAGTGAT-GGTGGTGATGATGACT
139	NheI_HISTag	5' GGTGGTGCTAGCTTATCAATGATGGT-GATGGTGGTGATGA
140	EcoRI_VHUCHT1	5' GGTGGTGAATTCGAAGTGCAGCTGGTT-GAAT
141	EcoRI_VLUCHT1	5' GGTGGTGAATTCGATATTCAGAT-GACACAGAGCCC

3.1.13. Plasmids

#	**Name**	**cloned by**
T001	pCMV-SPORT6_CD24	Havard Plasmid Database
T002	pDONR201_CD133	Havard Plasmid Database
T003	pENTR223_CD166	Havard Plasmid Database
T004	pDONR221_CEA	Havard Plasmid Database
T005	PB01_CD24	Hannes Gotthard
T006	PB02_CD24	Hannes Gotthard
T007	PB01_CD133	Hannes Gotthard
T008	PB02_CD133	Hannes Gotthard
T009	PB01_CD166	Hannes Gotthard
T010	PB02_CD166	Hannes Gotthard
T011	PB01_CEA	Hannes Gotthard
T012	PB02_CEA	Hannes Gotthard
T013	PB_superPiggyBacTransposae	System Biosciences
C65	pMA-T-VLdiL2K-scFvCD24	GeneArt
C66	pMA-T-scFvCD133	GeneArt
C67	pMA-T-scFvCD166	GeneArt
C68	pMA-T-VHdiL2K-scFvCEA	GeneArt

C69.1	CET1019AS-Hygro-diL2KVH-CD24	Hannes Gotthard
C69.2	CET1019AS-Puro-diL2KVH-CD24	Hannes Gotthard
C70.1	CET1019AS-Hygro-diL2KVL-CD24	Hannes Gotthard
C70.2	CET1019AS-Puro-diL2KVL-CD24	Hannes Gotthard
C75.1	CET1019AS-Hygro-diL2KVH-CD133	Hannes Gotthard
C75.2	CET1019AS-Puro-diL2KVH-CD133	Hannes Gotthard
C76.1	CET1019AS-Hygro-diL2KVL-CD133	Hannes Gotthard
C76.2	CET1019AS-Puro-diL2KVL-CD133	Hannes Gotthard
C77.1	CET1019AS-Hygro-diL2KVH-CD166	Hannes Gotthard
C77.2	CET1019AS-Puro-diL2KVH-CD166	Hannes Gotthard
C78.1	CET1019AS-Hygro-diL2KVL-CD166	Hannes Gotthard
C78.2	CET1019AS-Puro-diL2KVL-CD166	Hannes Gotthard
C79.1	CET1019AS-Hygro-diL2KVH-CEA	Hannes Gotthard
C79.2	CET1019AS-Puro-diL2KVH-CEA	Hannes Gotthard
C80.1	CET1019AS-Hygro-diL2KVL-CEA	Hannes Gotthard
C80.2	CET1019AS-Puro-diL2KVL-CEA	Hannes Gotthard
C83.1	CET1019AS-hygro-diL2KscFv_CD24	Hannes Gotthard
C83.2	CET1019AS-puro-diL2KscFv_CD24	Hannes Gotthard
C86.1	CET1019AS-hygro-diL2KscFv_CD133	Hannes Gotthard
C86.2	CET1019AS-puro-diL2KscFv_CD133	Hannes Gotthard
C87.1	CET1019AS-hygro-diL2KscFv_CD166	Hannes Gotthard
C87.2	CET1019AS-puro-diL2KscFv_CD166	Hannes Gotthard
C88.1	CET1019AS-hygro-diL2KscFv_CEA	Hannes Gotthard
C88.2	CET1019AS-puro-diL2KscFv_CEA	Hannes Gotthard
V3C	pRSFDUET-3CProtease	Boris Nowotny
V0500	pCold-VHdiL2K-scFvCD24	Hannes Gotthard
V0501	pCold-VHUCHT1-scFvCD24	Hannes Gotthard
V0502	pCold-VLUCHT1-scFvCD24	Hannes Gotthard
V0503	pCold-scFvUCHT1-scFvCD24	Hannes Gotthard
V0510	pCold-VHUCHT1-scFvCD133	Hannes Gotthard

V0511	pCold-VLUCHT1-scFvCD133	Hannes Gotthard
V0512	pCold-scFvUCHT1-scFvCD133	Hannes Gotthard
V0513	pCold-VHUCHT1-scFvCD166	Hannes Gotthard
V0514	pCold-VLUCHT1-scFvCD166	Hannes Gotthard
V0515	pCold-scFvUCHT1-scFvCD166	Hannes Gotthard
V0516	pCold-VHUCHT1-scFvCEA	Hannes Gotthard
V0517	pCold-VLUCHT1-scFvCEA	Hannes Gotthard
V0518	pCold-scFvUCHT1-scFvCEA	Hannes Gotthard
V0525	pCold_VLdiL2K_scFvCD24	Hannes Gotthard
V0526	pCold-BiTEdiL2K_scFvCD24	Hannes Gotthard
V0533	pCold_VHdiL2K_CD133	Hannes Gotthard
V0534	pCold_VLdiL2K_scFvCD133	Hannes Gotthard
V0535	pCold_scFvdiL2k_CD133	Hannes Gotthard
V0536	pCold_VHdiL2K_CD166	Hannes Gotthard
V0537	pCold_VLdiL2k_scFvCD166	Hannes Gotthard
V0538	pCold_scFvdiL2K_CD166	Hannes Gotthard
V0539	pCold_VHdiL2K_CEA	Hannes Gotthard
V0540	pCold_VLdiL2K_scFvCEA	Hannes Gotthard
V0541	pCold_scFvdiL2K_CEA	Hannes Gotthard
BN1	pMA-VHHSlamF7 Fc hole (kiHs-s)	Boris Nowotny
BN2	pMA-VHHSlamF7 Fc knob (kiHs-s)	Boris Nowotny
H137	pCEP4-VHUCHT1-Fc knob (kiHs-s)	Hannes Gotthard
H139	pCEP4-VLUCHT1-Fc knob (kiHs-s)	Hannes Gotthard
H140	pCEP4-scFvCD24-Fc hole (kiHs-s)	Hannes Gotthard
H144	pCEP4-scFvCD133-Fc hole (kiHs-s)	Hannes Gotthard
H146	pCEP4-scFvCD166-Fc hole (kiHs-s)	Hannes Gotthard
H148	pCEP4-scFvCEA-Fc hole (kiHs-s)	Hannes Gotthard
H162	pCEP4-scFvUCHT1-Fc Knob (kiHs-s)	Hannes Gotthard
H163	pCEP4-scFvCD24	Hannes Gotthard
H164	pCEP4-scFvCD133	Hannes Gotthard
H165	pCEP4-scFvCD166	Hannes Gotthard
H166	pCEP4-VLUCHT1-scFvCD24	Hannes Gotthard
H167	pCEP4-VLUCHT1-scFvCD166	Hannes Gotthard
H168	pCEP4-VLUCHT1-scFvCEA	Hannes Gotthard
H169	pCEP4-VHUCHT1-scFvCD133	Hannes Gotthard

3.1.14. Software

ExPASy Protparam	[https://web.expasy.org/protparam/]
ExPASy Translate	[https://web.expasy.org/translate/]
FlowJo Version 8.8.7	[Treestar, Ashland, USA]
Graphpad PRISM 7	[GraphPad Software, La Jolla, USA]
Serial Cloner 2.6	
ApE (A plasmid Editor v2.0.53c)	[M. Wayne Davis, University of Utah, USA]
ImageLab	[Biorad Laboratories, CA, USA]
Unicorn V6.3	[GE Healthcare Life Sciences, Chicago, USA]
Snapgene	[GSL Biotech LLC, CA, USA]
Bio-Rad CFX Manager	Bio-Rad Laboratories, CA, USA]
BBrowser	[Bioturing, San Diego, USA]

3.2. Methods

3.2.1. Cloning

3.2.1.1. Polymerase chain reaction

DNA was amplified using the Q5 hot start DNA polymerase and a PCR mixture (Table 2).

Table 2: Composition of PCR mixture

Components	**Volume [µl]**
Q5 Reaction Buffer	10
Q5 Enhancer	10
Forward Primer (100 µM)	1
Reverse Primer (100 µM)	1
dNTPs (10 mM)	2
Q5 Polymerase	0,5
Template	1
ddH_2O	24,5

Depending on the length of the amplified PCR construct elongation time for the Q5 polymerase must be adjusted (1000 nt/min).

The PCRs were performed using the PCR program shown in

Table ***3***. PCR products were loaded on a 1% agarose gel to separate them from template DNA and primers.

Table 3: PCR program

PCR step	Temperature [°C]	Time [min]	No. of cycles
Initial denaturation	98	3	1x
Denaturation	98	0,5	30x
Annealing	55	0,5	
Elongation	72	Dependent on PCR product	
Final elongation	72	5	1x

3.2.1.2. Restriction digestion

Restriction digestion was performed in a total volume of 20 µl comprising of 17 µl of H2O containing 1 µg DNA or a complete extracted PCR product from an agarose gel, 2 µl 10x FD Buffer and 1 µl restriction enzyme. To digest vector DNA, 1 µl of fast alkaline phosphatase (Fast AP) was added. Digestion was conducted at 37°C for 45 min. The digested insert DNA was separated from vector DNA using agarose gel electrophoresis.

3.2.1.3. Agarose gel electrophoresis and DNA gel extraction

To analyze and purify PCR-amplified or digested DNA fragments, agarose gel electrophoresis was used. 1 % (w/v) agarose was dissolved in 1 x TAE buffer by boiling. DNA was mixed with 5x DNA loading buffer and loaded onto an agarose gel containing 0,2 µg/ml Nancy-520. After 40 min at 80 V running time, DNA was visualized using ultraviolet light. Relevant bands were cut and purified with a MiniElute Gel Extraction and PCR Purification kit according to the manufacturer's protocol.

3.2.1.4. Ligation

Ligation was conducted at room temperature. Pre-digested Vector DNA and insert DNA were mixed with T4 Ligase buffer and T4 ligase according to Table 4.

Table 4: Composition of ligation reaction

Components	Volume/ Amount
Vector DNA	50 ng
Insert DNA	Insert:Vector ratio 3:1 (depending on size of Vector and Insert DNA)
T4 ligase buffer	2 µl
T4 ligase	1 µl
ddH_2O	Ad to 20 µl

After 2h of incubation, 5 µl of the ligated DNA was transformed into bacteria.

3.2.1.5. Transformation of competent MACH1 bacteria

50 µl of MACH1 bacteria were thawed on ice and added on top of 5 µl of the ligation mixture. After 20 min incubation on ice, the bacteria were heat shocked at 42°C for 45s, following 5 min of incubation on ice. 500 µl of LB medium was added and the mixture was shaken at 37°C for 1h at 660 rpm. 250 µl of this mixture was plated in agar plates containing carbenicillin (100 µg/ml). In a last step, the plates were incubated at 37°C overnight.

3.2.1.6. Screening of clones

To check for positive transformants containing the ligated plasmid, a colony PCR was conducted. Individual clones were picked from the agar plates and mixed with 20 µl containing REDTaq® ReadyMix™ and appropriate primers according to the manufacturers protocol. Colony PCR was performed as described

Table ***3*** considering a Taq-polymerase replication fidelity of 500 nt/min. Denaturation temperature was adjusted to 95 °C, initial denaturation was performed for 10 min. Annealing and denaturation were prolonged to 1 min. Positive clones were identified by agarose gel electrophoresis.

3.2.1.7. Plasmid DNA isolation

Overnight cultures of transformed MACH1 bacteria were inoculated in 100-200 ml (MIDI-preparation) LB-medium containing carbenicilin (100 µg/ml). Plasmid DNA was purified using the NucleoBond® Xtra Midi kit according to the manufacturer's instructions. The DNA pellet was resuspended in 200 µl H_2O and stored at -20°C. DNA concentration was measured with the NanoDrop 2000.

Subsequent DNA sequencing was performed by LGC Genomics (Berlin, Germany). Nucleotide BLAST was used to analyze the sequenced DNA (Serial cloner).

3.2.1.8. Cloning of constructs used in thesis

All DNA constructs were cloned using the above-mentioned. For cloning PiggyBac Plasmids to express target antigens in CHO-K1 cells, plasmids T001-T004 were purchased from Harvard Plasmid Database. Using the primers #7-#20, ECDs of respective antigens were amplified via PCR and cloned into PB01 and PB02 backbone.

Sequences for 1st generation Hemibodies were synthesized by GeneArt (Regensburg, Germany) (plasmids C65-C68). For stable expression in CHO suspension cells, Hemibody sequences were transferred into CET1019AS vector system via cut and paste cloning using the restriction enzymes NgoMIV and BmtI.

For production of 1st gen Hemibodies in Shuffle T7 cells, constructs were cloned into pCold vector system containing either diL2K or UCHT1 as a CD3 binder using the primers #47-51 in backbones. To produce these Hemibodies in ExpiHEK suspension cells, constructs were cloned into pCEP4 vectors via cloning in pMA vector using the primers #139, #140 and #141 for PCR amplification of Hemibodies out of the vectors V0510, V0502, V0514 and V0517. PCR fragments were cloned into pMA vector following the cloning into pCEP4 vector system using the primers #96 and #85.

2nd generation Hemibodies were only produced in ExpiHEK suspension cells. PCR amplification of target scFvs from the vectors V0510, V0502, V0514 and V0517 was performed with the primers #86-#95. PCR fragments were cloned into the pMA-Vectors BN1 and BN2 and via another PCR with the primers #96-#98 cloned into the pCEP4 vector system. Similarly, blocking scFvs were cloned into the pCEP vector system using the primers #86, #90, #92, #94, #139, #96 and #85.

3.2.2. Cell culture

The used cell lines were cultivated at 37°C, 5% CO_2 and 95% humidity in different media (see 3.1.11). Before reaching full confluence, cells were passaged using trypsin for detachment. Cell count per ml was determined with the Countess II [Thermo Fisher, Waltham, USA].

3.2.3. Isolation of PBMCs and activated CD8+ T-cells

Whole blood samples were received from patients of the University Hospital in Würzburg. To isolate PBMCs, a density-gradient centrifugation using Ficoll-based lymphocyte separation was performed. Briefly, blood was mixed at a 1:1 ratio with PBS and the mixture was slowly pipetted onto a Pancoll/ Ficoll layer. After 25 mins of centrifugation with 3400 rpm w/o brakes, the interlayer consisting of PBMCs was transferred to another falcon and washed twice in PBS. For removing residual erythrocytes, cells were mixed with 15 ml of Red Blood Cell lysis buffer and incubated for 15 min at RT. After two wash steps with PBS, PBMCs were cultured in F12-K medium and directly used for experiments.

For further isolation of activated CD8+ T-cells, the CD8+ T Cell Isolation Kit [Miltenyi Biotec, Bergisch-Gladbach] was used according to manufacturer's protocol. After isolation, T-cells were expanded and activated using the T Cell Activation/Expansion Kit [Miltenyi Biotec, Bergisch-Gladbach] according to manufacturer's instructions.

3.2.4. Stable transfection of adherent CHO-K1 cells

To establish a system for testing the killing efficacy of produced Hemibodies, CHO-K1 cells were transfected with several target antigens using the PiggyBac® Transposon system. Lipofectamine 3000 was used according to manufacturer's instructions to transfect native CHO-K1 cells with two different PiggyBac-vectors, namely PB01 and PB02, together with a plasmid containing the PiggyBac® Transposase. After antibiotic selection with puromycin at a concentration of 5 µg/ml, cells were FACS-sorted for positivity of the second antigen which wasn't under antibiotic selection.

3.2.5. Lentiviral transduction of established human cancer cell lines

A firefly luciferase plasmid containing lentivirus was used to make cells luciferase positive. The lentivirus was a kind gift of AG Hudecek (Würzburg, Germany). Briefly, tumor cells were seeded at a density of $1x10^4$ c/well in 500 µl in 24 wells together with 5 µg/ml polybrene. Lentivirus was thawed at RT and added on top at a multiplicity of infection (MOI) of 5. After 5 passages for viral cleaning, cells were directly used for experiments.

3.2.6. Expression and purification of recombinant proteins

3.2.6.1. Expression of recombinant proteins in Shuffle T7 cells

In a first step glycerol stocks of the respective plasmids were made for producing recombinant proteins in Shuffle T7 cells. The pCold vector system was used in these bacteria. Shuffle T7 cells were transformed with 100 ng pCold vector combined with 100 ng of the 3C protease containing vector V3C as described in 3.2.1.5 and cultured in 2xYT + 0,2% Glucose + 37,5 µg/ml Kanamycin + 37,5 µg/ml Carbenicilin. O/n cultures were frozen at -80°C as glycerol stocks in a 1:2 dilution of culture with glycerol stock buffer when reaching a OD of 0,5 - 0,7. Glycerol stocks were used to inoculate a o/n culture, which was used the next day to inoculate the working culture at an OD of 0,1. After reaching an OD of 1 – 1,5 while shaking at 125 rpm and 37°C, the incubator was set to 10°C for two hours. To start the overexpression of the recombinant protein, temperature was set to 14°C and IPTG was added to a final concentration of 0,1 mM. 18-20h later, cells were harvested by centrifugation for 30 min at 4200 rpm and 4°C. Cell pellets were resuspended in Co-IMAC loading buffer and disrupted by French Press. After two rounds of centrifugation at 15000 g and 4°C, supernatants were sterile filtrated and proteins were further purified as described in 3.2.6.4.

3.2.6.2. Transient expression of recombinant proteins in ExpiHEK cells

ExpiHEK293 cells were cultured in Freestyle293-medium. Once they reached a density of $1,5*10^6$ – $2*10^6$ c/ml, transfection was performed. For 100 ml of HEK culture, 100 µg DNA was mixed with 5 ml Freestyle293-medium and 300 µl of Polyethylenimine (PEI) (1mg/ml) was mixed with 5 ml of Freestyle293-medium. Both solutions then were mixed and incubated for 15 min at room temperature. After transferring the DNA-PEI mixture to the cell suspension for 24h at 37°C, tryptone N1 (TN1) was added to a final concentration of 0.5%. 96 hours later, the cell suspension was collected and centrifuged (300 g, 10 min, 4°C; 4000 g, 20 min, 4°C). The supernatant was sterile filtrated and proteins were further purified as described in 3.2.6.4.

For the production of 2nd generation Hemibodies, two heavy chain plasmids had to be transfected. Therefore, following transfection ratios were used:

- VHUCHT1-scFvCD133-KiH: 1:1 (H137:H144)
- VLUCHT1-scFvCD24-KiH: 1:1,5 (H139:H140)
- VLUCHT1-scFvCD166-KiH: 1:1,5 (H139:H146)
- VLUCHT1-scFvCEA-KiH: 1:1,5 (H139:H148)
-

3.2.6.3. Stable expression of recombinant proteins in CHO suspension cells

CHO cells were cultured in ActiSM medium at 37°C, 8% CO_2, 80% humidity, 120 rpm. With I-SCEI digested CET1019AS vectors, $2*10^6$ CHO suspension cells were electroporated with the Neon™ Transfection System 100 µL Kit according to manufacturer's instructions (1620 V/ 10 ms/ 3 pulses). 48 hours after electroporating, a puromycin containing CET1019AS vector, a hygromycin containing vector coding for the same recombinant protein was electroporated to the already transfected cells following the protocol above. For stable integration of the plasmids, CHO cells were further cultured in ActiSM selection medium containing 1,5 µg/ml Puromycin and 0,25 mg/ml Hygromycin for at least 14 days.

After stable integration of the plasmid, overexpression was performed by inoculating $0,3*10^6$ c/ml CHO cells in ActiSM expansion medium. Four days after seeding, cells were fed daily with 2% Feed A and 0,2% Feed B and cell viability was monitored daily. When viability dropped below 60%, cells were harvested (centrifugation 1h, 7000 g, 4°C) and sterile filtered. Further purification of the recombinant proteins is described in 3.2.6.5.

3.2.6.4. Purification by immobilized metal affinity chromatography (IMAC)

Proteins containing a His_6-tag were purified by Co-NTA-IMAC. Cell culture supernatant was incubated with Co-NTA-agarose beads at 4°C for at least three hours followed by loading the beads to a column and washing them with Co-IMAC loading buffer (20 CV). The presence of protein was determined by a Bradford test. When no undesired protein was detectable, the bound proteins were eluted with Co-IMAC elution buffer in 0.5 ml fractions. These fractions were pooled and analyzed via running a SDS-PAGE. When purifying bacterial supernatants an additional wash step with 50 column volumes (CV) Co-IMAC wash buffer was included for endotoxin removal.

3.2.6.5. Purification using Strep-Tactin®XT

Recombinant proteins produced in CHO suspension cells were purified using a Strep-Tactin®XT resin. Purification was done according to manurfacturer's protocol.

3.2.6.6. Fast protein liquid chromatography

Protein production containing multimers of the desired protein or contaminations were further purified by FPLC. A Superdex increase 10/300 200 pg column was used. Prior to usage, the column was washed with two column volumes of ddH_2O and equilibrated with two column volumes of sodium phosphate buffer (50mM sodium phosphate, 300mM NaCl, pH 7,5). Chromatography was performed at a flow rate of 0,4 ml/min at a pressure of 1.5 mPA. Protein fractions were collected at a volume of 400 µl and the desired fractions were pooled.

3.2.7. Protein characterization

3.2.7.1. Determination of protein concentration

To measure the concentration of protein productions, the NanoDrop ND 2000 was used, allowing to measure protein concentrations at 280 nm in a small volume. Extinction coefficient and molecular mass of a protein were determined using the online tool ProtParam (Expasy). Alternatively, a SDS-PAGE was loaded with a fixed amount of recombinant protein together with a protein standard of BSA ranging concentrations from 2000

ng/µl – 31,25 ng/µl. Using ImageLab software, protein concentration could be determined comparing gel bands with the standard curve.

3.2.7.2. SDS polyacrylamide gel electrophoresis (SDS-PAGE)

SDS-PAGE was performed to assess the purity and molecular mass of a protein. Depending on the expected molecular mass, gels with different acrylamide concentrations were prepared (Table 5). Protein samples were mixed with reducing or non-reducing 4x Laemmli-buffer, boiled at 95°C for 5 min and loaded onto a gel. After 20 min running time at 90V and another 60 min at 140V, the gel was washed 3 times with ddH_2O and stained with Coomassie for 30 min. In a last step, the gel was destained in destaining solution.

Table 5: Composition of polyacrylamid gels

Components	12% resolving gel	15% resolving gel	4% stacking gel
H_2O	2,8 ml	1,9 ml	2,3 ml
30% acrylamide mix	3,2 ml	4 ml	520 µl
1,5 M Tris (pH 8,8)	2 ml	2 ml	-
1,0 M Tris (pH 6,8)	-	-	400 µl
10% APS	80 µl	80 µl	32 µl
TEMED	3,2 µl	3,2 µl	3,2 µl

3.2.8. Functional characterization

3.2.8.1. Flow cytometric binding studies

To determine the binding of an antibody to different cancer cells, flow cytometry was used. Detached cells were diluted to concentration of $1{,}5*10^6$ cells/ml and 100 µl were transferred in each well of a 96-well V-bottom plate. After centrifugation (400 g, 5 min, 4 °C), supernatant was discarded and antibodies were serially diluted in FACS buffer, added to the cells and incubated for 1 h at 4 °C. Following 3 washing steps with FACS buffer, bound antibodies were detected with an AF488-conjugated anti-human IgG antibody which was incubated for 1h at 4°C. Again, three washing steps with FACS-buffer were performed. Emitted fluorescence was detected in a MACSQuant® 10. The relative MFI was calculated according to the following formula:

$$rel.MFI = \frac{probe - (detection\ system - cells)}{cells}$$

3.2.8.2. Flow cytometric characterization of cell lines

To find suitable cell lines for biological assays, established cancer cell lines and transfected CHO-K1 cell lines needed to be characterized for their expression of target antigens via FACS. Therefore, cells were adjusted to a concentration of $1*10^7$ c/ml in 100 µl FACS Buffer containing a directly labeled antibody against respective antigens. Used antibody dilutions are stated in 313.1.6. After 1h incubation at 4°C in the dark, cells were washed three times with FACS buffer and analyzed with either the MACSQuant® 10 or the BD facscalibur.

3.2.8.3. Single cell RNA-sequencing data analysis

For finding suitable target combinations for Hemibody based therapy of colorectal cancer stem cells, a publicly available single cell RNA-seq dataset from the single cell expression atlas with a total of 60000 analyzed cells was used (https://www.ebi.ac.uk/gxa/sc/experiments/E-MTAB-8410/results/tsne?geneId=ENSG00000001626&k=18&clusterId=%5B13%5D; Stand 17.09.21). “Raw scRNA-seq data of the SMC population are available in the European Genome-phenome Archive database (EGAS00001003779, EGAS00001003769). Processed scRNA-seq and metadata for the SMC populationss are available in the NCBI Gene Expression Omnibus (GEO) database under the accession codes GSE132465, GSE132257 and GSE144735. Clusters and gene expression data of the SMC compartment can be found on the User-friendly InteRface tool to Explore Cell Atlas (URECA) website (http://ureca-singlecell.kr). The raw gene expression matrix from the CellRanger pipeline was filtered, normalized using the Seurat R package, and selected according to the following criteria: cells with > 1,000 UMI counts, > 200 genes, and < 6,000 genes, and < 20% of mitochondrial gene expression in UMI counts. These are pre-determined cell filtration criteria excluding apoptotic cells and doublets. Next, we combined the Seurat and RCA pipelines for initial clustering and cell type identification, removing discordant cells from the downstream analysis. Before sub-clustering, cells with a number of genes exceeding the outliers were removed to eliminate doublets again” (Lee et al. 2020). Analysis and all plots were performed with BBrowser (Bioturing, San Diego, USA). For differential expression analysis and enrichment analysis a threshold of $p \leq 0,05$ was used. Data was clustered and statistically analyzed according to Lee et al. (Lee et al. 2020).

3.2.9. Biological characterization

3.2.9.1. Luciferase-based killing assay

A luciferase based killing assay was applied to test the killing efficacy of Hemibodies on eukaryotic cell lines. Firefly Luciferase expressing cells were grown in 96-well white plates ($1*10^4$ cells per well) overnight in 50 µl of complete growth medium. After 24h, $5*10^4$ activated CD8+ T-cells were added to each well in 50 µl complete growth medium together with different Hemibody combinations in concentrations ranging from 100 – 0,03 nM in 20 µl complete growth medium. The next day, D-Luciferin was pipetted to a final concentration of 3,5 mM and incubated for 30 mins at 37°C and 5% CO_2. Relative light units (RLU) were measured using the TECAN Spark and values were normalized to the control cells with T-cells without Hemibodies. Because only living cells are able to convert D-Luciferin, RLUs are proportional to the number of living cells in each well. Killing efficacy was calculated in % killing compared to control without Hemibodies according to the following formula:

$$Killing\ [\%] = 100 - \frac{treatment_{RLU}}{cells\ with\ Tcells_{RLU}} * 100$$

3.2.9.2. Luciferase-based killing assay with receptor blocking

Because different cell lines express varying amounts of target antigens, an assay was established to test killing efficacy and off target effects on the same double antigen positive cell line. For producing a single positive cell line out of the double positive, target cells were incubated with a blocking scFv (combination CD133xCD166: blocking with 1 µM scFv-aCD133 and 4 µM scFv-aCD166; combination CD133xCD24: blocking with 1 µM scFv-aCD133 and 2 µM scFv-aCD24) targeting one antigen for 2h at 37°C and 5% CO_2. Otherwise, the killing assay was conducted as described in 3.2.9.1

3.2.9.3. Luciferase-based Caspase assay

The luciferase-based Caspase assay was performed according to 3.2.9.1. Instead of assessing killing by addition of D-Luciferin, Caspase 3/7 activity was measured using the Caspase-Glo® 3/7 Assay Systems from Promega according to manufacturer's protocol.

3.2.9.4. FACS-based killing assay with mixed populations

Since the main advantage of Hemibodies is its highly specific targeting of double positive cells, an assay was developed coculturing three cell lines expressing either both target antigens or only one respective antigen. The three cell lines were grown in a total of 500 µl in complete medium with 60.000 cells for each cell line in a 24-well plate. The double

positive cell line was GFP+, one single positive cell line was stained with CellTrace violet according to manufacturer's protocol and the remaining cell line remained native for distinction of the three cell lines by FACS. 24h later, activated CD8+ T-cells were added in a 5:1 (E:T) ratio in 500 µl, similar to the luciferase based killing-assay. After addition of different Hemibody combinations at a fixed concentration, cells were incubated overnight at 37°C and 5% CO_2. On the next day, cells were detached using TrypLE, washed with FACS-buffer and 7-AAD was added in a 1/1000 dilution. Cells were incubated for 20 min in the dark at 4°C and then analyzed using the MACSQuant 10. 7-AAD served as a marker for dead cells.

3.2.9.5. Colonosphere assay

The colorectal cancer cell line HCT116 was used in a colonosphere assay. $1*10^7$ cells were stained with a commercial FACS antibody against CD133 coupled to APC and a FACS antibody against CD166 coupled to PE. Antibodies were used in dilutions indicated in 3.1.6. After 1h incubation at 4°C in the dark, cells were passed through a cell strainer (70 µm) and sorted in the following 4 populations using the FACS Aria III cell sorter:

- CD133+ CD166+
- CD133+ CD166-
- CD133- CD166+
- CD133- CD166-

Each population was seeded in triplicates with $3*10^3$ cells per well of a 24-well ultra-low adherence plate in tumorsphere medium. Cells were incubated at 37°C and 5% CO_2 and medium was renewed every three days. Only cells inheriting stem cell characteristics are described to survive under these conditions. With this approach, CD133 and CD166 should be validated as CSC targets. After 10 days in culture photos of each well were taken using the Motic AE31E microscope. Amount and size of colonospheres were analyzed using ImageJ.

4. Results

4.1. Single cell RNA-seq analysis of colorectal cancer and adjacent normal tissue

The expression of the selected target antigens CD133, CD24, CD166 and CEA in a single cell RNA-seq dataset totaling ca. 60.000 single cells was analyzed. Beforementioned target antigens were utilized to identify a subset of cells further termed as cancer stem cells. Its specific expression on cancerous tissue to avoid off target toxicity was checked and via differential expression analysis and enrichment analysis this subset was characterized for CSC specific traits like the expression of CSC specific genes, pathways or transcription factors.

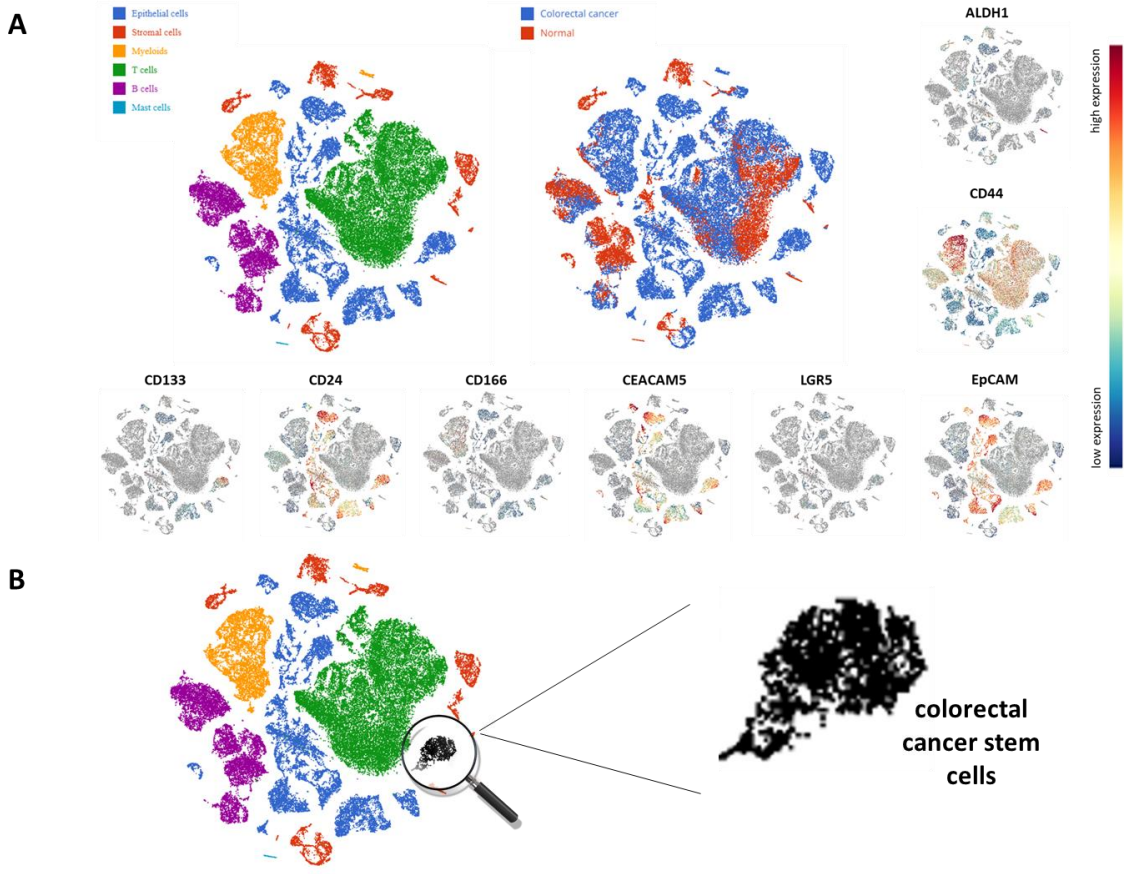

Figure 7: Expression of target antigens in a dataset of colorectal cancer cells and its adjacent normal tissue: (A) Using BBrowser the single cell RNA-seq dataset was analyzed for expression of several CSC related antigens depicted in t-SNE plots. High expression is visualized in red, whereas low expression is depicted in blue. Via specific marker genes cell subtypes were identified and the discrimination of cancerous tissue against normal tissue was made. (B) On the basis of antigen expression, a subset of cells coexpressing above-mentioned antigens was identified.

As seen in Figure 7 using BBrowser several cell subtypes, namely epithelial cells, stromal cells, myeloid cells, T-cells, B-cells and mast-cells could be identified. Furthermore, a discrimination of cancerous tissue against normal adjacent tissue was made (Le et al. 2020). Comparing these data with the expression of the markers CD133, CD24 and CD166, especially their co-expression, clearly shows an expression profile only on cancerous tissue without localization on healthy adjacent tissue. Co-expression analysis of CD133, CD24, CD166 and other CSC-related antigens including LGR5, EpCAM, CD44 and ALDH1 revealed a subset of cancer cells, which was consequently identified as the CSC subpopulation (Figure 7B). Based on this finding the subpopulation from Figure 7B should be further characterized by identifying genes which are overexpressed in CSCs compared to the remaining cell subtypes, which confer these cells typical CSC characteristics including self-renewal, resistance to conventional therapy and its ability to form new tumors (Figure 8).

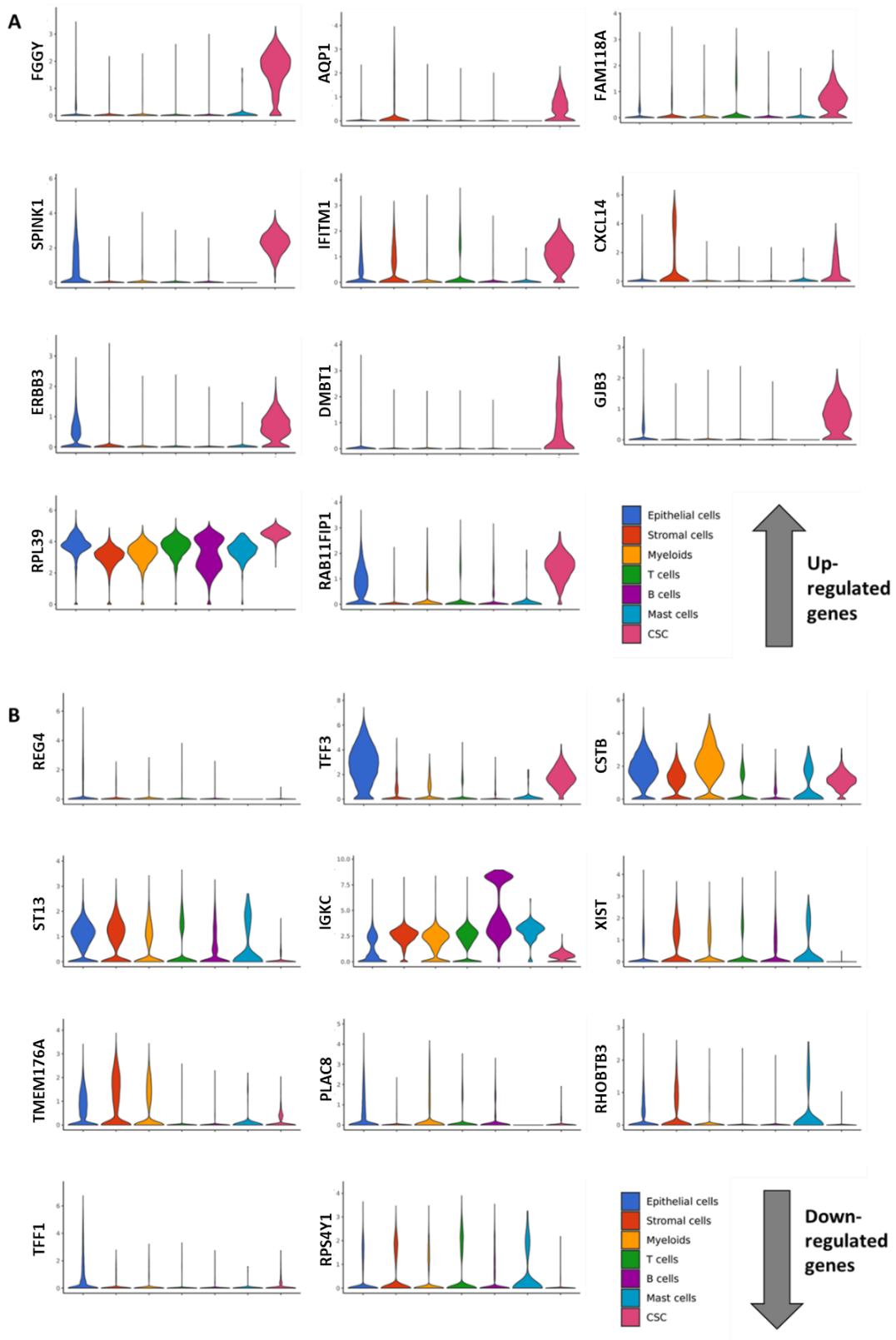

Figure 8: Differential expression analysis of single cell RNA-seq Dataset: Using BBrowser a differential expression analysis was performed between CSCs and epithelial cancerous tissue. A selection of up- and downregulated genes was visualized in violin plots showing the expression between cell subtypes. (A) genes upregulated in CSCs. (B) genes downregulated in CSCs.

Figure 8 exemplifies genes which are up- or downregulated in the putative CSC population compared to epithelial cancerous cells visualized as violin plots. The top 11 hits of up and downregulated genes interfering with stemness related traits with a $-\log_{10}$(FDR) value in the range of 10 – 322 (≡ q-value/FDR value of ca. $1*10^{-10}$ – $2{,}5*10^{-322}$) and a $\log_2$(foldchange) of 1,5 – 3,2 (foldchange of x ~ 3-10) were selected for further analysis.

Upregulated genes were FGGY, SPINK1, ErbB3, RPL39, AQP1, IFTM1, RAB11FIPI, FAM118A, DMTB1, CXCL14 and GJB3. The genes ST13, TMEM176A, TFF1, TFF3, IGKC, PLAC8, RPS4YI, CSTB, RHOBTB3, REG4 and XIST were downregulated compared to the epithelial cancerous cell population.

In summary, it can be said that genes were found conferring cancer stemness traits and genes contradicting these traits. Overall, there was a clear tendency towards supporting cancer stemness. The exact function and role of each gene is further examined in 5.1.

Similarly, to the differential expression analysis an enrichment analysis was performed to identify pathways, which are upregulated in the CSC compartment compared to the epithelial cancer tissue.

Table 6: Top 20 hits of enrichment analysis with a p- value below 0,05

ID	Name and function	ES	p-value
R-HSA-9032759	NTRK2 activates RAC1	0,99559	0,01161
R-HSA-9664535	LTC4-CYSLTR mediated IL4 production	0,99376	0,01354
R-HSA-1483115	Hydrolysis of LPC	0,98202	0,04449
R-HSA-426117	Cation-coupled Chloride cotransporters	0,96258	0,02372
R-HSA-2562578	TRIF-mediated programmed cell death	0,88778	0,03647
R-HSA-9013957	TLR3-mediated TICAM1-dependent programmed cell death	0,88778	0,03647
R-HSA-389948	PD-1 signaling	0,83467	0,03992
R-HSA-445095	Interaction between L1 and Ankyrins	0,83456	0,03992
R-HSA-111459	Activation of caspases through apoptosome-mediated cleavage	0,83214	0,03992
R-HSA-111469	SMAC, XIAP-regulated apoptotic response	0,83214	0,03992
R-HSA-975110	TRAF6 mediated IRF7 activation in TLR7/8 or 9 signaling	0,8254	0,01341
R-HSA-174403	Glutathione synthesis and recycling	0,78331	0,03403
R-HSA-5676594	TNF receptor superfamily (TNFSF) members mediating non-canonical NF-kB pathway	0,77129	0,04537
R-HSA-9014325	TICAM1,TRAF6-dependent induction of TAK1 complex	0,75317	0,0364
R-HSA-209543	p75NTR recruits signalling complexes	0,74953	0,03429
R-HSA-9008059	Interleukin-37 signaling	0,74788	0,00186
R-HSA-190861	Gap junction assembly	0,73368	0,03232
R-HSA-9013973	TICAM1-dependent activation of IRF3/IRF7	0,73181	0,03232
R-HSA-936964	Activation of IRF3/IRF7 mediated by TBK1/IKK epsilon	0,72308	0,03371
R-HSA-168927	TICAM1, RIP1-mediated IKK complex recruitment	0,71455	0,00931

In Table 6 the top 20 hits of the enrichment analysis using BBrowser with a p-value below 0,05 is visualized. Upregulated pathways of the reactome pathway database (Jassal et al. 2020) were further analyzed for biological function. 14 out of the 20 pathways could be linked to cancer stem cell promoting pathways (highlighted in green in Table 6), whereas only one pathway indicates contradictory findings (highlighted in red in Table 6).

In summary, there is a clear tendency of overexpressed genes as well as pathways indicated in CSC homeostasis, metabolism and generation underlining the right choice of antigens for identifying and targeting colorectal cancer stem cells.

4.2. Establishment of CHO-based system for testing Hemibodies in vitro

After finding suitable antigens for targeting colorectal cancer stem cells via single cell RNA-seq analysis, a suitable system for testing Hemibodies' killing efficacy and specificity. Therefore, CHO-K1 cells were transfected with the respective antigens using the PiggyBac Transposon System.

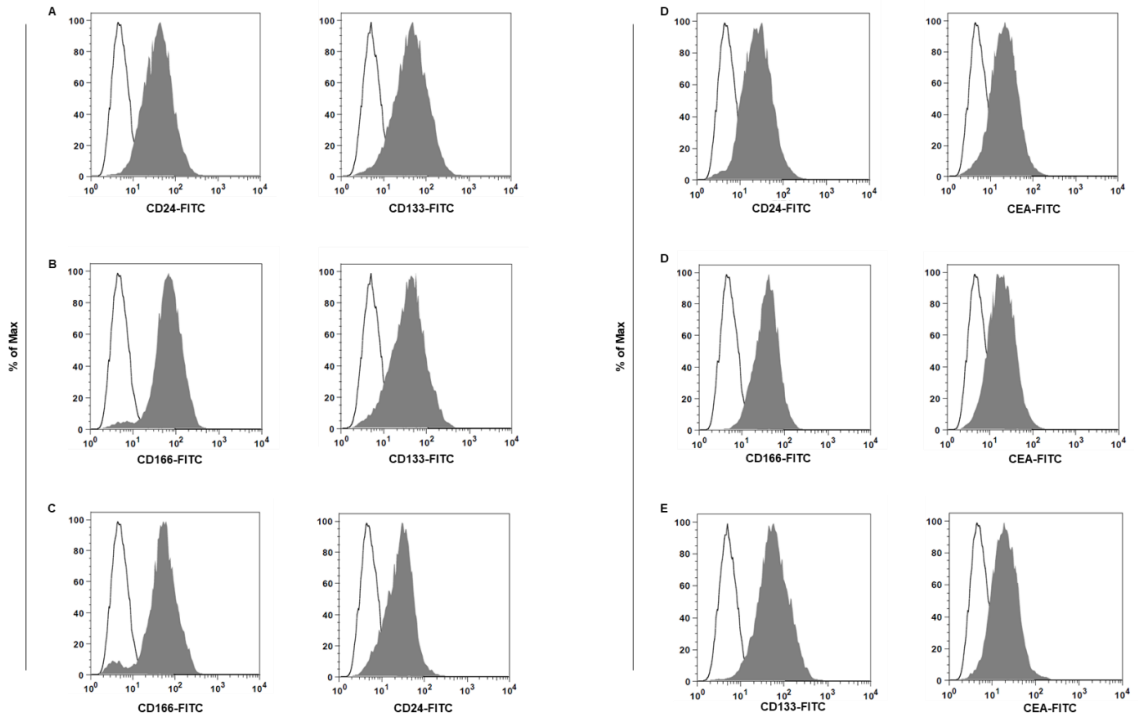

Figure 9: transfected CHO cells after sorting: adherent CHO-K1 cells were transfected with the indicated antigens. In total six cell lines were constructed, expressing different antigen combinations. After FACS-sorting for antigen expressing cells, cells were further analyzed for antigen positivity after sorting via FACS. (A-E) Histograms showing the expression of target antigens (grey) vs untransfected CHO cells (white).

In total six cell lines were generated expressing several target antigens for the combinations CD133xCD24, CD133xCD166 and CD133xCEA (Figure 9). In addition to the antigens, a gene for firefly luciferase (Fluc) was cotransfected as a readout of killing. All cell

lines were highly positive for the expression of its respective antigens (Figure 9). Furthermore, luciferase activity was measured leading to RLUs around 100000 (Data not shown). For testing the different Hemibody combination, the following cell lines were used:

CD133xCD24:	Cell line A (further termed as $CHO^{CD24+CD133+}$, double antigen positive) Cell line C (further termed as CHO^{CD24+}, single antigen positive) Cell line B (further termed as CHO^{CD133+}, single antigen positive)
CD133xCD166:	Cell line B (further termed as $CHO^{CD133+CD166+}$, double antigen positive) Cell line C (further termed as CHO^{CD166+}, single antigen positive) Cell line A (further termed as CHO^{CD133+}, single antigen positive)
CD133xCEA:	Cell line E (further termed as $CHO^{CEA+CD133+}$, double antigen positive) Cell line D (further termed as CHO^{CEA+}, single antigen positive) Cell line B (further termed as CHO^{CD133+}, single antigen positive)

4.3. FACS characterization of established cancer cell lines

After transfecting CHO cells as a test system, Hemibodies' efficacy and specificity should be determined using established cancer cell lines. Therefore, several cell lines were analyzed for antigen positivity using FACS.

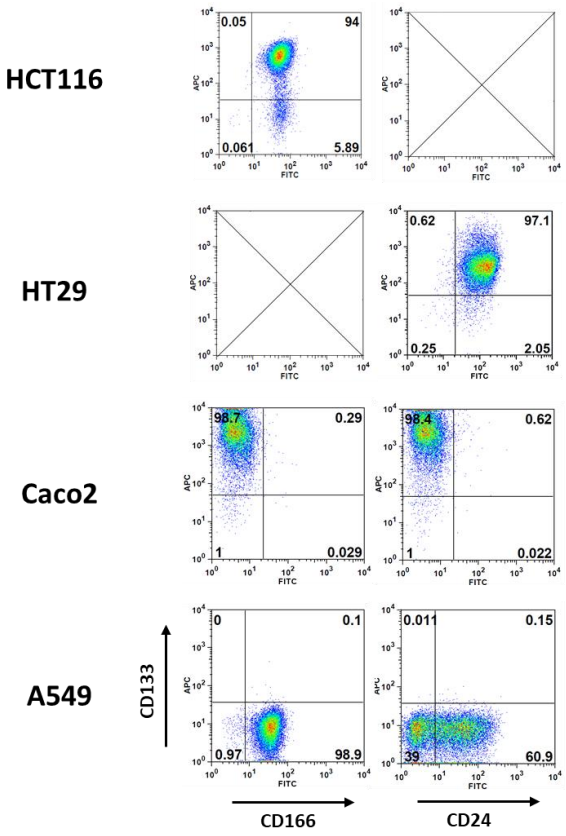

Figure 10: Cancer stem cell marker expression in human established colorectal cancer (CRC) cell lines: CRC cell lines were double-stained with FITC-labeled anti-CD166 or anti-CD24 antibody and an APC labeled anti-CD133. Representative dot pots are shown.

Figure 10 shows the results of the FACS analysis of the expression of analyzed CSC markers depicted as dot plots. On the y-axis, CD133 expression and on the X-axis either CD166 or CD24 expression is visualized. HCT116 cells were nearly 100% double positive for the CSC markers CD133 and CD166, HT29 cells were nearly 100% positive for the CSC markers CD133 and CD24, whereas the cell lines Caco2 and A549 were only single positive for CD133 and CD24 respectively (Figure 10). As a CD133 detection antibody, an antibody binding the glycosylation dependent epitope AC133 was used. All tested cell lines were colorectal cancer cell lines except for A549, originating from a lung cancer patient.

To test killing efficacy and specificity analogously as in CHO cells, the cancer cell lines were furthermore transduced using a lentivirus harboring a plasmid expressing Fluc and GFP. Luciferase activity was measured after transduction leading to RLUs around 1000000 (Data not shown).

4.4. Hemibody production

4.4.1. Stable expression of 1st Gen Hemibodies (diL2K based) in CHO suspension cells

Hemibodies and respective control BiTEs were produced in CHO suspension cells and purified by Strep-Tactin®XT chromatography. Protein size and purity were confirmed by SDS-PAGE (Figure 11).

Under reducing conditions, calculated masses of Hemibodies ranged from 40-43 kDa and 50-55 kDa for BiTEs. Looking at Figure 11 for all purifications, two bands at the height of 30 and 35 kDa are visible. Mass spectrometry analysis revealed that these bands arise from N-terminally degraded Hemibody fractions (Figure S 1). At the expected heights, only VL-Hemibody fragments and control BiTEs are visible. VH-Hemibodies yielded no band at the expected height (Figure 11).

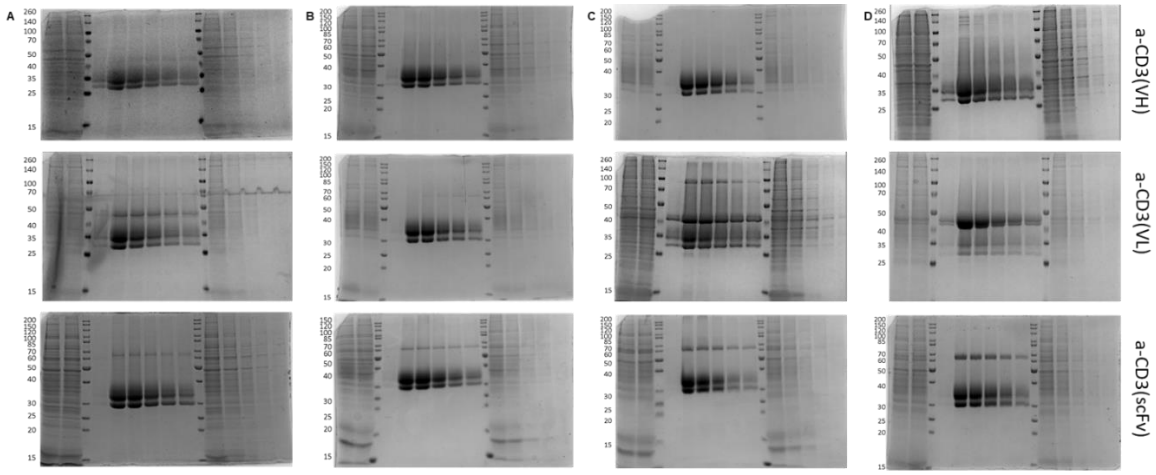

Figure 11: Overview of Hemibody Productions out of 200 ml CHO suspension cell culture: Polyacrylamidgels were loaded according to following scheme: supernatant (SN)|flowthrough (FT)|Marker|elution (E)1-E6|Marker|W1-5. (A)Anti-CD24 constructs, (B) anti-CD133 constructs, (C) anti-CD166 constructs, (D) anti-CEA constructs

Since no VH-Hemibodies could be produced, no Hemibody combinations could be used for further testing. Consequently, no further purification steps, including FPLC, were performed.

The addition of a commercially available protease inhibitor cocktail, as well as the addition of FBS as a protease inhibitor, did not recover degraded protein (Figure S 2).

4.4.2. Expression of 1st Gen Hemibodies (diL2K based) in Shuffle T7 cells

Because no VH-fragments could be produced in CHO suspension cells, production in a different host system was tested. Shuffle T7 cells express different proteases as CHO cells, giving the perspective of receiving VH-fragments in this system. After production in the above-mentioned E.Coli strain, cells were disrupted and the supernatants were purified by IMAC. Protein yield, purity and protein size were confirmed by SDS-PAGE (Figure 12).

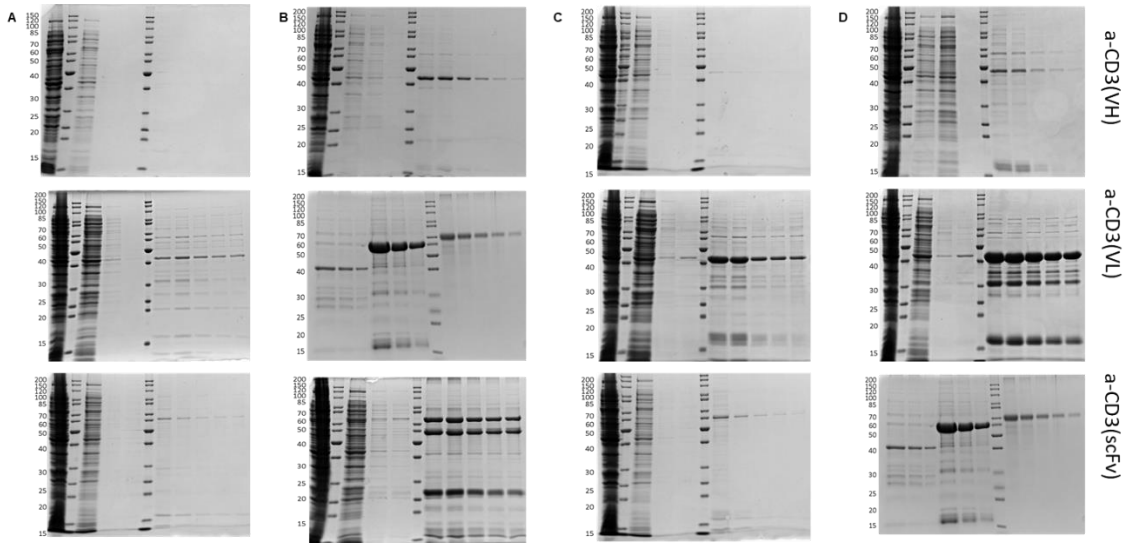

Figure 12: Overview of Hemibody Productions in Shuffle T7 suspension cell culture: Polyacrylamidgels were loaded according to following scheme: lysate SN|Marker|W1-3|Marker|E1-5|. Polyacrylamidgel B2 and D3 show following scheme: VLCD3-scFvCD133 20 µl |10 µl | 5 µl | scFvCD3-scFvCEA 20 µl | 10 µl| 5 µl | Marker | BSA-Standard (2000 – 125 ng; 1:2 dilutions). (A) Anti-CD24 constructs, (B) anti-CD133 constructs, (C) anti-CD166 constructs, (D) anti-CEA constructs

Calculated masses of Hemibodies equaled the masses from 4.4.1. As seen in Figure 12 production of VHdiL2K-scFvCD24 and VHdiL2K-scFvCD166 yielded no recombinant protein at the expected height at all (Figure 12A/C top graphs). VHdiL2K-scFvCD133 and VHdiL2K-scFvCEA could be produced in low quantities (Figure 12B/D top graphs). Remaining constructs were produced in sufficient amounts for in vitro testing. Unfortunately, productions in Shuffle T7 cells resulted in low purity of the construct, visualized in several unspecific bands seen in the SDS-PAGEs. Because of low purity and yield of the recombinant proteins, no further purification steps like FPLC were performed and proteins were directly used for downstream applications including luciferase-based killing assays.

4.4.3. Expression of 1st Gen Hemibodies (UCHT1 based) in Shuffle T7 cells

The solubility, stability and yield of heavy chain variable domains is highly influenced by framework core residues (Honegger et al. 2009). Honegger et al. identified the human VH3 domain as the framework having the best biophysical properties among human subtypes (Honegger et al. 2009). Consequently, to greatly improve Hemibody producibility, the CD3 binding domain was switched from diL2K having a VH1 framework to UCHT1 having the stable VH3 framework. These Hemibodies and respective control BiTEs were produced in Shuffle T7 cells and purified by IMAC. Again, Protein yield, purity and protein size were confirmed by SDS-PAGE (Figure 13).

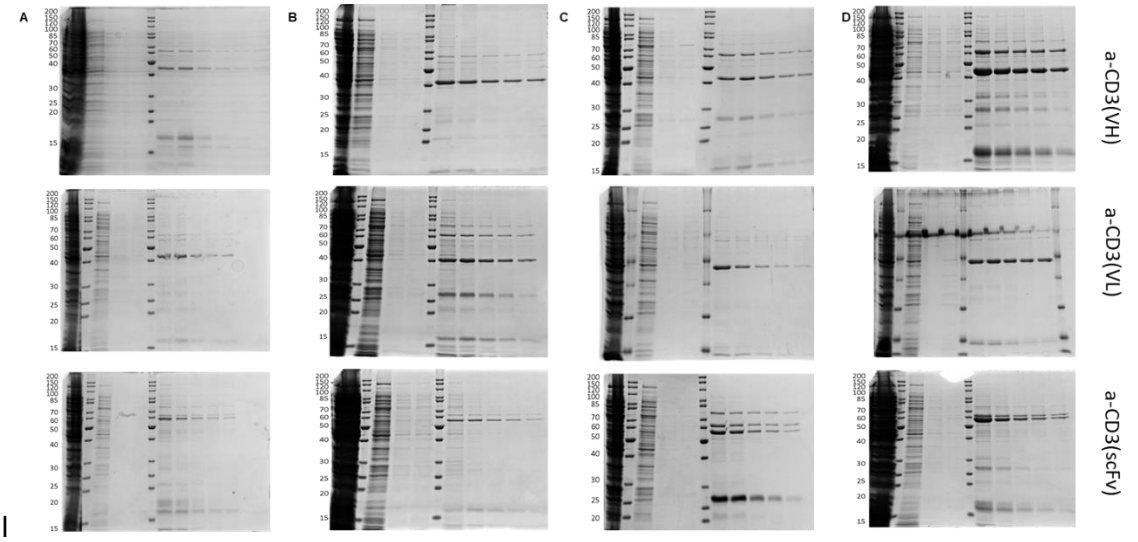

Figure 13: Overview of Hemibody Productions in Shuffle T7 suspension cell culture: Polyacrylamid-gels were loaded according to following scheme: lysate SN|Marker|W1-3|Marker|E1-5|. Polyacrylamidgel A1 and B1 show following scheme: lysate SN | W1-3|Marker|E1-5|. (A) Anti-CD24 constructs, (B) anti-CD133 constructs, (C) anti-CD166 constructs, (D) anti-CEA constructs

Arrangement of the graphs and calculated masses again approximately match results stated in 4.4.2. As seen in Figure 13, the constructs VHUCHT1-scFvCD24 and VHUCHT1-scFvCD166 could be produced using the UCHT1 framework in contrast to the corresponding diL2K constructs. Remaining construct could also be produced in sufficient amounts for in vitro experiments. Despite an enhanced producibility of UCHT1 constructs compared to diL2K constructs, productions only reached yields from 10 µg/L – 50 µg/L as determined by a BSA-standard curve. Purity was also low as seen by unspecific bands.

Constructs were further concentrated using Amicon Ultra centrifugal filters and directly used for downstream in vitro assays.

4.4.4. Expression of 1st Gen Hemibodies (UCHT1 based) in ExpiHEK293 suspension cells

To further improve yield and purity, expression host was again switched to a different host, namely ExpiHEK293 cells. 1st generation Hemibodies were transiently transfected to ExpiHEK suspension cells and supernatants were purified by IMAC. Protein yield, purity and protein size were confirmed by SDS-PAGE and FPLC (

Figure ***14***; Figure 15).

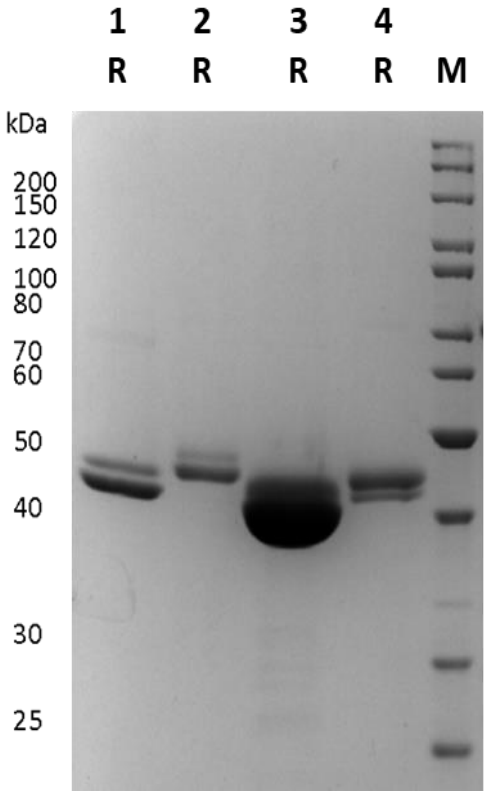

Figure 14: Protein integrity and purity analysis of 1st generation Hemibodies: SDS-PAGE analysis under reduced conditions (R). M, protein standard marker. Lane 1: VH-UCHT1_scFvCD133; Lane 2: VL-UCHT1_scFvCD24; Lane 3: VL-UCHT1_scFvCD166; Lane 4: VL-UCHT1_scFvCEA

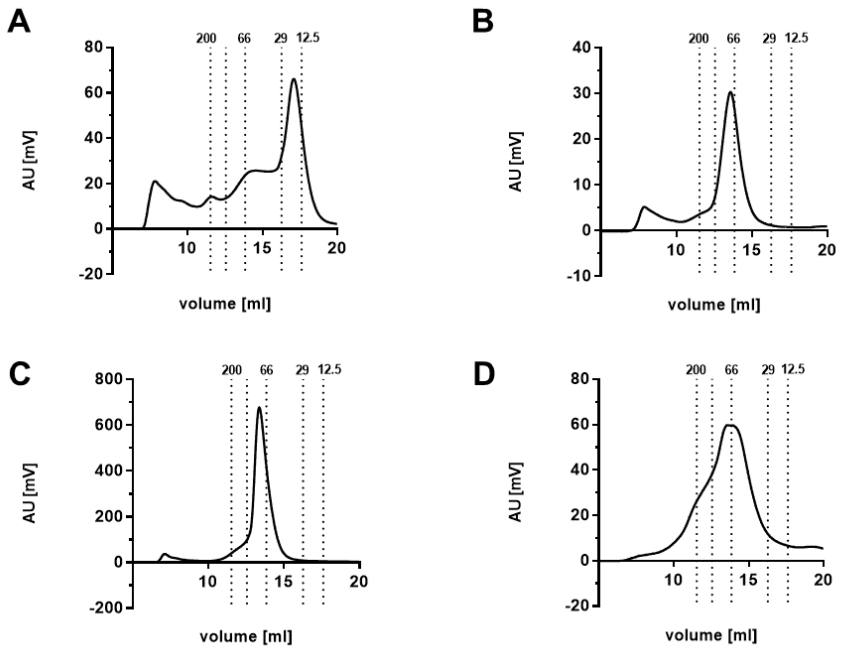

Figure 15: Protein integrity and purity analysis of 1st generation Hemibodies: FPLC-SEC analysis on Superdex 10-300 200 pg of (A) VH-UCHT1_scFvCD133, (B) VL-UCHT1_scFvCD24, (C) VL-UCHT1_scFvCD166 and (D) VL-UCHT1_scFvCEA

Lane 1-4 show 1st generation Hemibodies under reducing conditions. Only one double band at the expected heights is visible indicating a high purity. The double band arises due to glycosylation of the construct at the glycolinker introduced into the linker of the target scFv for better production yield. PNGase F digestion confirmed this assumption showing only one protein band after digestion (Figure S 3). FPLC analysis revealed monomeric peaks and only little aggregation at higher molecular weights (Figure 15). For the VL-fragments, the calculated size is a slightly bigger than the expected sizes. The VH-fragment showed higher levels of aggregation indicated by many peaks eluting before the monomeric peak. The monomeric peaks elute later than expected at a molecular mass of ca. 20 kDa. Looking at production yields, the change of the expression host to ExpiHEK293 cells resulted in an 10x increase in comparison to 1st generation Hemibodies produced in Shuffle T7 cells.

4.4.5. Expression of 2nd Gen Hemibodies (UCHT1 based) in ExpiHEK293 cells

A final attempt to improve the above-mentioned functional properties of Hemibodies was done by antibody engineering techniques. Out of the 1st generation Hemibody constructs, a second generation was developed introducing human constant IgG domains, namely the Fc-portion of a human IgG1 antibody via the knob into hole technology (KiH) to greatly enhance solubility and stability of the constructs and thereby their producibility and yield (Figure 6A). These so-called 2nd generation Hemibodies were again produced transiently in ExpiHEK293 suspension cells. Protein yield, purity and protein size were confirmed by SDS-PAGE and FPLC (Figure 16/ Figure 17).

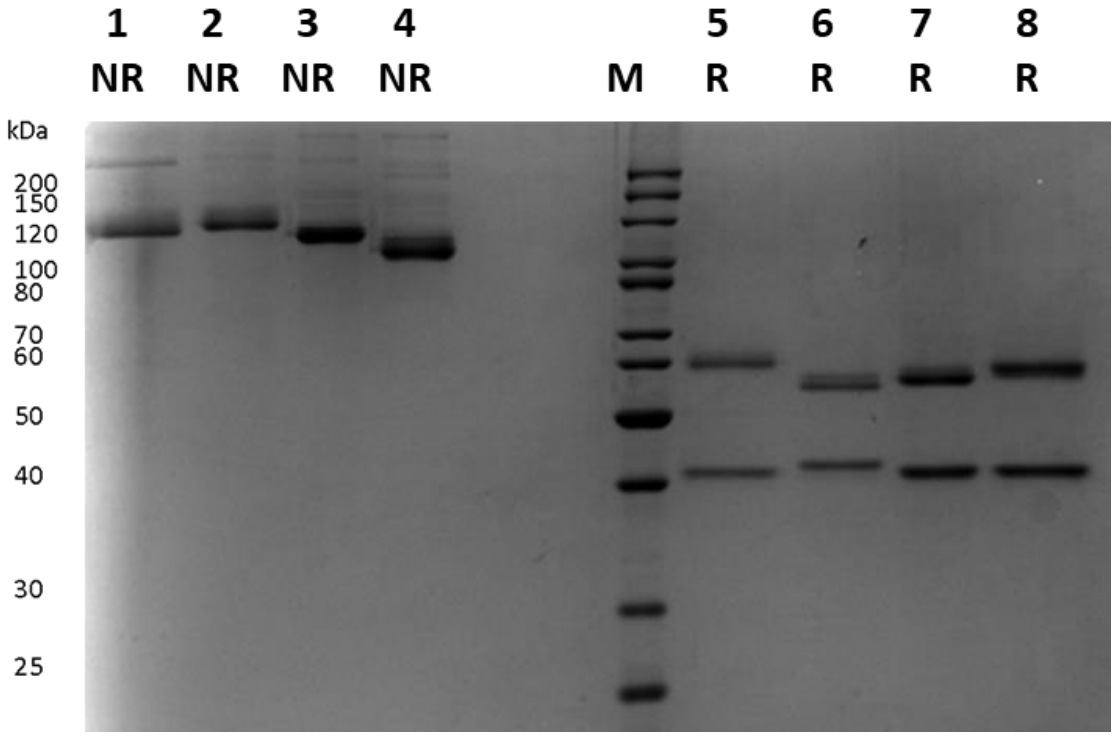

Figure 16: Protein integrity and purity analysis of the used antibodies: SDS-PAGE analysis under reduced (R) and non-reduced (NR) conditions. M, protein standard marker. Lane 1/5: VL-UCHT1_scFvCD24-FcKiH; Lane 2/5: VH-UCHT1_scFvCD133-FcKiH; Lane 3/7: VL-UCHT1_scFvCD166-FcKiH; Lane 4/8: VL-UCHT1_scFvCEA-FcKiH

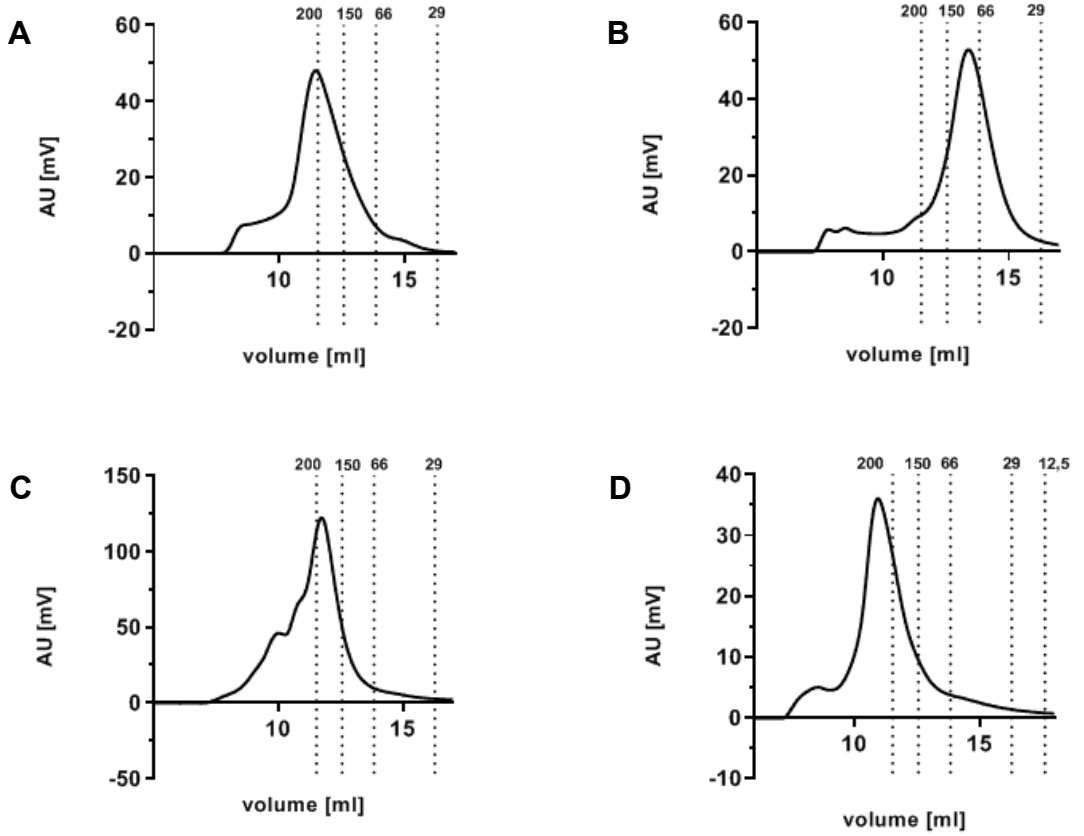

Figure 17: Protein integrity and purity analysis of the used antibodies: FPLC-SEC analysis on Superdex 10-300 200 pg of (A) VL-UCHT1_scFvCD24-FcKiH, (B) VH-UCHT1_scFvCD133-FcKiH, (C) VL-UCHT1_scFvCD166-FcKiH and (D) VL-UCHT1_scFvCEA-FcKiH

Under non reducing conditions, the 2nd generation Hemibodies ran at a height of approximately 100 -120 kDa, a little higher than the calculated masses of around 90 kDa (Figure 16, lane 1-4). Under reducing conditions (lane 5-8), two bands were visible displaying the two heavy chains of the antibodies which assemble to the whole Hemibody fragment through disulfide bridges and the kih technology. Except for slight additional bands above the expected band under non-reduced conditions, high purity of all proteins was confirmed via SDS-PAGE (Figure 16, lane 1-4). In FPLC-SEC analysis, besides a major peak at 80-200 kDa, minor peaks at higher masses not included in the protein standard were indicating the presence of possible multimers (Figure 17). To remove these multimers (minor peak), only fractions containing the monomeric protein were pooled leading to a yield of 1,2mg/ml to 2,42 mg/ml. FPLC purified constructs were used for all downstream assays including the functional and biological characterization.

Combining the above-mentioned production data, through antibody engineering techniques the yield could be improved significantly up to 20x more compared to 1st generation Hemibodies produced in Shuffle T7 cells and up to 2x compared to 1st generation

Hemibodies produced in ExpiHEK293 cells. Also, the purity was greatly improved compared to bacterial productions.

4.5. Receptor binding of Hemibodies

The binding of the 2nd generation Hemibodies was analyzed via flow cytometry using the transfected CHO cell lines and CSC expressing tumor cell lines. For 1st generation Hemibodies, the purity and yield was too low to perform such analysis.

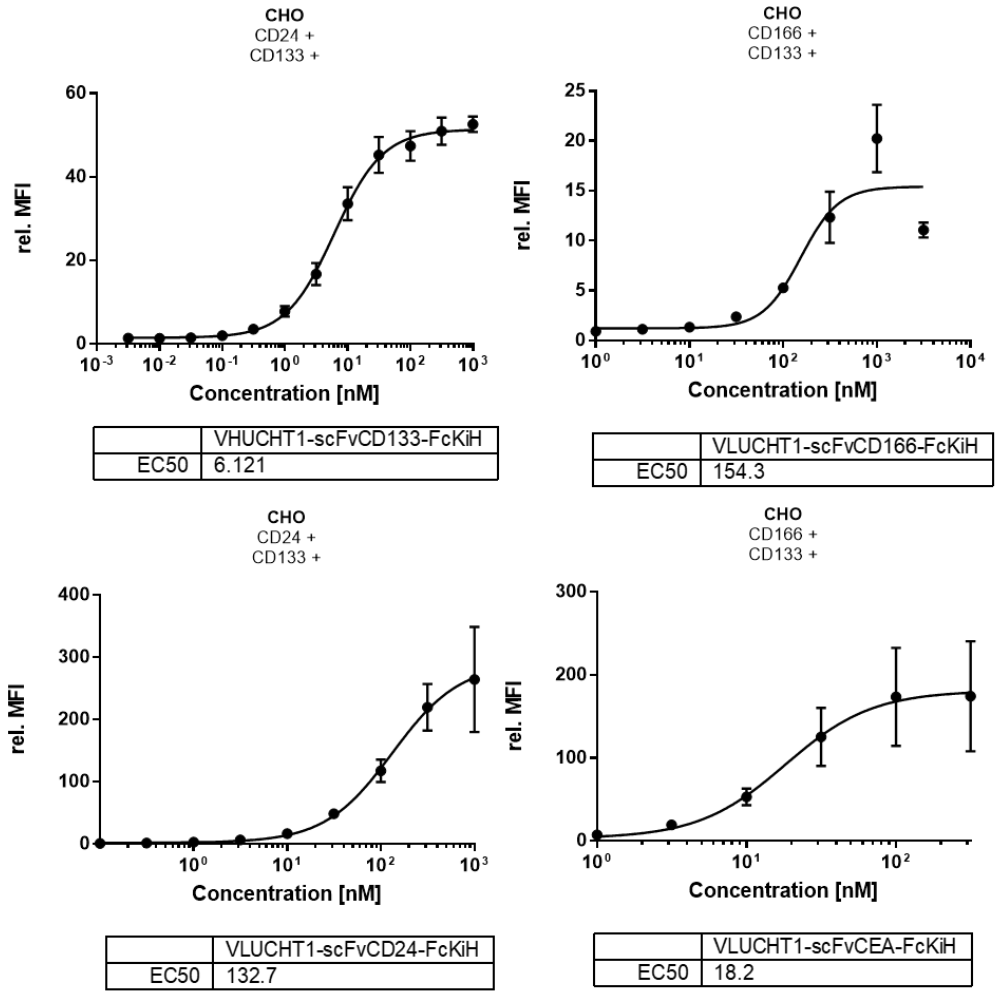

	VHUCHT1-scFvCD133-FcKiH
EC50	6.121

	VLUCHT1-scFvCD166-FcKiH
EC50	154.3

	VLUCHT1-scFvCD24-FcKiH
EC50	132.7

	VLUCHT1-scFvCEA-FcKiH
EC50	18.2

Figure 18: Cell surface binding analysis of selected Hemibodies: Binding of titrated Hemibodies (VH-UCHT1_scFv-CD133-FcKiH, VL-UCHT1_scFv-CD24-FcKiH, VL-UCHT1-scFv-CD166-FcKiH) was measured by flow cytometry. Antibodies were detected by AF488-conjugated α-human Fc antibody. 2 colorectal cancer stem cell marker expressing CHO cell lines were tested: CHO CD24+ CD133+, CHO CD166+ CD133+. Respective EC50 Values are shown below each graph. Data represented as mean ± SD of three independent experiments.

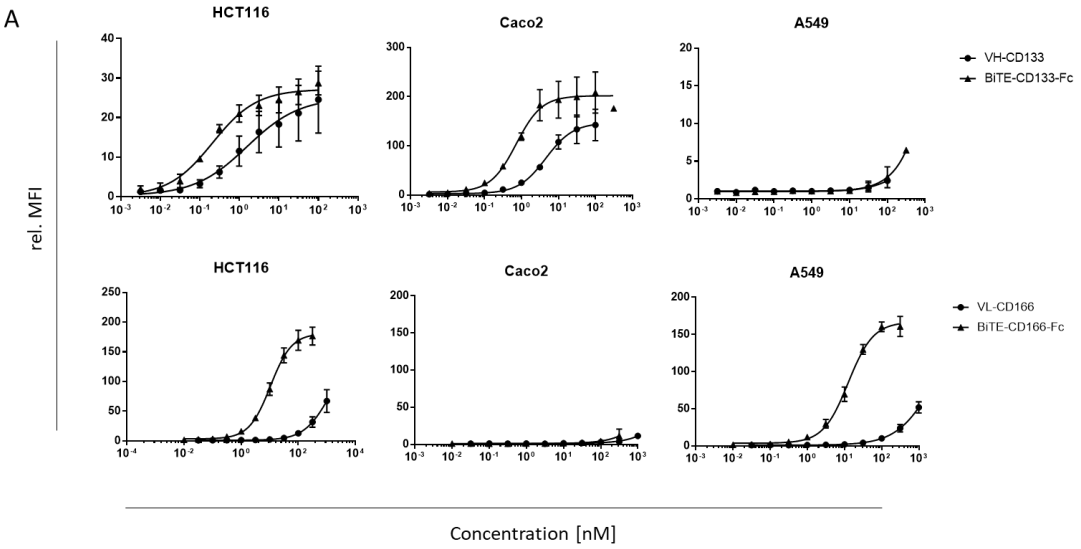

	HCT116		Caco2		A549	
	VH-CD133-Fc	*BiTE-CD133-Fc*	*VH-CD133-Fc*	*BiTE-CD133-Fc*	*VH-CD133-Fc*	*BiTE-CD133-Fc*
EC50 [nM]	1,57	0,21	4,59	0,72	148,30	~12220
	VL-CD166-Fc	*BiTE-CD166-Fc*	*VL-CD166-Fc*	*BiTE-CD166-Fc*	*VL-CD166-Fc*	*BiTE-CD166-Fc*
EC50 [nM]	1217,00	10,59	~3342544	~23782	2373	12,66

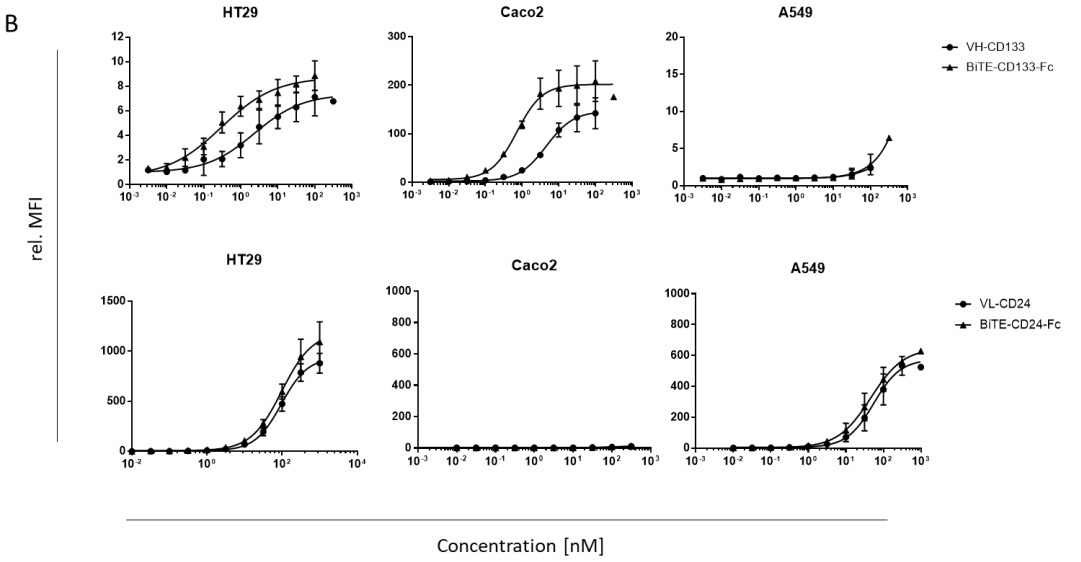

	HT29		Caco2		A549	
	VH-CD133-Fc	*BiTE-CD133-Fc*	*VH-CD133-Fc*	*BiTE-CD133-Fc*	*VH-CD133-Fc*	*BiTE-CD133-Fc*
EC50 [nM]	2,35	0,30	4,59	0,72	148,30	~12220
	VL-CD24-Fc	*BiTE-CD24-Fc*	*VL-CD24-Fc*	*BiTE-CD24-Fc*	*VL-CD24-Fc*	*BiTE-CD24-Fc*
EC50 [nM]	95,48	97,39	656,10	273,10	55,25	46,00

Figure 19:Cell surface binding analysis of selected Hemibodies: Binding of titrated Hemibodies (VH-UCHT1_scFv-CD133-FcKiH, VL-UCHT1_scFv-CD24-FcKiH, VL-UCHT1-scFv-CD166-FcKiH) and their corresponding BiTEs was measured by flow cytometry. Antibodies were detected by AF488-conjugated α-human Fc antibody. Four colorectal cancer cell lines were tested: HCT116, HT29, Caco2, A549. Respective EC50 Values are shown below each graph. Data represented as mean ± SD of three independent experiments. (A) analysis of the combination CD133xCD166 (B) analysis of the combination CD133xCD24

As seen in Figure 18, the constructs could bind to CD24, CD133, CD166 and CEA expressed on CHO cells in a concentration dependent manner as indicated by the sigmoidal binding curves. The calculated EC_{50} value for binding of VHUCHT1-scFvCD133-KiH to CD133 was 6,1 nM, for VLUCHT1-scFvCD24-KiH to CD24 132,7 nM, for binding of VLUCHT1-scFvCD166-KiH to CD166 154,3 nM and for binding of VLUCHT1-scFvCEA-KiH to CEA 18,2 nM, respectively. As the sigmoidal curve for VLUCHT1-scFvCD24-KiH was not saturated, the exact EC_{50} value is most probably way lower than determined. Binding of the constructs to established cancer cell lines is depicted in Figure 19. Expression profiles of each cell line were already illustrated in 4.3. On HCT116 cells, VHUCHT1-scFvCD133-KiH could bind as expected with an EC_{50} value of 1 nM and VLUCHT1-scFvCD166-KiH with an EC_{50} value of more than 1 µM. Also, here it is needed to be mentioned that saturation was not reached with VLUCHT1-scFvCD166-KiH indicating a lower EC_{50} value as determined. On Caco2 cells, only VHUCHT1-scFvCD133-KiH was able to bind with an EC_{50} value of 3,9 nM, VLUCHT1-scFvCD166-KiH could not bind at all. For the A549 cell line binding behavior was contrary, VHUCHT1-scFvCD133-KiH was not able to bind, whereas VLUCHT1-scFvCD166-KiH binds with an affinity of 667,8 nM. Analyzing the combination CD133xCD24, similar binding patterns were measured. On HT29 cells, the constructs VHUCHT1-scFvCD133-KiH and VLUCHT1-scFvCD24 could bind with EC_{50} values of 2,34 nM and 95,4 nM respectively. Saturation was not reached with VLUCHT1-scFvCD24, again indicating a lower EC_{50} value as determined. On A549 cells, VLUCHT1-scFvCD24 bound with an EC_{50} value of 55,3 nM. Compared to the control BiTE antibodies, binding was 10x weaker and for CD166 binding even more than 1000x weaker. For CD24 binding EC_{50} values were comparable (Figure 19).

4.6. Biological characterization of Hemibodies

4.6.1. Killing efficacy and specificity of 1st generation Hemibodies (diL2K based)

Killing efficacy and specificity of 1st generation Hemibodies, using diL2K as a CD3 binder, was tested with luciferase based killing assays on the CHO cell lines generated in 4.2. In this section constructs produced in Shuffle T7 cells were used. Briefly, the Hemibody combinations CD133xCD24, CD133xCD166 and CD133xCEA were tested on double antigen positive vs single antigen positive target cells.

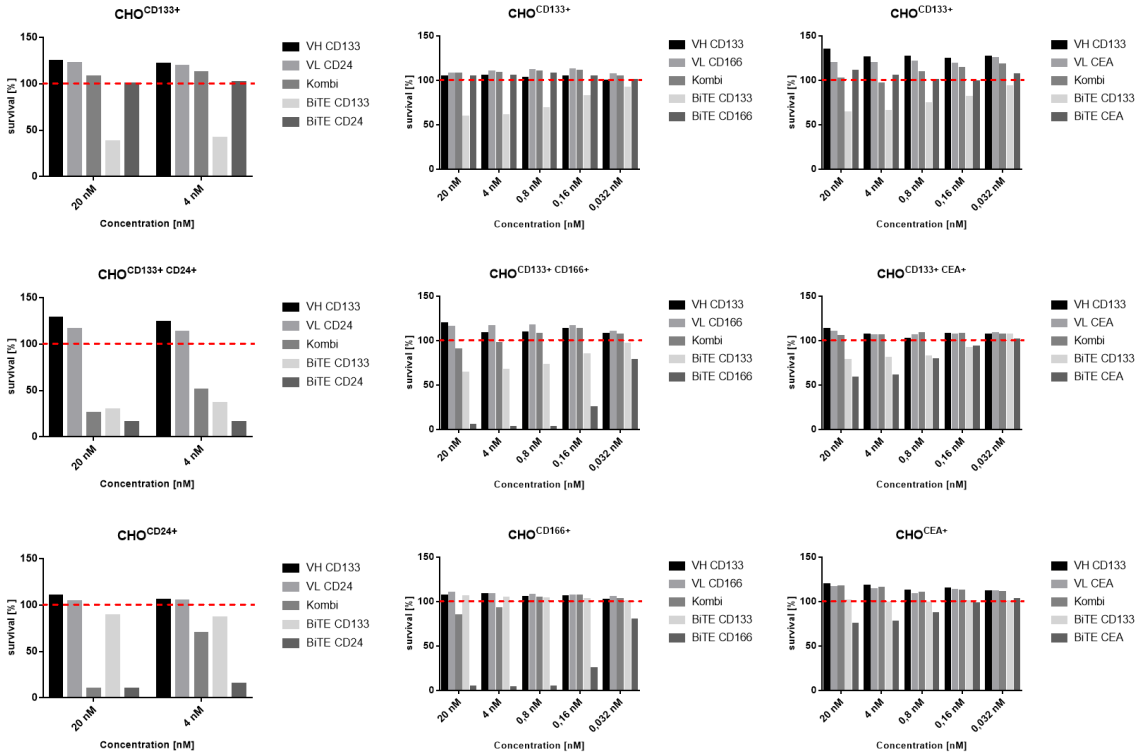

Figure 20: Luciferase Viability Assay: Firefly Luc+ CHO cells transfected with depicted antigens were co-cultured with CD8+ T-cells in a 1:5 ratio and treated with different Hemibody combinations 24h after seeding. Respective BiTE molecules served as positive controls. After another 24h incubation at 37°C Luciferase Signal was measured. Data was normalized to untreated cells with T-cells.

As seen in Figure 20, viability after treatment was depicted in bar graphs showing the different treatment regimens including single Hemibody controls, Hemibody combinations (Kombi) as well as respective BiTE controls. Cells were treated in a titration series ranging from 20 nM for both Hemibody fragments to 0,032 nM.

From left to right, the combinations CD133xCD24, CD133xCD166 and CD133xCEA were analyzed. Specificity was tested by treating single antigen positive cells (upper and lower panel) and double antigen positive cells (middle panel) separately (Figure 20). For all tested combinations, the single Hemibody controls showed no killing indicated by viability values of around 100% compared to untreated cells. Starting with CD133xCD24 the Hemibody combination consisting of the Hemibody fragments VHdiL2K-scFvCD133 and VLdiL2K-scFvCD24 lead to a killing of ca. 80% at the highest tested concentration. Compared to the killing on the single antigen positive cell line CHO^{CD24+}, killing was comparable or even higher for the highest concentration. At a concentration of 4 nM, the combination therapy reached killing efficacies of around 50% on the double antigen positive whereas only a killing of around 20% was observed on the single antigen positive cell line CHO^{CD24+}. On the single antigen positive cell line CHO^{CD133+}, no killing at all was seen (Figure 20, left panel). Control BiTE treatments showed killings as expected:

around 90% killing for the cell lines positive for the target antigen and no killing for the antigen negative cell lines confirming the correct expression of antigens on the used target cells. Similar killing patterns could be observed for the remaining combinations. On the single antigen positive cell line CHO^{CD133+}, no killing is observed, as well as for the single Hemibody controls. BiTE antibodies only induced efficient killing on antigen positive cell lines. For the combination CD133xCD166, target cell elimination of around 15% is only seen for the highest tested concentration on the double antigen positive cell line $CHO^{CD133+CD166+}$. Induced killing of the combination was similar on the antigen single positive cell line CHO^{CD166+} indicating a lack of specificity. The last tested combination CD133xCEA showed no killing on all cell lines (Figure 20).

4.6.2. Killing efficacy and specificity of 1st generation Hemibodies (UCHT1 based)

For testing the killing efficacy and specificity of 1st generation Hemibodies using UCHT1 as a CD3 binder, the same experiments were performed as stated in 4.6.1. Constructs produced in Shuffle T7 cells were used. Here, only the first produced combinations CD166xCD24 and CEAxCD24 were tested. In contrast to 4.6.1, PBMCs instead of expanded and activated CD8+ T-cells were used as effector. Looking at Figure 21 depicting the double antigen positive cell lines on the left and the respective single antigen positive cell line on the right, a similar killing behavior is observed. Killing was induced efficiently for the Hemibody combinations and BiTE antibodies on the double positive cell line but also on the single antigen positive cell line CHO^{CD24+} for both tested combinations. Titrating the concentration down to 0,16 nM, led to only killing of the double antigen positive cell lines $CHO^{CD166+CD24+}$/ $CHO^{CEA+CD24+}$, indicating a clear tendency of killing double antigen positive cell lines compared to single antigen positive cell lines. Since there was no detectable killing at 0,032 nM, the specificity for the UCHT1 based Hemibodies in both tested combinations specificity is still too low for eliminating only double positive cells without off-target toxicity (Figure 21).

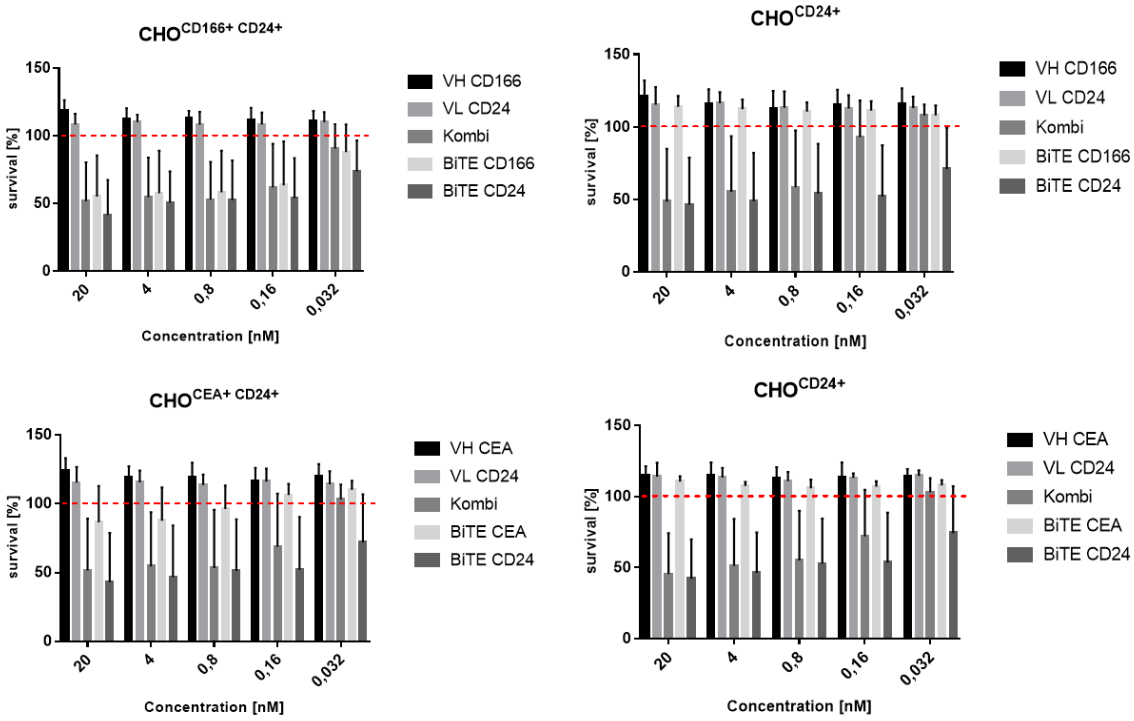

Figure 21: Luciferase Viability Assay: Firefly Luc+ CHO cells transfected with depicted antigens were co-cultured with PBMCs in a 1:5 ratio and treated with different Hemibody combinations 24h after seeding. Equivalent BiTE molecules served as positive controls. After another 24h incubation at 37°C Luciferase Signal was measured. Data was normalized to untreated cells with PBMCs.

Because multimerization of the constructs to dimers or oligomers can highly influence the specificity of Hemibodies by binding several target antigens at a time and thereby increasing the amount of split CD3 binders in close contact to single antigen positive cells and thereby increasing the affinity to CD3 by an avidity effect, 1st generation Hemibodies with UCHT1 were also produced in ExpiHEK293 suspension cells. Due to the increased yield and purity, FPLC purification for exclusion of multimeric proteins was possible. 1st generation Hemibodies produced in ExpiHEK293 cells were tested on the lentiviral transduced cancer cell lines HCT116 (double antigen positive for CD133 and CD166), HT29 (double antigen positive for CD133 and CD24), Caco2 (single antigen positive for CD133) and A549 (single antigen positive for CD166/ CD24).

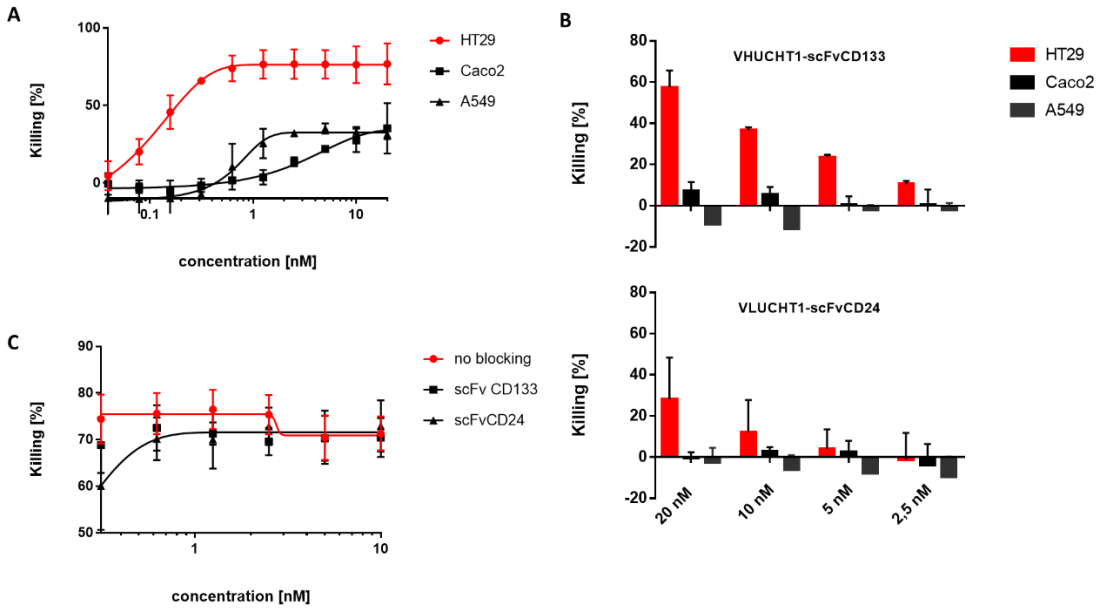

Figure 22: 1st gen Killing-Assays on colorectal cancer cell lines with the Hemibody combination CD133xCD24: Cancer cell lines expressing Fluc were treated with different concentrations of Hemibody combinations one day after seeding. CD8+ T-cells were added in a 5:1 (E:T) ratio together with the constructs. 24h later luminescence was measured. (A) Target cell Killing using the Hemibody combination CD133xCD24 (VH-UCHT1_scFvCD133 x VL-UCHT1_scFvCD24) on HT29, Caco2, A549 (B) Target cell killing with single Hemibody constructs (C) Killing of HT29 cells with Hemibody combination CD133xCD24 after blocking with an scFv against CD133 (c = 1 µM) and CD24 (c = 2 µM)

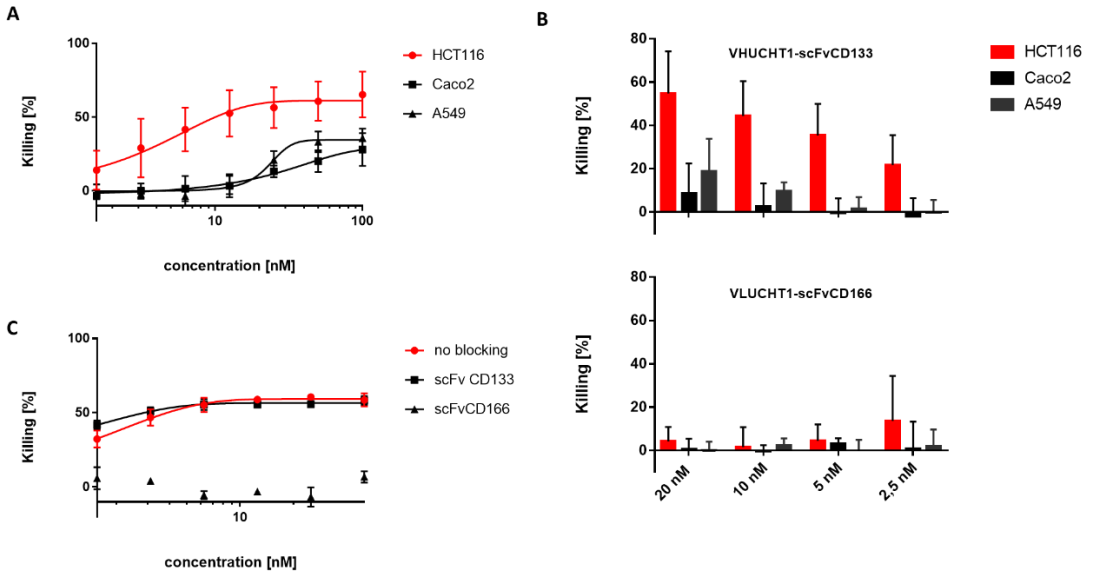

Figure 23: 1st gen Killing-Assays on colorectal cancer cell lines with the Hemibody combination CD133xCD166: Cancer cell lines expressing Fluc were treated with different concentrations of Hemibody combinations one day after seeding. CD8+ T-cells were added in a 5:1 (E:T) ratio together with the constructs. 24h later luminescence was measured. (A) Target cell Killing using the Hemibody combination CD133xCD166 (VH-UCHT1_scFvCD133 x VL-UCHT1_scFvCD166) on HCT116, Caco2, A549 (B) Target cell killing with single Hemibody fragments (C) Killing of HCT116 cells with Hemibody combination CD133xCD166 after blocking with an scFv against CD133 (c = 1 µM) and CD166 (c = 4 µM)

FPLC purified monomeric 1st gen Hemibodies showed increased killing on colorectal cancer cell lines compared to the killing of Hemibodies produced in Shuffle T7 cells on CHO cells (Figure 22; Figure 23). For both combinations (CD133xCD24, CD133xCD166) a clear killing tendency towards the double positive cancer cell line is visible over two log levels. Only at higher concentrations, killing occurs on single antigen positive cancer cells (Figure 22; Figure 23). Looking into the effect of single Hemibody constructs on the colorectal cancer cell lines shows high killing up to 60% for the VH-fragment. The respective VL-constructs alone only show low killing. Strikingly, single fragment killing is most obvious on double antigen positive cells (Figure 22B; Figure 23B).

To exclude killing specificity arises from different resistances to immunotherapy of the three used cancer cell lines, the double antigen positive cell line was artificially transformed into a single antigen positive cell line by blocking one antigen with an excessive amount of scFv against this antigen. For the combination CD133xCD24 no difference is seen between blocked cells and native cells (Figure 22C). At low concentrations the cell line blocked with scFvCD24 shows slightly less killing compared to the native cell line. For the combination CD133xCD166 a similar killing pattern is visible. Only when HCT116 cells are blocked with an scFv against CD166 killing could be blocked almost completely (Figure 23C). Importantly to mention, killing of BiTE controls could not be blocked at all on both used cell lines using the respective scFv in great excess (Data not shown).

4.6.3. Killing efficacy and specificity of 2nd generation Hemibodies (UCHT1 based)

According to 4.6.1 also the 2nd generation Hemibodies were tested similarly. Superiority of 2nd generation Hemibodies should be demonstrated in terms of efficacy and specificity compared to 1st generation Hemibodies. All tested constructs were purified via FPLC to exclude interference of multimers. In these experiments, an additional treatment regimen was introduced where the VHUCHT1 Hemibody fragment was titrated on the target cells in 10x lower concentration compared to the VLUCHT1 constructs, which greatly increased specificity as detected in preliminarily data (Data not shown). Figure 24 depicts the results of the combinations CD133xCD24, CD133xCD166 and CD133xCEA from left to right. The upper panel shows the treatment regimen where both Hemibody fragments are administered at the same concentration, the lower panel shows the treatment regimen where the construct VHUCHT-scFvCD133-KiH was administered in a 10x lower concentration as the VLUCHT fragments. In the graphs below killing is depicted in concentration range from 100 nM to 0,1 nM showing killing of the double antigen positive CHO cell line in red and the respective single antigen positive cell lines in black. When

both Hemibody fragments were given at the same concentration killing reached values of 60-80% for the highest concentrations for all tested combinations. Furthermore a therapeutic window ranging approximately 1 log level, 0,1 nM to 1 nM for CD133xCD24 and CD133xCEA (Figure 24A/C, upper graph) and 1 nM to 10 nM for CD133xCD166 (Figure 24B, upper graph), where only double antigen positive target cells were eliminated with high specificity. Comparing these results to the treatment regimen where the VHUCHT1-scFvCD133-KiH is administered at a 10x lower concentration, it is striking that a significant improvement of the therapeutic window was achieved. Therapeutic window could be widened to almost 2 log levels, 0,1 nM to 10 nM for CD133xCD24 and CD133xCEA and 1 nM to 100 nM for CD133xCD166 (Figure 24).

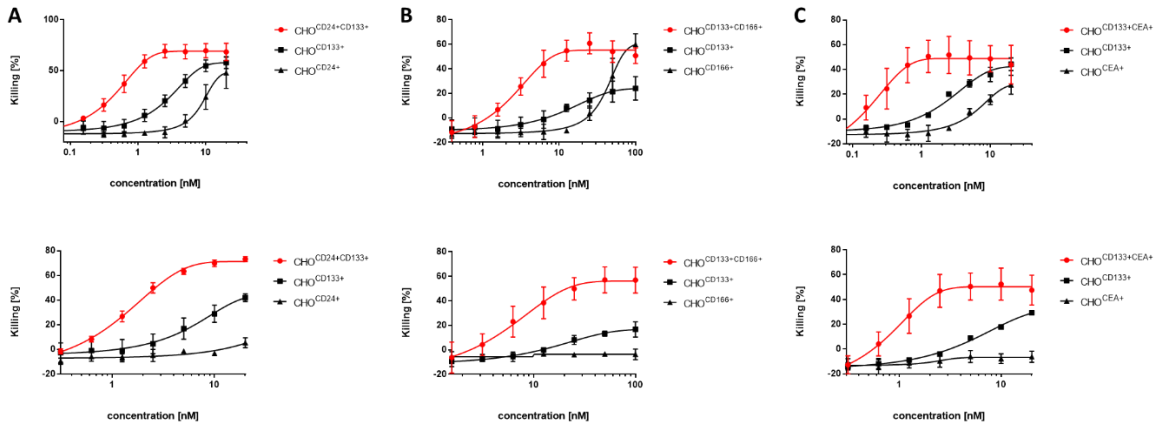

Figure 24: Killing-Assay using different Hemibody combinations: Stably transfected Fluc+ CHO cell lines were treated with different concentrations of Hemibody combinations one day after seeding. CD8+ T-cells were added in a 5:1 (E:T) ratio together with the constructs. 24h later luminescence was measured. (A) Target cell Killing using the Hemibody combination CD133xCD24 (VH-UCHT1_scFvCD133-FcKiH x VL-UCHT1_scFvCD24-FcKiH). (B) Target cell Killing using the Hemibody combination CD133xCD133 (VH-UCHT1_scFvCD133-FcKiH x VL-UCHT1_scFvCD166-FcKiH). (C) Target cell Killing using the Hemibody combination CD133xCEA (VH-UCHT1_scFvCD133-FcKiH x VL-UCHT1_scFvCEA-FcKiH). Data was normalized to untreated cells + T-cells and represented as mean ± SD of three independent experiments.

To verify that the readout of luciferase values represents actual target cell killing, a further experiment, namely a Caspase assay was performed. Results are shown exemplary for the combination CD133xCD24 in Figure 25.

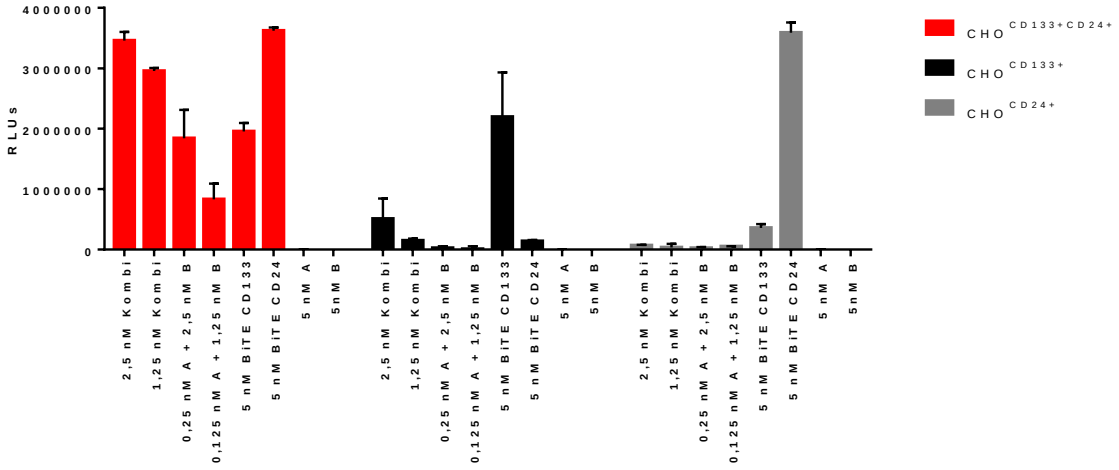

Figure 25: Caspase-Glo® 3/7 Assay: CHO cell lines expressing the cancer stem cell targets CD133 and CD24 were seeded in complete growth medium. After 24h cells were treated with the constructs A (VH-UCHT1_scFvCD133-FcKiH), B (VL-UCHT1_scFvCD24-FcKiH), combinations of both or BiTEs against CD133 or CD24 and CD8+ T-cells were added in a 5:1 (E:T) ratio. On day 3, plates were analyzed using Caspase-Glo® 3/7 Assay System. Data is represented as mean ± SD of three independent experiments.

Caspase activity was measured as RLUs using the Caspase® 3/7 assay [Promega, Madison, Wisconsin, USA]. Red bar graphs illustrate the caspase activity on the double antigen positive CHO cell line $CHO^{133+CD24+}$. High activity was measured for both above mentioned treatment regimens ranging from 2,5 nM to 1,25 nM with RLUs between $1*10^6$ to almost $4*10^6$. In the single antigen positive cell lines CHO^{CD133+} and CHO^{CD24+} low or no activity was detected for all tested concentrations. Single constructs did not activate any caspases and administered control BiTEs only induced caspase activity when the respective antigen was present on the cell line (Figure 25).

In summary it can be stated that 2nd generation Hemibodies have a high efficacy and specificity in an artificial CHO cell-based system and the Caspase assay validated the readout of luciferase-activity in target cells as a correct measure for target cell killing.

4.6.4. Killing efficacy and specificity of 2nd generation Hemibodies on established cancer cell lines

Since transfected CHO cell lines represent a highly artificial testing system, killing efficacy and specificity should be validated in a final experiment in established cancer cell lines. Therefore, the lentiviral transduced cancer cell lines HCT116, HT29, Caco2 and A549 (all originating from the colon except for A549 originating from the lung) were used in a similar manner as described in 4.6.1. For the combination CD133xCD24, the cell line HT29 was utilized as the double antigen positive cell line, whereas the cell lines Caco2 and A549 served as single antigen positive target cells for CD133 and CD24 respectively (Figure 26AB). For the combination CD133xCD166, the cell line HCT116

was used as the double antigen positive cell line and the cell lines Caco2 and A549 as the single antigen positive targets for CD133 and CD166, respectively (Figure 27AB). Besides measuring the killing on three different cell lines, an experiment where both antigens were blocked sequentially using a scFv against each to exclude the possibility that the therapeutic window arises from an antigen expression independent resistance to immunotherapy (Figure 26C, Figure 27C).

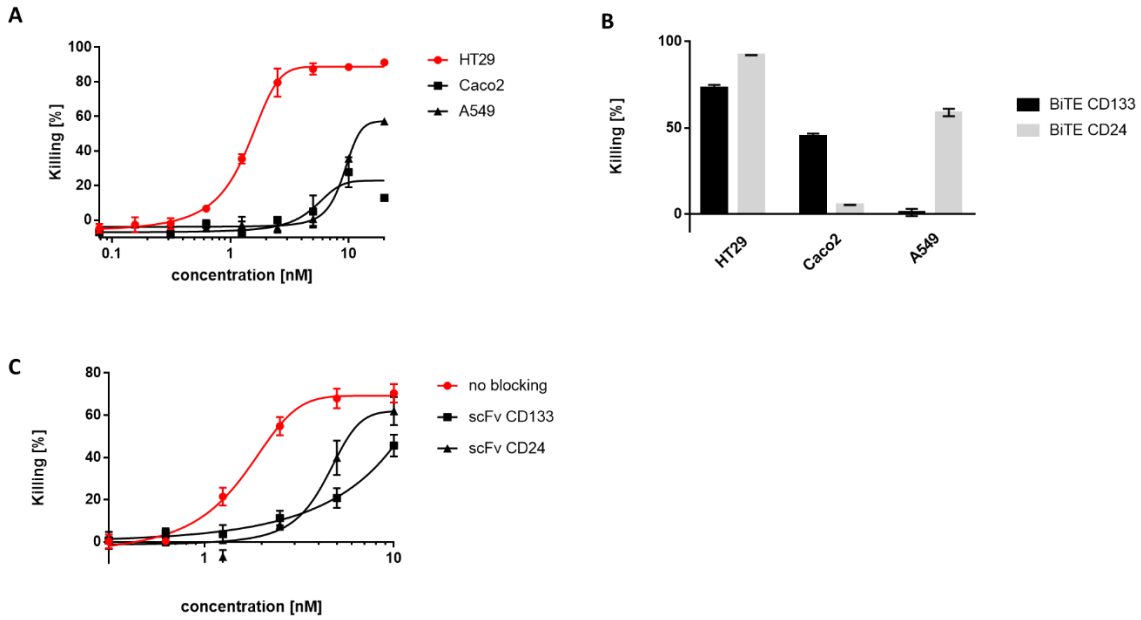

Figure 26: Killing-Assays on colorectal cancer cell lines with the Hemibody combination CD133xCD24: Cancer cell lines expressing Fluc were treated with different concentrations of Hemibody combinations one day after seeding. CD8+ T-cells were added in a 5:1 (E:T) ratio together with the constructs. 24h later luminescence was measured. (A) Target cell Killing using the Hemibody combination CD133xCD24 (VH-UCHT1_scFvCD133-FcKiH x VL-UCHT1_scFvCD24-FcKiH) on HT29, Caco2, A549 (B) Target cell killing with BiTE controls at c = 0,8 nM (C) Killing of HT29 cells with Hemibody combination CD133xCD24 after blocking with an scFv against CD133 (c = 1 µM) and CD24 (c = 2 µM)

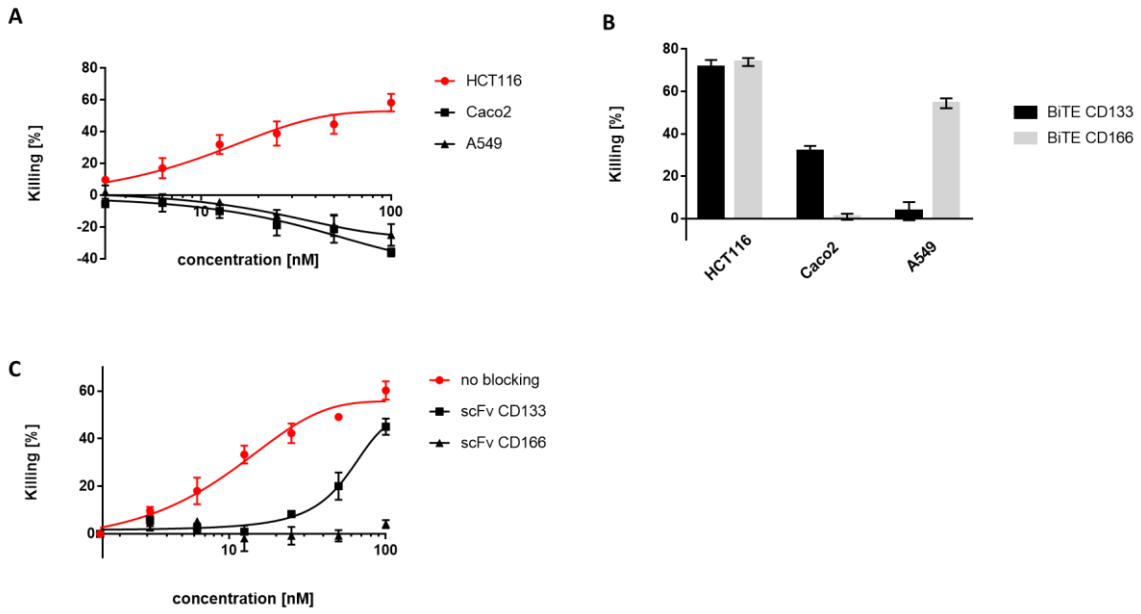

Figure 27: Killing-Assays on colorectal cancer cell lines with the Hemibody combination CD133xCD166: Cancer cell lines expressing Fluc were treated with different concentrations of Hemibody combinations one day after seeding. CD8+ T-cells were added in a 5:1 (E:T) ratio together with the constructs. 24h later luminescence was measured. (A) Target cell Killing using the Hemibody combination CD133xCD166 (VH-UCHT1_scFvCD133-FcKiH x VL-UCHT1_scFvCD166-FcKiH) on HCT116, Caco2, A549 (B) Target cell killing with BiTE controls at c = 0,8 nM (C) Killing of HCT116 cells with Hemibody combination CD133xCD166 after blocking with an scFv against CD133 (c = 1 µM) and CD166 (c = 4 µM)

Starting with the combination CD133xCD24, only the treatment regimen with the VH fragment being 10x underrepresented compared to the VL fragment was tested. At the highest tested concentration equaling 20 nM VLUCHT1-scFvCD24-KiH combined with 2 nM of VHUCHT1-scFvCD133, the double antigen positive cell line HT29 is eradicated almost completely whereas the single antigen positive cell lines are only killed to approximately 50%. Titrating down the concentration leads to a highly specific killing of the double antigen positive cell line sparing the single antigen positive cell lines completely, thus creating a therapeutic window of almost 2 log levels which is comparable to the data collected with the CHO cell system (Figure 26A). For the combination of CD133xCD166 a comparable result was achieved. Over a concentration range from 1 to 100 nM, no killing is detectable for the cell lines Caco2 and A549. At the highest tested concentration, a slight proliferative effect (max. 40% proliferation compared to the untreated cells) is visible (Figure 27A). Control killings of the BiTE antibodies on the established cell lines, validated the expression profile determined by FACS (see 4.3). BiTE molecules only induced killing in cell lines expressing their respective target antigen (Figure 26B; Figure 27B). The blocking experiments revealed a slightly smaller therapeutic window for both tested combinations ranging from 0,1 nM to 2,5 nM (CD133xCD24) and 1 nM to 25 nM (CD133xCD166) (Figure 26C; Figure 27C). Control BiTE molecules could not be blocked at all despite an over 200x excess of blocking scFv in each well (Data not shown).

Another possible mechanism of off-target activity of Hemibodies could be induced by close proximity of single and double antigen positive cell lines. When all three tested cell lines for each combination are cultivated in the same vessel both antigens e.g. CD133 and CD24 for the first combination, could be expressed on both single antigen positive cell lines. Because of proximity of both cell lines Hemibodies could crosslink these cells each by one Hemibody fragment and reconstitute its CD3 binding domain leading to unspecific killing of the single antigen positive cell lines Caco2 and A549. To exclude this mechanism from being existent, a FACS-based killing experiment was developed, where both single and double antigen positive cell lines are cultivated together in one well. For distinction of the three cell lines, they were stained differently and killing was measured using 7-AAD. Results of this assay are depicted in Figure 28. T- cells were excluded by their smaller size via the FSC/ SSC. With the above-mentioned staining regimen, the three cell lines could be clearly distinguished. Unstained Caco2 cells were slightly overlapping with unstained T-cells (Figure 28A). The Hemibody combination against CD133 and CD24 induced killing on the double positive cell line HT29, indicated by a shift in the 7AAD channel, whilst sparing the single antigen positive cell lines Caco2 and A549. Single fragments (Hemibody A = VHUCHT1-scFvCD133-Fc/ Hemibody B = VLUCHT1-scFvCD24-Fc) had no effect on all cell lines. BiTE B (BiTE against CD24), as seen in Figure 28B, induced killing in the double antigen positive cell line HT29 and in the single antigen positive cell line A549. BiTE A targeting CD133 only induced small killing effects on the cell lines HT29 and Caco2. Combining these results with the FACS characterization in Figure 10, it is clear that 2nd generation Hemibodies are working as expected by only killing double antigen positive cells. Also, the effect of single fragment killing seen with 1st generation Hemibodies was overcome.

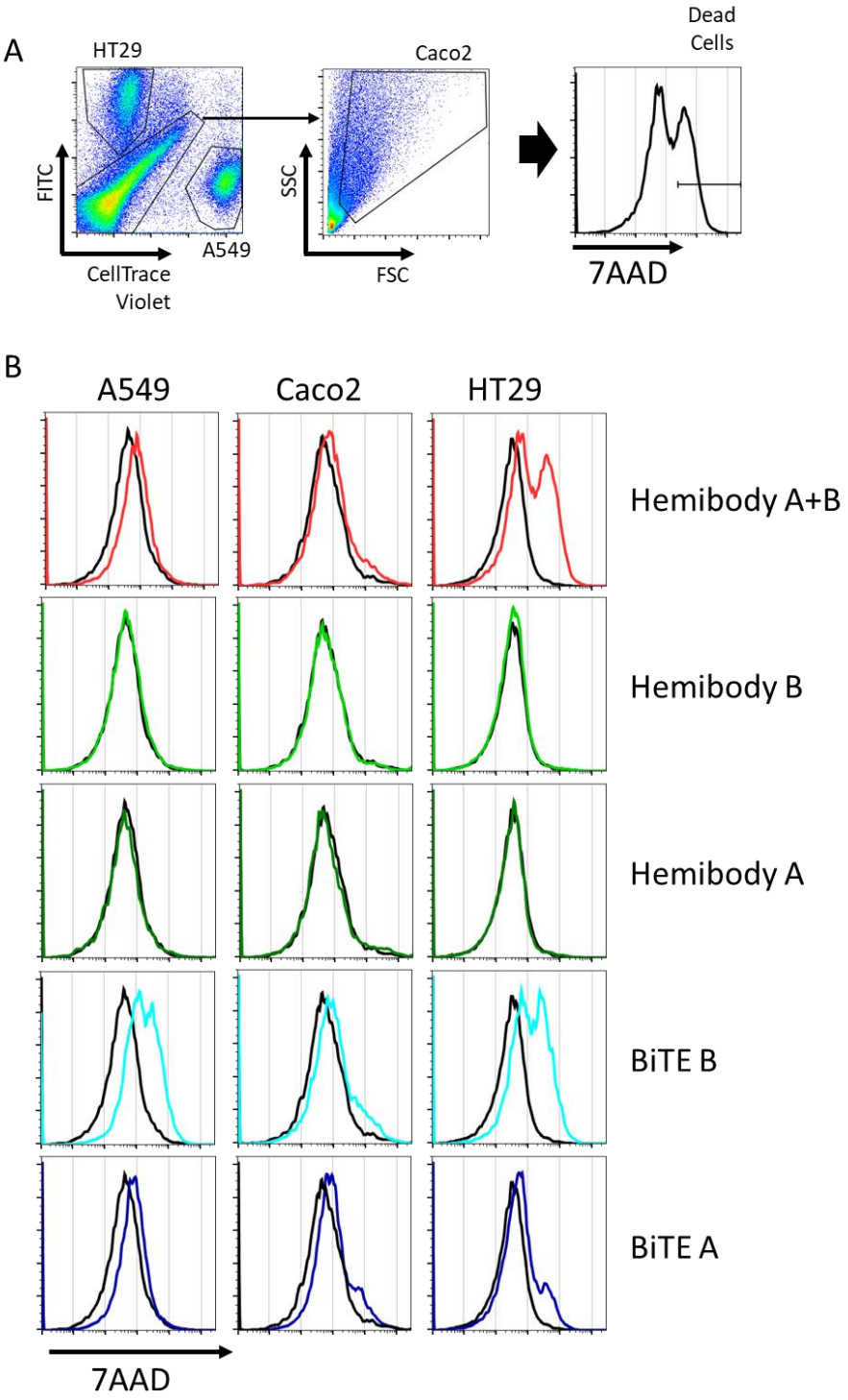

Figure 28: mixed killing with the combination CD133xCD24: established cancer cell lines were stained with cell trace violet (A549), GFP (HT29) or remained unstained for distinguishment of the cell lines. 24h after seeding cells were treated with either single fragments, the combination or control BiTEs against respective antigens and T-cells were added in a 5:1 (E:T) ratio. Further 24h later, killing was measured using the MACSQuant analyzer 10 as 7AAD signal. (A) gating of the cultivated cell lines in each vessel. (B) Killing measured as 7AAD signal using the different treatment regimens on the three different cancer cell lines. Data shows one representative plot of n=2 experiments.

5. Discussion

5.1 Single cell RNA sequencing analysis

For targeting CSC in colorectal cancer with Hemibodies, suitable surface markers have to be identified. After literature research several CSC markers were chosen as qualified for targeting and were further characterized in a single cell RNA sequencing analysis. Briefly, a publicly available dataset of 60.000 colorectal cancer cells with adjacent normal tissue was analyzed for coexpression, expression on healthy and cancerous tissue and via differential expression analysis (DE) and enrichment analysis (EA) for really being involved in stemness. Out of an initial set of 10 candidate CR-CSC marker (EpCAM, CD133, CD24, CEA, CD166, LGR5, ALDH1, CD29, CD44, DCAMKL-1), four CSC markers were identified as suitable for Hemibody therapy including CD24, CD133, CEA and CD166. In terms of expression on cancerous tissue compared to normal healthy tissue, these markers showed an exclusive expression on cancerous tissue except for CEA and CD24. Since Hemibodies are a dual antigen restricted targeting strategy, the combinations CD133xCD24, CD133xCD166 and CD133xCEA have an excellent safety profile only eliminating diseased tissue. CD133 and CD166 had an expression pattern localized to small subsets of cancerous tissue, whereas CD24 and CEA showed broad expression throughout diseased tissue. By applying above-mentioned combinations, specific elimination of only a subgroup of cancerous tissue can be achieved. LGR5, CD44, EpCAM among others were excluded for further testing because of either expression on adjacent healthy tissue or expression at only a basal level.

After having identified a putative CSC compartment, this subset was analyzed for genes conferring stemness and tumorigenic potential. Differential expression analysis with the remaining epithelial cancer cells revealed a list of genes being significantly up- or downregulated in the putative CSC population. Visualization by violin plots clearly distinguishes between up- and downregulated genes between different cell types in the dataset (Figure 8). Among these genes some could be identified for promoting stemness whereas others indicated controversy results. Consequently, upregulated genes could be divided into two subgroups.

The first subgroup consisting of the genes FGGY, SPINK1, ErbB3, RPL39, AQP1, IFTM1, RAB11FIPI and FAM118A which can be clearly linked to cancer stem cell traits including the involvement in cancer proliferation, metastasis, drug resistance and poor prognosis (Zhang et al. 2019; Lin 2021; Rau et al. 2020; Dave et al. 2014; Imaizumi et al. 2018; Sari et al. 2016; Wang et al. 2018; Stangeland et al. 2015). In a field study of prostate cancer the knockdown of SPINK1 resulted in a decrease of sphere formation

ability (Tiwari et al. 2020) which was also validated using the 22RV1 cell line by regulating the expression of genes involved in stemness and EMT, including SNAI1 (SNAIL), SNAI2 (SLUG) and TWIST1 (Bhatia et al. 2019). In breast cancer Rau et al. could emphasize HER3s role in stemness. Treatment of triple negative breast cancer (TNBC) with a bispecific antibody targeting EGFR and HER3 inhibited the proliferation and oncosphere formation efficiency driven by HER3 signaling (Rau et al. 2020). Using the COGNOSCENTE database, a positive correlation of FAM118A with the increment levels of MTOR, DLL3 (Notch), PDGFB and STAT3 was found in GBM. Western blot analysis further revealed the overexpression of FAM118A in glioblastoma stem cell (GSC) cultures (Stangeland et al. 2015). In colorectal cancer tissues RAB11FIPI was found to promote migration and invasion correlating with poor prognosis (Wang et al. 2018). Contrary to the first subgroup the second consisting of only 3 genes (compared to 8 genes in the first group) conveys traits of tumor suppressors. Namely, DMTB1, CXCL14 and GJB3 were linked to inhibition of proliferation and tumor suppression by several researchers (Park et al. 2018; Lin et al. 2014; Sjöberg et al. 2016; Wu und Wang 2019).

For the downregulated genes, a similar subgrouping was done, 9 genes clearly indicated an association with stemness and tumorigenic potential when being downregulated whereas only two genes contradicted these traits.

The first group consists of the genes ST13, TMEM176A, TFF1, TFF3, IGKC, PLAC8, RPS4YI, CSTB and RHOBTB3 (Bai et al. 2012; Wang et al. 2017; Gao et al. 2017; Buache et al. 2011; Yamaguchi et al. 2018; Espinoza et al. 2021; Schmidt et al. 2012; Jia et al. 2018; Zhang et al. 2016; Ji und Rivero 2016). In colorectal cancer cells lentiviral based down-regulation of ST13 with short hairpin RNA (shRNA) significantly increased cell proliferation and cloning efficiency in vitro, in vivo down-regulation of ST13 expression resulted in increased tumorigenicity of CRC (Bai et al. 2012). Furthermore, decreased expression of CSTB and TFF3 promoted cell proliferation and migration while suppressing apoptosis in CRC and gastric cancer (Zhang et al. 2016; Espinoza et al. 2021). Jia et al. could unveil a novel signaling pathway including the well-known CSC transcription factor KLF4 together with PLAC8 with an inverse correlation between both in lung cancer (Jia et al. 2018).

Representatives of the second group are the genes REG4 and XIST. REG4 is a transcriptional target of GATA6 which makes it essential for colorectal tumorigenesis (Kawasaki et al. 2015). Furthermore, REG4 is described to bind with CD44 increasing cell proliferation and stemness (Sninsky et al. 2021). XIST, a long non-coding RNA is described as a prognostic factor in colorectal cancer which can inhibit 5-fluoruracil cell toxicity (Xiao

et al. 2017b). Besides its role in promoting cancer stemness, the genes TFF1, TFF3 and PLAC8 were also related to decreased proliferation, invasion and malignant behavior by some researchers (Yusufu et al. 2019; Cui et al. 2021; Li et al. 2014).

In summary there was a clear tendency towards genes confirming the population being CSC, 17 up- or downregulated genes could be linked to conferring stemness, proliferation and tumorigenic potential whereas only 5 indicated contrary outcomes in a list of 22 analyzed genes.

In addition to the results of the differential expression analysis, the enrichment analysis confirmed the identified subset to be the CSC compartment. The 20 top hits of upregulated pathways compared to the remaining epithelial cancer cells with a p-value below 0,05 mostly conferred stem cell traits. Highlighted in green are pathways with an association to CSC, in red pathways resulting in opposite effects and not highlighted pathways are not involved in any proliferative or stemness properties (Table 6).

Many of the above-mentioned pathways are involved in the NfκB-pathway, which plays an important role in cancer stem cell formation and maintenance as stated in 2.2.1. Namely, R-HSA-5676594, R-HSA-9014325 and R-HSA-209543 (Rinkenbaugh und Baldwin 2016; Zhu et al. 2019) are either directly or indirectly involved in the activation of the NfκB-pathway.

Cytokines, especially interleukins and interferons, are also very important in proliferation and differentiation processes of cancer cells. The pathways R-HSA-9664535, R-HSA-975110, R-HSA-9013973 and R-HSA-936964 which are upregulated in the CSC population are linked to exactly these.

R-HSA-9664535 for example is a pathway for the LTC4-CYSLTR mediated IL4 production. As stated in 2.2.1 a crucial characteristic of CSC is their resistance to conventional chemotherapy. Interleukin-4 (IL-4) plays a vital role in the survival of colon cancer stem cells. Recent work showed that this resistance is mediated by an autocrine response to the immune cytokine IL-4. Blockade of IL-4 signaling could restore therapeutic efficacy and increase the in vivo efficacy of cytotoxic therapy (Francipane et al. 2008). The pathways R-HSA-975110, R-HSA-9013973, R-HSA-936964 and R-HSA-168927 regulates tumor immunity and prognosis of CRC patients via the interferons 3 and 7 (IRF 3/7). Chen et al. could show that IRF3 and IRF7 overexpression, despite a higher CD4+ T cell, CD8+ T cell, B-cell, and macrophage activation and infiltration, resulted in a shorter overall survival (OS). Dysfunction of T cells with high level of infiltration or distinct

exclusion of T cells from infiltrating tumors are proposed as possible mechanisms of tumor immune evasion (Chen et al. 2021).

Another often found mechanism of immune evasion is based on overexpression of immune checkpoints (Wei et al. 2019). As seen in Table 6 PD-1 signaling is significantly upregulated in the CSC compartment underlining the identification of the right cell subgroup.

In recent publications activated choline and glutathione metabolism showed an essential role for self-renewal, chemoresistance, carcinogenesis and tumor progression (Sonkar et al. 2019; Jagust et al. 2020). With the pathways R-HSA-1483115 and R-HSA-174403 exactly these metabolisms are overly activated in the CSC group.
R-HSA-9032759 activates Rac1, a small GTPase, through NTKR2. This small GTPase is involved in a variety of biological processes including cell proliferation, cell survival, EMT, cell motility and invasiveness. Orchestrating signaling networks like actin skeleton remodeling, activation of protein kinases (PAKs, MAPKs) and transcription factors (NfκB, Wnt/β-catenin/TCF, STAT3, Snail) this pathway may promote crucial CSC specific traits including self-renewal and tumorigenesis (Kotelevets und Chastre 2020).
At last, the pathways R-HSA-445095 and R-HSA-190861 are significantly enriched in the CSC population compared to the remaining epithelial cancer cells. Both pathways are described to play an important role in the pathophysiology and function of CSC. R-HSA-445095 is linked to malignancy and therapy resistance. Aberrantly expressed L1 cell adhesion molecule (L1CAM) was found in a variety of tumors including colorectal cancer. It was identified as a target of the β-catenin/TCF signaling and NfκB signaling explaining its contribution to chemoresistance and stemness (Giordano und Cavallaro 2020).
R-HSA-190861 is involved in GAP junction assembly. Despite the expression of Gap junction proteins in cancer stem cells and non-stem cancer cells of many tumors, in breast cancer and glioblastoma it could be demonstrated that gap junctions are relevant in cancer stem cells especially in the communication of CSC with their surrounding cells for dissemination of CSC via blood and lymphatic vessels. Intercellular communication is mediated via paracrine secretion of interleukins, cytokines and pro-angiogenic factors or via gap junctional intercellular communication. They are crucial to maintain stem cell properties, recruiting tumor associated cells including tumor associated macrophages (TAMs) and tumor associated fibroblasts (TAFs) which transform cells in the vicinity of the tumor or induce angiogenesis. TNBC cells for example expressed high levels of Cx26, a gap junction protein, which was essential for self-renewal via formation of a complex with focal adhesion kinase (FAK) and the well-known CSC transcription factor

NANOG (Beckmann et al. 2019). Furthermore, overexpression of Cx26 in non CSC resulted in an increase in the transcription factors OCT4, Sox2, as well as Nanog which were already introduced in association with stemness in 2.2.1 (Beckmann et al. 2019).

Only the pathway R-HSA-9008059, which was found enriched, contradicts the above-mentioned findings. IL-37 overexpression in colorectal cancer is described to suppress cell migration, invasion, proliferation, colony formation and cancer stem cells via suppressing β-catenin (Yan et al. 2017).

Combining findings of the DE and EA suggests that the identified compartment has many characteristics also described for CR-CSC. Consequently, the found subset can be called cancer stem cells and as the markers CD24, CD133, CD166 and CEA were found on this population, Hemibody therapy targeting those antigens could be a suitable strategy.

5.2 Production and functional characterization of Hemibodies

Hemibodies were produced in a variety of expression hosts including CHO suspension cells, Shuffle T7 cells and ExpiHEK293 suspension cells. Starting with the 1st generation of Hemibodies using diL2K as a CD3 binder, Hemibodies were further optimized to a more stable 1st generation with UCHT1 as a CD3 binder. In a last step, these UCHT1 based 1st generation Hemibodies were further developed into the final 2nd generation of Hemibodies with enhanced producibility, stability and in vivo half-life. Produced Hemibodies combine binding to either CD133 and CD24, CD133 and CD166 or CD133 and CEA.

Beginning with 1st generation Hemibodies stably produced in CHO suspension cells, SDS-PAGE analysis showed bands at the expected heights for fragments carrying the VL portion of dIL2K or the whole scFv of diL2K. Besides the expected bands, two prominent bands at 30 and 35 kDa are visible for all constructs. VH-Hemibodies could not be produced for any target, only the above-mentioned prominent bands at 30 and 35 kDa respectively are visible. As confirmed by mass spectrometry analysis, these two bands are the result of proteolytic degradation of the constructs from the N-terminus (Figure S 1). The addition of protease inhibitor cocktails could not rescue degraded protein. Especially non-antibody glycoproteins are described to face major hurdles in production due to cell-related proteolytic degradation (Laux et al. 2018). Laux et al. for example could identify Matripase-1 to be a critical protease involved in the degradation of recombinant proteins expressed in CHO-K1 cells. Deletion of Matripase-1 resulted in a reduced or no degradation activity at all in a panel of several recombinantly produced proteins (Laux et

al. 2018). Since 1st generation Hemibodies are only derived from an antibody by extracting variable domains and a glycolysation motif present in the linker in the target scFv, Matripase-1 could be the protease responsible for low yield of full length Hemibodies.

CRIPR-Cas9 based genome editing approaches to delete Matripase-1 are very time consuming, because of what a different approach was used for improving producibility of 1st generation Hemibodies. Despite also having a lot of proteases the E.Coli strain Shuffle T7 does not glycosylate the constructs in the linker region and isn´t harboring Matripase-1, making it a possible production host for reducing degradation.

SDS-PAGE analysis revealed that the switch of the expression host indeed led to an improved yield. VH-Hemibodies could be produced in sufficient amounts for in vitro studies for the targets CD133 and CEA. VH-Hemibodies against CD24 and CD166 again were not producible. Unspecific bands most probably occur due to nonspecific binding of untagged proteins having two or more adjacent histidine residues (Bornhorst und Falke 2000). For a better purity, stricter washing steps with Washing Buffers having higher imidazole molarities could be used in the future. Furthermore, using less IMAC resin can lead to more specific binding for low producing recombinant proteins as it is the case for 1st generation hemibodies (Bornhorst und Falke 2000).

Switching the CD3 binding domain from diL2K to the more stable UCHT1 resulted in better producibility especially for the VH-Hemibodies (Figure 13). Unfortunately, low purity still remains a problem indicated by many unspecific bands. Since the unspecific bands are partially almost the same size as the Hemibodies, FPLC purification can not distinguish between unspecific band and Hemibody. Consequently, no FPLC purification was applied to constructs produced in Shuffle T7 cells. Higher purity could be achieved with methods mentioned above for the production of 1st generation Hemibodies with diL2K as a CD3 binder.

Production yields in ExpiHEK293 cells of 1st generation Hemibodies with UCHT1 as a CD3 binder greatly increased yield and purity as indicated by SDS-PAGE analysis. The appearance of double bands for each construct could be explained via a PNGase digest indicating the second band on the SDS-PAGE to be glycosylated (Figure S 1). In FPLC-SEC analysis, besides major peaks at around 45 kDa, minor peaks at higher molecular masses were observed for these Hemibodies (Figure 15). Because of differences of size of the monomeric Hemibodies (major peak) to the putative multimers (minor peaks), FPLC -SEC was performed leading to only monomeric protein in the elution fractions. The recombinant protein VHUCHT1-scFvCD133 eluted way later than the expected molecular mass should elute, leading to a calculated mass of only 15 kDa. A possible reason

could be interactions between the Hemibody and the superdex matrix. Since Hemibodies have a split binding domain against CD3, hydrophobic residues, which are normally buried in the VH/VL interface, are accessible for the matrix. Reducing the salt concentration, increasing the pH or adding a suitable detergent or organic solvent in the running buffer could solve this issue (Cytiva 2021). As the protein is still eluting but only later no changes in buffer formulation were made.

Finally, 2nd generation Hemibodies were again produced in ExpiHEK293 cells and purified via IMAC. SDS-PAGE analysis shows that only the expected band is visible, ranging from 100-120 kDa under non reducing conditions. Comparing it to the calculated sizes of ca. 90 kDa, Hemibodies run a little bit higher than expected. At higher molecular weights, only slight unspecific bands are visible. Two bands are visible under reducing conditions, one at ca. 40 kDa and one at ca 50-60 kDa. These bands represent the two heavy chains VH/VL-UCHT1-FcKnob and scFvTarget-Fchole respectively (Figure 16). The heavy chain scFvTarget-Fchole shows a slight double band. This is due to glycolyzation of the construct at the glycolyzation site present in the linker of the target scFv. Again FPLC-SEC revealed multimers present in the elution fraction indicated by minor peaks upwards the main monomeric peak. Extrapolated masses exceed the calculated masses almost by 100 kDa for the VL-fragments, the VH-Hemibody again ran at a lower molecular mass of 84 kDa (Figure 16). This can be explained by the discrepancy between a molecules weight and its hydrodynamic radius. A recombinant protein runs through a FPLC column according to its hydrodynamic radius, which is dependent on the tertiary structure. The split binding domain against CD3 probably does not fold to a globulary structure as the full scFv would do expanding its hydrodynamic radius. Furthermore, the protein is glycosylated changing its running behavior. To circumvent this discrepancy, absolute methods such as SEC-MALS for molecular weight determination could be used for further characterization. The lower extrapolated weight for the VH-fragment again can be explained by many exposed hydrophobic residues interacting with the superdex matrix.

In summary, the best improvement in terms of yield and producibility was the switch from diL2K to UCHT1 and from a prokaryotic expression host to ExpiHEK293 cells. Changing the Hemibodies architecture from a 1st generation to the 2nd generation doubled the yield and had a major effect on its half-life considering the incorporation of a Fc-portion into the molecule.

Binding of the 2nd generation Hemibodies was examined by FACS, resulting in a 10-fold weaker binding compared with the respective BiTE antibodies. As the EC50 value was

determined in the nanomolar range, this difference is negligible for the constructs binding to CD133 and CD24. For the constructs binding to CD166, EC50 values are approximately 1000x weaker than the BiTE, which also translates into a reduced killing efficacy at lower concentrations. Increased EC50 values could be a result of the new split T-cell -engaging antibody format. Although the linkers are designed in a manner that no interaction between the target scFv and the split CD3 binder should occur (short linker between target scFv and αVH/VLCD3, long linker between VH and VL of target scFv) there is still the possibility of the αVH/VLCD3 to bind to either the VH or VL domain of the target scFv. This reversible mismatch pairing of variable domains could interfere with binding to target antigens resulting in higher EC50 values. Higher EC50 values in Hemibody combinations may not be disadvantageous but rather be beneficial. By having a lower binding capability, recruiting T-cells to double positive cells could be even more specific because only when both fragments are bound to the target cells binding affinity is high enough via avidity effects to retarget T-cells.

5.2.1 Establishment of testing systems for Hemibody killing efficacy and specificity

To assess killing efficacy and specifity of the Hemibody constructs, a read out system was established, expressing both target antigens (killing efficacy) and or only one target antigen (killing specificity). In a first attempt, adherent CHO cells were transfected with PiggyBac vectors expressing the target antigens. After sorting a FACS analysis confirmed expression of respective antigens. Obviously, all target antigens were expressed in almost 100% of CHO cells (Figure 9). Following the measurement of luciferase activity which has to be at least 50000 RLU for efficient determination of cell death cells could be used for downstream experiments.

Since the CHO cells are a highly artificial system, established colorectal cancer cell lines were transduced with lentivirus expressing firefly luciferase and GFP. GFP signal confirmed successful integration of the plasmid into target cells (Data not shown). Suitable cell lines expressing both antigens or only one were identified using FACS and transduction resulted in RLUs of almost $1 * 10^6$ RLUs allowing efficient measurement of cell killing. The usage of colorectal cancer cell lines allows the analysis of important factors, which influence killing, including the expression of co-receptors.

In summary a highly specific test system could be established successfully.

5.3 Biological characterization of Hemibodies

5.3.1 Killing efficacy and specifity

As stated earlier, CHO cells and established cancer cell lines were used in luciferase based killing assays for assessing the killing specificity and efficacy.

Starting with the 1st generation Hemibodies with diL2K as a CD3 binder, it is obvious that the combination CD133xCD24 showed a high killing efficacy with almost 80% killing in the nanomolar range. Looking at the single antigen positive CHO cells unfortunately killing is visible for the CHO^{CD24+} cell line indicating a lack of specificity. On the single antigen positive CHO cell line CHO^{CD133+} no killing was seen as expected. Titrating the concentration at lower concentrations a tendency to the double antigen positive CHO cells is visible. Off target killing on CHO^{CD24+} cells can be explained by a restoration of the split CD3 binding domain without the need of binding of the VH-Hemibody fragment. This can be due to a high affinity of the ternary complex consisting of αVH/VLCD3 together with CD3, resulting in binding of CD3 without the need of the Hemibody to be bound to a target cell. Reducing the affinity of the ternary complex via introduction of specific mutations into either the framework or CDR regions of the variable heavy and light chain domains of diL2K. Attempts to mutate diL2K failed in the lab so far due to lack of producibility of the mutants or a greatly reduced killing efficacy (Data not shown). Since random mutagenesis and testing of mutants via phage display technologies is very time consuming switching the CD3 clone from diL2K to UCHT1 was the easier and more promising attempt. In addition to that, the combinations CD133xCD166 and CD133xCEA also lacked in killing efficacy indicating the need for a CD3 binder inducing better killing. 1st generation Hemibodies with diL2K were produced in Shuffle T7 cells without further purifications steps including FPLC. Therefore, there is a high chance of multimers being present in the protein solution. Multimers could also be a possible reason for decreasing killing specificity. Several VH or VL fragments bound together in a multimer could result in recruiting a T-cell via avidity without the need of binding to a target cell. The above-mentioned results clearly justify the decision of switching the clone of the CD3 binder for better performance.

1st generation Hemibodies with UCHT1 as a CD3 binder produced in Shuffle T7 cells were also directly tested without further purification steps like FPLC-SEC. Killing efficacy was greatly enhanced compared to Hemibodies using diL2K indicated by efficient killing at all tested combinations already with using PBMCs as effector cells compared to pre-activated CD8+ T-cells. In terms of specificity, the switch to UCHT1 resulted in deterioration of the specificity as killing efficacy showed no tendency towards the

double antigen positive CHO cell line even when titrating the concentrations. Again, the presence of multimers could be an explanation for low specificity. Since production yields are also too low for UCHT1-Hemibodies produced in Shuffle T7 cells FPLC-SEC was not possible. Consequently, to exclude interference of multimers with specificity and efficacy production yield and purity had to be increased at first. As seen in

Figure ***14***/ Figure ***15*** the problem of low production yield and purity could be solved in ExpiHEK293 cells.

In terms of killing of killing, the 1st generation Hemibodies produced in ExpiHEK293 cells showed a great killing efficacy as seen in Figure 22/Figure ***23***. For both tested combinations a therapeutic window of at least one log level was achieved. Unfortunately, also the single fragment VHUCHT1-scFvCD133 induced high killings mainly on the double antigen positive cell line. Multimerization of this construct after binding could be a reason for that. Avidity of several VH-fragments could lead to a binding of T-cells inducing killing. Since the double antigen positive cell line seems to be more responsive to Hemibody induced killing, a therapeutic window could be achieved. Looking into the blocking experiment (Figure 22Figure 23C) only excess of scFvCD166 could efficiently block killing, indicating that either blocking is insufficient or the therapeutic window is indeed only achieved because of different sensitivities towards immunotherapy. More stable constructs, e.g. 2nd generation Hemibodies incorporating a Fc-portion could overcome the killing of single fragments. The enhanced size of these constructs could sterically hinder multimerization and the incorporation of the Fc-portion could lead to a different folding shielding the multimerization-prone hydrophobic split CD3 domain.

Preliminary in vivo half-life studies revealed a short half-life of only minutes to hours of 1st generation Hemibodies (Banaszek et al. 2019). As a result, treatment regimens need to include daily doses of Hemibody therapy for remission of tumors, which means a high burden for the patient. To overcome this issue and the issue of single fragment killing, 2nd generation Hemibodies incorporate a Fc-portion resulting in a more stable framework and in antibody recycling via FcRn receptors leading to extended half-lifes (Unverdorben et al. 2016) and less multimerization. The higher molecular weight also participates in half-life extension via a reduced renal clearance (Ahmad et al. 2012). To exclude the possibility of ADCC or CDC usually conferred by Fc portions, several mutations including the well published LALA mutation among others were introduced (Saunders 2019). Because of a changed architecture of the Hemibody, killing specificity and efficacy had to be determined again.

Again, this was tested on the artificial CHO system in a first attempt for the combinations CD133xCD24, CD133xCD166 and CD133xCEA. When applying both Hemibody fragments in a molar ratio of 1:1 over a concentration range of 0,01 nM to 20 nM for the combinations CD133xCD24 and CD133xCD166 and 0,1 nM to 100 nM for the combination CD133xCD166, killing was induced efficiently on the dual antigen positive cell lines with efficacies of almost 80% at the highest tested combinations. For all combinations, there was a clear tendency towards the double positive cell line. Unfortunately, off-target killing of single positive cells occurred at higher concentrations. Administering the Hemibodies in a 1:10 ration of VL:VH solved this issue opening a therapeutic window of one to two log levels without inducing off-target toxicity Figure 24. The reason for a shifted therapeutic window of the combination CD133xCD166 from 0,01 nM – 20 nM for the remaining combinations to 0,1 nM - 100 nM is a greatly decreased EC50 for the construct binding CD166. Due to its low affinity, killing is induced at higher concentrations. Despite having to use higher concentrations, off-target toxicity is significantly reduced compared to the remaining combinations. Administration of Hemibodies in a 1:10 ratio basically mimics lower affinity of one Hemibody, leading to the same effect of less off-target toxicity. Applying a CaspaseGlo 3/7 assay in parallel with luciferase based killing assays could validate the luciferase readout as a specific measurement for apoptosis and cell elimination (Figure 25).

Consequently, further improvements in Hemibodies specificity could be accomplished by mutating the target scFvs to reduce its affinity. Phage-Display technologies for introducing random mutations and screening could be a way to improve Hemibodies safety profile.

After testing 2nd generation Hemibodies on CHO cells, its efficacy and specificity needed to be tested on established cancer cell lines to see if the results are translatable into a less artificial system. Cancer cell lines have a more complex metabolism showing immune evasion strategies including immune check point variations what makes it crucial to check if Hemibdies confer toxicity in this setting, too.

Figure 26 depicts the combination CD133xCD24. Double antigen positive HT29 cells were used together with the single antigen positive cell lines Caco2 and A549. Killing was induced in HT29 cell to almost 100% at the highest tested combinations compared to almost no killing in the single positive cell lines. Only at higher concentrations above 10 nM, off-target toxicity is visible. A similar pattern is seen for the combination CD133xCD166, where efficient killing is induced in the double antigen positive cell line HCT116 whereas in the single antigen positive cell lines Caco2 and A549 no killing is

visible for all tested concentrations. Again, the combination CD133xCD166 shows a superior safety profile compared to the combination CD133xCD24 highlighting the importance of target scFv affinity. For the cell lines Caco2 and A549, a small proliferative effect is visible at higher concentrations. If the observed effect really is translated into a proliferation has to be further characterized, as higher RLUs compared to the negative control can also result from an enhanced luciferase expression per cell instead of more cells. CFSE based proliferation assays could clarify this phenomenon.

Since different cancer cell lines can be more or less resistant to different therapies, the above-described specificity could also result from more resistant single antigen positive cell lines. BiTE control killings already indicated a higher sensitivity of the double antigen positive towards immunotherapeutic targeting. Consequently, an experiment was performed where the double antigen positive cell lines were artificially transformed into single antigen positive cells by blocking target epitopes with scFvs in high excess against respective antigens. In this experiment a clear tendency towards the non-blocked cell lines is seen for both tested combinations (Figure 26; Figure 27). Since BiTE killing could not be blocked with scFvs efficiently, blockade of the epitopes was not sufficient. In further experiments, a higher excess of blocking agents or genetic deletion of respective antigens should be considered. Because there still was a significant tendency towards the non-blocked cell line, results from the killing assay performed on three separated cell lines could be confirmed. In addition to that a therapeutic window was also achieved in the artificial CHO cell system, which clearly has the same sensitivity towards therapy.

A last in-vitro assay was developed to further outline specificity of Hemibody combinations. All three cell lines (HT29, Caco2, A549) which were used in Figure 26 and Figure 27 were co cultivated, stained with CellTracker dyes for distinction and treated with the Hemibody regimens. By this it should be checked if the single Hemibody fragments are able to bind to single positive cells in close proximity to each other and thereby reconstitute the split CD3 moiety to redirect T-cells. This would lead to unwanted off-target toxicity and had to be clearly excluded. As seen in Figure 28, mixing of single and double antigen positive cell lines had no effect on Hemibodies' specificity. Only double antigen positive cells were killed whilst sparing the single antigen positive cell lines A549 and Caco2. Unfortunately, 7AAD staining was only slightly positive for the cell lines Caco2 and HT29. In future experiments other viability dyes like AnnexinV or PI could be included to increase the sensitivity of the killing readout. Besides above-mentioned adjustments, the mixed killing assay could exclude the last possible off target effect of 2nd generation Hemibodies.

In summary it can be said that in this thesis two fully functional Hemibody combinations could be developed which show great killing efficacy and specificity. Using Hemibody therapies in comparison to BiTE or CAR technologies could overcome their inherent and potentially fatal adverse effects including cytokine release syndromes by highly specific targeting of CSCs without off-target toxicities on healthy tissue (PubMed Central (PMC) 2021).

The fact that other labs also started developing dual antigen restricted strategies to redirect the immune system emphasizes the need for more specific immunotherapeutics. Revitope Oncology for example developed a similar approach of an antibody with a split CD3 domain termed as PrecisionGATE Technology (Revitope 2021). They further introduced a so-called stabilizing domain shielding the split CD3 domain from binding into a ternary complex together with CD3 and the other split CD3 domain. Once bound on tumor tissue, cancer specific proteases cleave off this stabilizing domain freeing αVH/VL domains for complementation. For half-life extension they included a half-life extender to the stabilizing domain instead of incorporating a Fc-part into the construct. Another lab tried to apply a dual antigen restricted targeting approach with CAR-T cells. They developed novel colocalization dependent protein switches (Co-LOCKR) expressed on CAR-T cells which enable the cells to be redirected against tumor cells expressing two surface antigens while avoiding off-target toxicity on single antigen cells and which add another level of recognition that allows to avoid or include cells expressing a third antigen (Lajoie et al. 2020).

Nonetheless, with the development of 2nd generation Hemibodies a huge step towards clinical applicability was made and translation into clinical studies can be pursued after confirming the above-mentioned in-vitro results with in vivo PDX models.

6. Outlook

This thesis mainly focused on the development of Hemibody pairs against CRC-CSC, its production and testing in vitro. Since a good producible 2nd generation Hemibody format with desired killing efficacy and specificity could be constructed in vitro, Hemibodies have to be tested in settings closer to actual tumors of patients in future experiments.

The first projected experiments are treatments of so called PDMs. Since PDMs are multicellular, hierarchical organized structures resembling the original tumor of patients, several more parameters influencing the functionality of Hemibodies including tumor infiltration, inhibitory effects of the TME and the effects of TILs other than CD8+ T-cells, can be addressed. Using single cell RNA-seq analysis the smallest effects of treatment on tumor signaling networks and metabolism can be revealed. In a projected cooperation with the NMI, Reutlingen under supervision of Prof. Dr. Christian Schmees Hemibodies efficacy, specificity and biological effect will be examined in future experiments according to the following working plan.

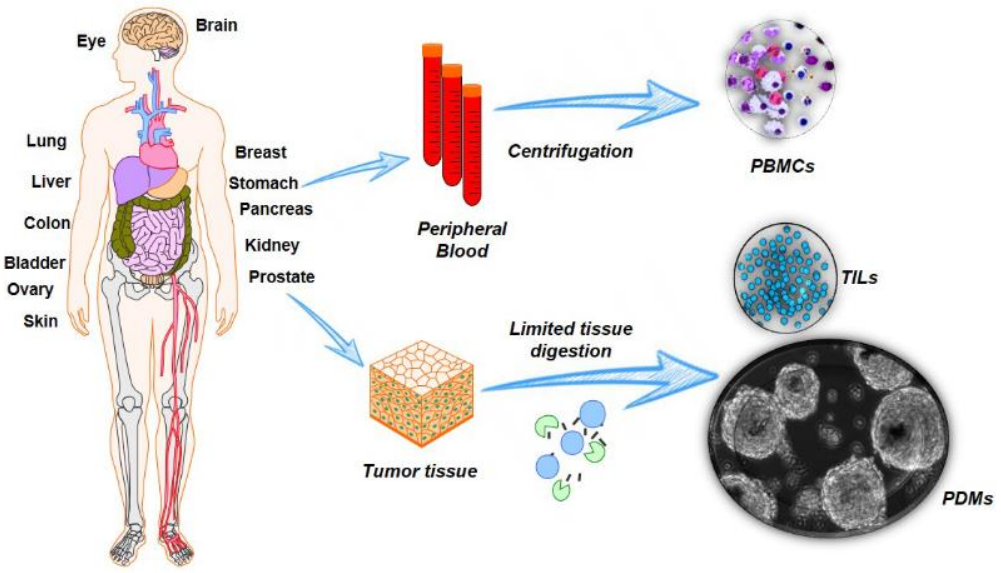

Figure 29: scheme of isolation of micro-tumors: via biopsies diseased tumor tissue is extracted from patients and transformed into micro-tumors via limited tissue digestion and cultivation under highly defined conditions. Furthermore autologous PBMCs can be extracted from the same patient to test the killing efficacy of several recombinant antibody fragments on micro-tumors (adapted from (Christian Schmees 2021)

As seen in Figure 29 micro tumors are developed by extraction of diseased tissue out of cancer patients and in vitro cultivation under defined conditions (for further information see (Przystal et al. 2021). These PDMs therefore reflect the heterogeneity of the original tumor consisting of cancer cells, CSCs, fibroblasts, epithelium and tumor infiltrating lymphocytes (TILs). In a first step micro-tumors resected from the colon are used to validate

co-expression of the combinations CD133xCD24 and CD133xCD166. Therefore, micro-tumors are stained using IHC with antibodies against respective antigens. Suitable PDMs were further used for testing the killing efficacy and specificity of Hemibodies. The combinations CD133xCD24 and CD133xCD166 are administered to PDMs together with autologous T-Cells in a 1:5 ratio. After several days treated tumors are again stained via IHC to see which subset of cancer cells was depleted. By counterstaining the tissue with several cell type specific markers exact determination of the cell type which was diminished could be achieved. Furthermore, RNA-single sequencing analysis shall be performed before and after administration of Hemibodies to check for efficient lysis of target cells and possible alterations of signaling or metabolic networks of the whole PDM.

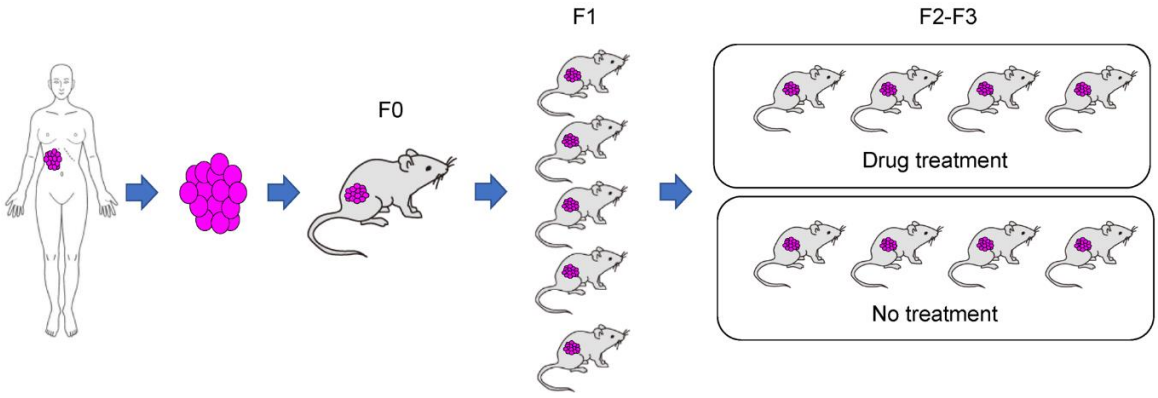

Figure 30: PDX model: resected tumor material is cultivated under defined conditions to micro tumors. Micro-tumors can be either directly treated with Hemibodies and subsequently transplanted into mice or transplanted into mice and treated afterwards (adapted from https://www.mdpi.com/2075-4426/10/3/64).

In a second step micro-tumors can be transplanted into PDX mouse models. Treatment regimens can be administered either before transplantation or after xeno-transplantation. Treating tumors after transplantation would include several new parameters including vascularization, treating tumors before transplantation could more specifically reveal the efficacy of 2nd generation Hemibodies against colorectal stem cells inhibiting the growing of a new tumor in vivo (Figure 30).

When all the above-mentioned experiments show promising results, 2nd generation Hemibodies could be translated into clinics for first trials on human tumors. In this thesis only the small fraction of cancer stem cells is targeted. Using different combinations, several other tumor populations ranging from small subfractions to very large tumor bulks can be targeted. This flexibility combined with its high specificity makes Hemibodies a promising immunotherapy with great potential for the future.

7. Supplementary data

7.1. Experimental data

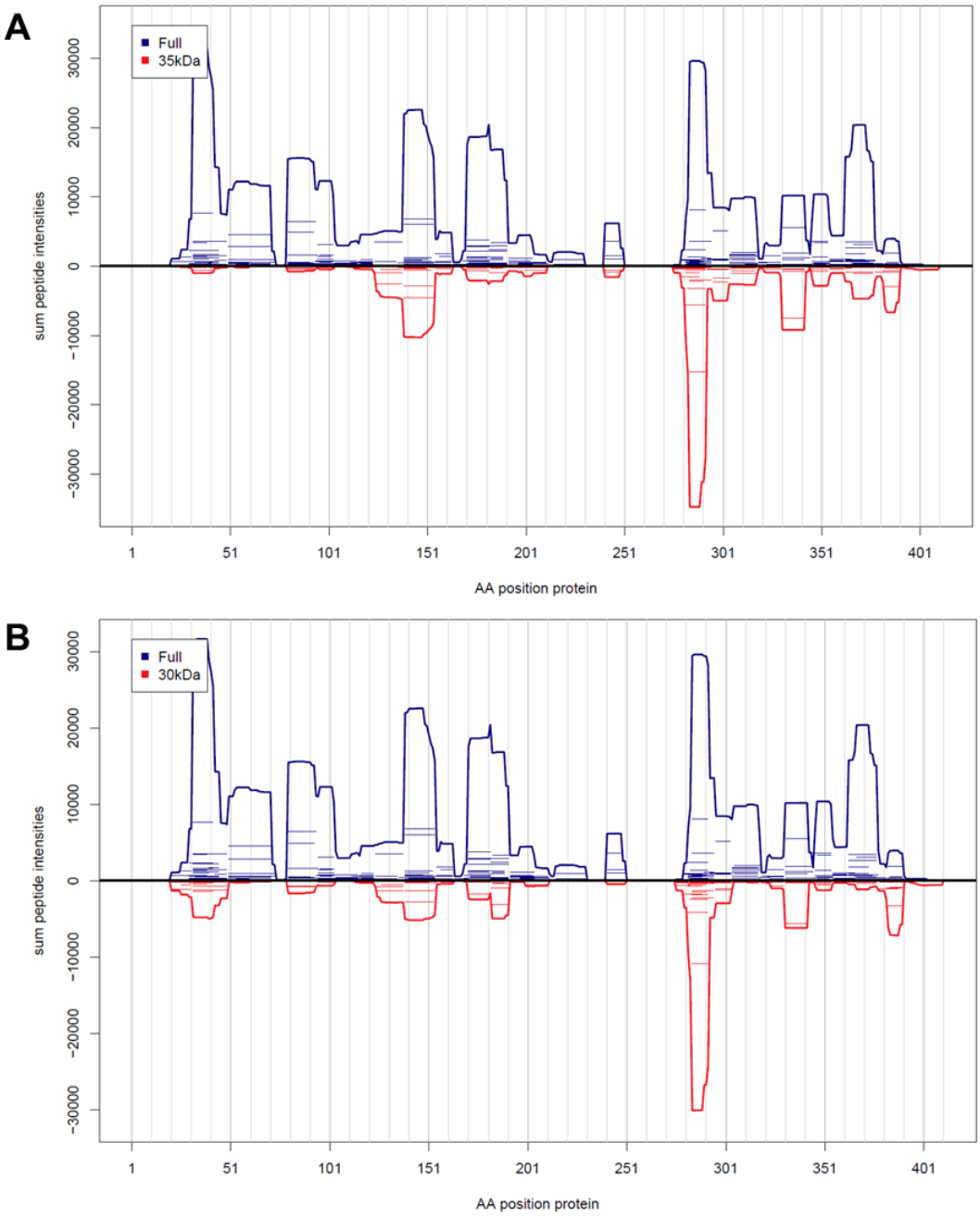

S 1: Peptide coverage of full length Hemibody vs 30 and 35 kDa degradation products: Mass spec analysis revealed the peptide coverage of a full hemibody compared to the (A) 35 kDa fragment and (B) 30 kDa fragment

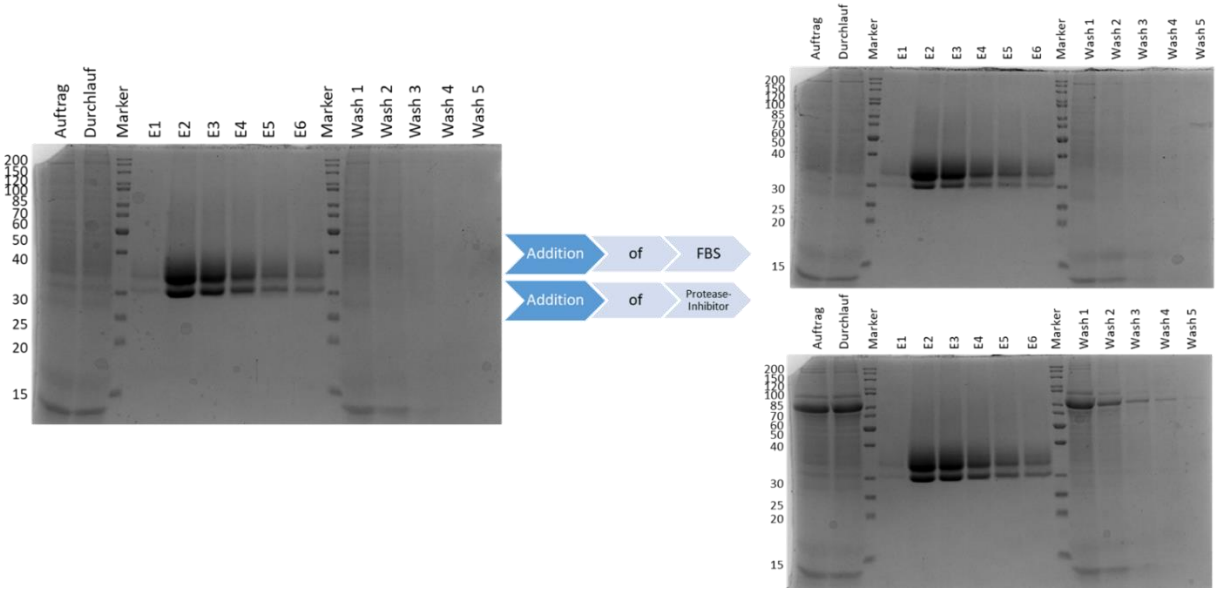

S 2: Hemibody production with the addition of protease inhibitors: Protease inhibitors (FBS, complete Protease inhibitor) were added to CHO suspension cultures. On the left a polyacrylamid gel w/o addition of inhibitors is shown, on the right the corresponding productions with FBS or complete protease inhibitor are depicted.

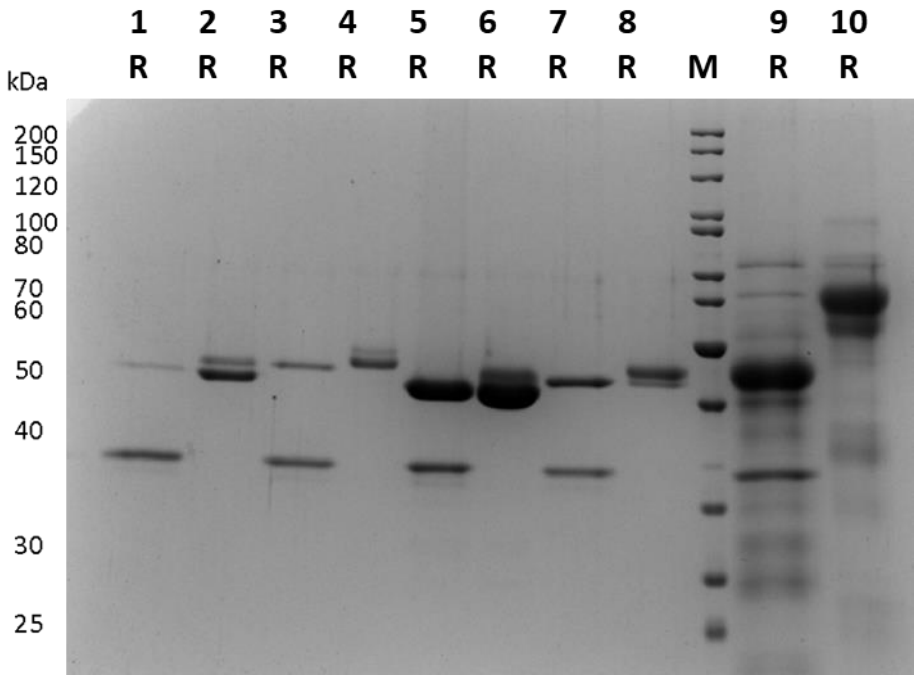

S 3: PNGase F digestion of 1st gen Hemibodies: SDS-PAGE analysis under reduced conditions (R). M, protein standard marker. Lane 1: VH-UCHT1_scFvCD133 digested; Lane 2: VH-UCHT1_scFvCD133 native; Lane 3: VL-UCHT1_scFvCD24 digested; Lane 4: VL-UCHT1_scFvCD24 native; Lane 5: VL-UCHT1_scFvCD166 digested; Lane 6: VL-UCHT1_scFvCD166 native; Lane 7: VL-UCHT1_scFvCEA digested; Lane 8: VL-UCHT1_scFvCEA native; Marker; Lane 9: Fetuin digested; Lane 10: Fetuin native

7.2. Sequences

7.2.1. Sequences of used scFvs against CSC markers

Target	Patent	Sequenz
CD24	Nadir Arber,Tel-Aviv US 8,614,301 B2 Dec. 24, 2013	DVHLQESGPDLVKPSQSLSLTCTVTGY- SITSGYTWHWIRQFPGNTVEWMGYIQYTG- STRYNPALRGRLSISRDTSKNQFFLQLISVTTADTGTYFCAR GTTASFDYWGQGTTLT- VASAGSAGGGGSGSGSGNGSGGGGSDIVMSQSPSSLNVS VGEKVTMRCRSSQSLLYSSDQKNYLTWYQQKPGQSPKLLIS WASTRASGVPDRFTGSGSGTDFTLTISSV- KAEDLGVYYCQQYFIYPLTFGVGTKLGLK
CD133	Universitätsklinikum Freiburg WO 2014/128185 A1 Aug. 28, 2014	QVQLQQSGAELVRPGASVKLSCKASGYTFSD- FEMHWVKQTPVHGLEWIG- DIDPGTGDTAYNLKFKGKATLTTDKSSSTAYMELRSLTSEDS AVYYCTLGAFVY- WGQGTLVTVSSGGGGSGSGSGNGSGGGGSDVVVTQT- PLSLPVSFGDQVSISCRSSQSLANSYGNTYLSWYLHKPGQS PQLLIYGISNRFSGVPDRFSGSGSGTDFTLKISTIKPED- LGMYYCLQGTHQPYTFGGGTKLEIK
CD166	CytomX Therapeutics Inc. WO 2016/179285 A1 Nov. 10, 2016	QITLKESGPTLVKPTQTLTLTCTFSGFSLSTYG- MGVGWIRQPPGKALEWLANI- WWSEDKHYSPSLKSRLTITKDTSKNQVVLTMTNMDPVDTAT YYCVQIDYGNDYAFTYWGQGTLVTVSSGGGGSGSGSGNGS GGGGSDIVMTQSPLSLPVTPGEPASISCRSSKSLLHSNGITY- LYWYLQKPGQSPQLLI- YQMSNLASGVPDRFSGSGSGTDFTLKISRVEAEDVGVYYCA QNLELPYTFGQGTKLEIK
CEA	Immunomedics Inc US 6,676,924 Jan. 13, 2004	EVQLVESGGGVVQPGRSLRLSCSSSGFDFTTYWMSWVR- QAPGKGLEWVAEIHPDSSTI- NYAPSLKDRFTISRDNSKNTLFLQMDSLRPEDTGVYFCASLY FGFPWFAY- WGQGTPVTVSSGGGGSGSGSGNGSGGGGSDIQLTQSPSS LSASVGDRVTITCKASQDVGTSVAWYQQKPGKAPKLLI- YWTSTRHTGVPSRFSGSGSGTDFTFTISSLQPEDIATYYCQQ YSLYRSFGGGTKVGIK

7.2.2. Sequences of used CD3 binders

7.2.2.1. dll2K

αCD3(VH) GS-Linker α-CD3(VL)

DVQLVQSGAEVKKPGASVKVSCKASGYTFTRYTMHWVRQAPGQGLEWIGYINPSRGYTN-
YADSVKGRFTITTDKSTSTAYMELSSLRSEDTATYYCARYYDDHYCLDYWGQGTTVTVSSG
GGGSGGGGSGGGGSDIVLTQSPATLSLSPGERATLSCRASQSVSYMNWYQQKPGKAP-
KR-
WIYDTSKVASGVPARFSGSGSGTDYSLTINSLEAEDAATYYCQQWSSNPLTFGGGTKVEIK

7.2.2.2. UCHT1

αCD3(VH) GS-Linker α-CD3(VL)

EVQLVESGGGLVQPGGSLRLSCAASGYSFTGYTMNWVRQAPGKGLEWVALINPYK-GVSTYNQKFKDRFTISVDKSKNTAYLQMNSLRAEDTAVYYCARSGYYGDSDWYFDVWGQ GTLVTVSSGGGGSGGGGSGGGGSDIQMTQSPSSLSAIVG-DRVTITCRASQDIRNYLNWYQQKPGKAPKLLIYYTSRLESGVPSRFSGSGSGTDYTLTISSL QPEDFATYYCQQGNTLPWTFGQGTKVEIK

7.2.3. Signal leader/ Tags

7.2.3.1. Thioredoxin Tag

Trx-Tag GS-Linker 3C-Protease restriction site

MSDKIIHLTDDSFDTDVLKADGAILVDFWAEWCGPCKMIAPILDEIADEYQGKLTVAKL-NIDQNPGTAPKYGIRGIPTLLLFKNGEVAATKVGALSKGQLKEFLDANLAGGSGGGGGSLEV LFQGP

7.2.3.2. 3C-Protease

GPNTEFALSLLRKNIMTITTSKGEFTGLGIHDRVCVIPT-HAQPGDDVLVNGQKIRVKDKYKLVDPENINLELTVLTLDRNEKFRDIRGFISEDLEGVDATLV VHSNNFTNTILEVGPVTMAGLINLSSTPTNRMIRYDYATKTGQCGGVLCATGKIF-GIHVGGNGRQGFSAQLKKQYFVEKQ

7.2.3.3. 6xHIS-Tag/ 8xHIS-Tag

HHHHHH/ HHHHHHHH

7.2.3.4. Twin-Strep-TagII

AWSHPQFEKGGGSGGGSGGSAWSHPQFEK

7.2.3.5. Signal Leader CHO/ ExpiHEK suspension cells

METDTLLVFVLLVWVPAGNG

7.2.4. Sequences of target antigens

7.2.4.1. CD24

MGRAMVARLGLGLLLLALLLPTQIYSSETTTGTSSNSSQSTSNSGLAPNPTNATTKAAG-GALQSTASLFVVSLSLLHLYS

7.2.4.2. CD133

MALVLGSLLLLGLCGNSFSGGQPSSTDAPKAWNYELPATNYETQDSHKAGPIGILFEL-
VHIFLYVVQPRDFPEDTLRKFLQKAYESKIDYDKIVYYEAGIILCCVLGLLFIILMPLVGYFFCM
CRCCNKCGGEMHQRQKENGPFLRKCFAISLLVICIIISIGIFYGFVANHQVRTRIKRS-
RKLADSNFKDLRTLLNETPEQIKYILAQYNTTKDKAFTDLNSINSVLGGGILDRLRPNIIPVLDEI
KSMATAIKETKEALENMNSTLKSLHQQSTQLSSSLTSVKTSLRSSLNDPLCLVHPS-
SETCNSIRLSLSQLNSNPELRQLPPVDAELDNVNNVLRTDLDGLVQQGYQSLNDIPDRVQR
QTTTVVAGIKRVLNSIGSDIDNVTQRLPIQDILSAFSVYVNNTESYIHRNLPTLEEYD-
SYWWLGGLVICSLLTLIVIFYYLGLLCGVCGYDRHATPTTRGCVSNTGGVFLMVGVGLSFLF
CWILMIIVVLTFVFGANVEKLICEPYTSKELFRVLDTPYLLNEDWEYYLSGKLFNKSKMKLT-
FEQVYSDCKKNRGTYGTLHLQNSFNISEHLNINEHTGSISSELESLKVNLNIFLLGAAGRKNL
QDFAACGIDRMNYDSYLAQTGKSPAGVNLLSFAYDLEAKANSLPPGNLRNSLKRDAQTIK-
TIHQQRVLPIEQSLSTLYQSVKILQRTGNGLLERVTRILASLDFAQNFITNNTSSVIIEETKKYG
RTIIGYFEHYLQWIEFSISEKVASCKPVATALDTAVDVFLCSYIIDPLNLFWFGIGKAT-
VFLLPALIFAVKLAKYYRRMDSEDVYDDVETIPMKNMENGNNGYHKDHVYGIHNPVMTSPS
QH

7.2.4.3. CD166

MESKGASSCRLLFCLLISATVFRPGLGWYTVNSAYGDTIIIPCRLDVPQNLM-
FGKWKYEKPDGSPVFIAFRSSTKKSVQYDDVPEYKDRLNLSENYTLSISNARISDEKRFVCM
LVTEDNVFEAPTIVKVFKQPSKPEIVSKALFLETEQLKKLGDCISEDSYPDGNITWYRNG-
KVLHPLEGAVVIIFKKEMDPVTQLYTMTSTLEYKTTKADIQMPFTCSVTYYGPSGQKTIHSEQ
AVFDIYYPTEQVTIQVLPPKNAIKEGDNITLKCLGNGNPPPEEFLFYLPGQPEGIRSSN-
TYTLTDVRRNATGDYKCSLIDKKSMIASTAITVHYLDLSLNPSGEVTRQIGDALPVSCTISASR
NATVVWMKDNIRLRSSPSFSSLHYQDAGNYVCETALQEVEGLKKRESLTLIVEGKPQIKMT-
KKTDPSGLSKTIICHVEGFPKPAIQWTITGSGSVINQTEESPYINGRYYSKIIISPEENVTLTCT
AENQLERTVNSLNVSAISIPEHDEADEISDENREKVNDQAKLIVGIVVGLLLAAL-
VAGVVYWLYMKKSKTASKHVNKDLGNMEENKKLEENNHKTEA

7.2.4.4. CEA

MESPSAPPHRWCIPWQRLLLTASLLTFWNPPTTAKLTIESTPFNVAEGKEVLLLVHNLPQHL-
FGYSWYKGERVDGNRQIIGYVIGTQQATPGPAYSGREIIYPNASLLIQNIIQNDTGFYTLHVIK
SDLVNEEATGQFRVYPELPKPSISSNNSKPVEDKDAVAFTCPETQDATYLWWVNNQSLPV-
SPRLQLSNGNRTLTLFNVTRNDSASYKCETQNPVSARRSDSVILNVLYGPDAPTISPLNTSY
RSGENLNLSCHAASNPPAQYSWFVNGTFQQSTQELFIPNITVNNSGSYTCQAHNSDT-
GLNRVTTITVYAEPPKPFITSNNSNPVEDEDAVALTCEPEIQNTTYLWWVNNQSLPVSPRLQ

LSNDNRTLTLLSVTRNDVGPYECGIQNELSVDHSDPVILNVLYGPDDPTISPSY-
TYYRPGVNLSLSCHAASNPPAQYSWLIDGNIQQHTQELFISNITEKNSGLYTCQANNSASGH
SRTTVKTITVSAELPKPSISSNNSKPVEDKDAVAFTCEPEAQNTTYLWWVNGQSLPV-
SPRLQLSNGNRTLTLFNVTRNDARAYVCGIQNSVSANRSDPVTLDVLYGPDTPIISPPDSSYL
SGANLNLSCHSASNPSPQYSWRINGIPQQHTQVLFIAKITPNNNGTYACFVSNLATGRNN-
SIVKSITVSASGTSPGLSAGATVGIMIGVLVGVALI

7.2.5. Example sequences of Hemibodies/ BiTEs/ target antigens

7.2.5.1. Shuffle T7/ pCold constructs (pCold-VHUCHT1-scFvCD24)

Trx-Tag GS-Linker 3C-Protease restriction site αCD3(VH) GS-linker
αCD24(VH) GS-Linker αCD24(VL) 8xHIS-Tag

MSDKIIHLTDDSFDTDVLKADGAILVDFWAEWCGPCKMIAPILDEIADEYQGKLT-
VAKLNIDQNPGTAPKYGIRGIPTLLLFKNGEVAATKVGALSKGQLKEFLDANLAGGSGGGGG
SLEVLFQGPMEVQLVESGGLVQPGGSLRLSCAASGYSFTGYTMNWVR-
QAPGKGLEWVALINPYKGVSTYNQKFKDRFTISVDKSKNTAYLQMNSLRAEDTAVYYCARS
GYYGDSDWYFDVWGQGTLVTVSSGGGGSDVHLQESGPDLVKPSQSLSLTCTVTGY-
SITSGYTWHWIRQFPGNTVEWMGYIQYTGSTRYNPALRGRLSISRDTSKNQFFLQLISVTTA
DTGTYFCARGTTASFDYWGQGTTLT-
VASAGSAGGGGSGSGSGNGSGGGGSDIVMSQSPSSLNVSVGEKVTMRCRSSQSLLYSSD
QKNYLTWYQQKPGQSPKLLISWASTRASGVPDRFTGSGSGTDFTLTISSV-
KAEDLGVYYCQQYFIYPLTFGVGTKLGLKVDGGGGSHHHHHHHH*

7.2.5.2. CHO/ pCET1019AS constructs (CET1019AS-Hygro-diL2KVH-CD24)

Signal Leader αCD3(VH) GS-linker αCD24(VH) GS-Linker αCD24(VL)
Twin-Strep-TagII

METDTLLVFVLLVWVPAGNGDVQLVQSGAEVKKPGASVKVSCKAS-
GYTFTRYTMHWVRQAPGQGLEWIGYINPSRGYTNYADSVKGRFTITTDKSTSTAYMELSSL
RSEDTATYYCARYYDDHYCLDYWGQGTTVTVSSGGGGSDVHLQESGPDLVKPSQSLSLT-
CTVTGYSITSGYTWHWIRQFPGNTVEWMGYIQYTGSTRYNPALRGRLSISRDTSKNQFFLQ
LISVTTADTGTYFCARGTTASFDYWGQGTTLTVASAGSAGGGGSGSGSGNGSGGGGS-
DIV-
MSQSPSSLNVSVGEKVTMRCRSSQSLLYSSDQKNYLTWYQQKPGQSPKLLISWASTRASG
VPDRFTGSGSGTDFTLTISSVKAEDLGVYYCQQYFIYPLTFGVGTKLGLKS-
SSSSSAWSHPQFEKGGGSGGGSGGSAWSHPQFEK*

7.2.5.3. ExpiHEK/ pCEP4 constructs 1st generation Hemibodies (VLUCHT1-scFvCD24)

Signal Leader αCD3(VL) GS-linker αCD24(VH) GS-Linker αCD24(VL) 8xHIS-Tag

METDTLLVFVLLVWVPAGNGEFDIQMTQSPSSLSASVG-
DRVTITCRASQDIRNYLNWYQQKPGKAPKLLIYYTSRLESGVPSRFSGSGSGTDYTLTISSL
QPEDFATYYCQQGNTLPWTFGQGTKVEIKSGGGGSDVHLQESGPDLVKP-
SQSLSLTCTVTGY-
SITSGYTWHWIRQFPGNTVEWMGYIQYTGSTRYNPALRGRLSISRDTSKNQFFLQLISVTTA
DTGTYFCARGTTASFDYWGQGTTLT-
VASAGSAGGGGSGSGSGNGSGGGGSDIVMSQSPSSLNVSVGEKVTMRCRSSQSLLYSSD
QKNYLTWYQQKPGQSPKLLISWASTRASGVPDRFTGSGSGTDFTLTISSV-
KAEDLGVYYCQQYFIYPLTFGVGTKLGLKVDGGGGSHHHHHHHH*

7.2.5.4. ExpiHEK/ pCEP4 constructs 2nd generation Hemibodies

pCEP4-scFvCD24-Fc hole (kiHs-s)

Signal Leader GS-linker αCD24(VH) GS-Linker αCD24(VL) Fc hole

METDTLLVFVLLVWVPAGNGEFDVHLQESGPDLVKPSQSLSLTCTVTGY-
SITSGYTWHWIRQFPGNTVEWMGYIQYTGSTRYNPALRGRLSISRDTSKNQFFLQLISVTTA
DTGTYFCARGTTASFDYWGQGTTLT-
VASAGSAGGGGSGSGSGNGSGGGGSDIVMSQSPSSLNVSVGEKVTMRCRSSQSLLYSSD
QKNYLTWYQQKPGQSPKLLISWASTRASGVPDRFTGSGSGTDFTLTISSV-
KAEDLGVYYCQQYFIYPLTFGVGTKLGLKSGGGGSDKTHTCPPCPAPEAAGGPSVFLFPPK
PKDTLMISRTPEVTCVVVDVSHEDPEVKFNWYVDGVEVHNAK-
TKPREEQYASTYRVVSVLTVLHQDWLNGKEYKCKVSNKALPAPIEKTISKAKGQPREPQVC
TLPPSRDELTKNQVSLSCAVKGFYPSDIAVEWESNGQPENNYKTTPPVLDSDGS-
FFLVSKLTVDKSRWQQGNVFSCSVMHEALHNHYTQKSLSLSPGK*

pCEP4-VLUCHT1-Fc knob (kiHs-s)

Signal Leader GS-linker αCD3(VL) GS-Linker αCD24(VL) Fc knob 6xHIS-Tag

METDTLLVFVLLVWVPAGNGDIQMTQSPSSLSASVGDRVTIT-
CRASQDIRNYLNWYQQKPG-
KAPKLLIYYTSRLESGVPSRFSGSGSGTDYTLTISSLQPEDFATYYCQQGNTLPWTFGQGTK
VEIKSGGGGSDKTHTCPPCPAPEAAGGPSVFLFPPKPKDTLMISRTPE-
VTCVVVDVSHEDPE-
VKFNWYVDGVEVHNAKTKPREEQYASTYRVVSVLTVLHQDWLNGKEYKCKVSNKALPAPIE
KTISKAKGQPREPQVYTLPPCRDELTKNQVSLWCLVKGFYPSDIAVEWESNGQPENNYKT-
T-
PPVLDSDGSFFLYSKLTVDKSRWQQGNVFSCSVMHEALHNHYTQKSLSLSPGKVDGSHHH
HHH*

7.2.5.5. CHO-K1 adherent/ PiggyBac constructs

PB01_CD24

ECD CD24 mRuby PuroR T2A

MGRAMVARLGLGLLLLALLLPTQIYSSETTTGTSSNSSQSTSNSGLAPNPT-
NATTKAAGGALQSTASLFVVSLSLLHLYS*
MASSEDVIKEFMRFKVKMEGSVNGHEFEIEGEGEGRPYEGTQTAKLKVTKGGPLPFSWDIL-
SPQFQYGSKAYVKHPADIPDYLKLSFPEGFKWERFMNFEDGGVVTVTQDSTLQDGEFIYKV
KLRGTNFPSDGPVMQKKTMGWEASTERMYPEDGALKGEIKMRLKLKDGGHYDAEV-
KTTYKAKKQVQLPGAYMTDIKLDIISHNGDYTIVEQYERAEGRHSTGAGEGRGSLLTCGDVE
ENPGPMTEYKPTVRLATRDDVPRAVRTLAAAFADYPATRHTVDPDRHIERVTEL-
QELFLTRVGLDIGKVWVADDGAAVAVWTTPESVEAGAVFAEIGPRMAELSGSRLAAQQQM
EGLLAPHRPKEPAWFLATVGVSPDHQGKGLGSAVVLPGVE-
AAERAGVPAFLETSAPRNLPFYERLGFTVTADVEVPEGPRTWCMTRKPGA*

PB02_CD24

ECD CD24 Firefly Luciferase

MGRAMVARLGLGLLLLALLLPTQIYSSETTTGTSSNSSQSTSNSGLAPNPTNATTKAAG-GALQSTASLFVVSLSLLHLYS*
MEDAKNIKKGPAPFYPLEDGTAGEQLHKAMKRYALVPGTIAFTDAHIEVDITYAEYFEMSVR-LAEAMKRYGLNTNHRIVVCSENSLQFFMPVLGALFIGVAVAPANDIYNERELLNSMGISQPTV VFVSKKGLQKILNVQKKLPIIQKIIIMDSKTDYQGFQSMYTFVTSHLPPGFNEYDFVPESF-DRDKTIALIMNSSGSTGLPKGVALPHRTACVRFSHARDPIFGNQIIPDTAILSVVPFHHGFGM FTTLGYLICGFRVVLMYRFEEELFLRSLQDYKIQSALLVPTLFSFFAKSTLIDKYDLSNL-HEIASGGAPLSKEVGEAVAKRFHLPGIRQGYGLTETTSAILITPEGDDKPGAVGKVVPFFEAK VVDLDTGKTLGVNQRGELCVRGPMIMSGYVNNPEATNALIDKDGWLHSGDIAYWDE-DEHFFIVDRLKSLIKYKGYQVAPAELESILLQHPNIFDAGVAGLPDDDAGELPAAVVVLEHGK TMTEKEIVDYVASQVTTAKKLRGGVVFVDEVPKGLTGKLDARKIREILIKAKKGGKIAV*

7.3. Plasmids

7.3.1. pColdIV

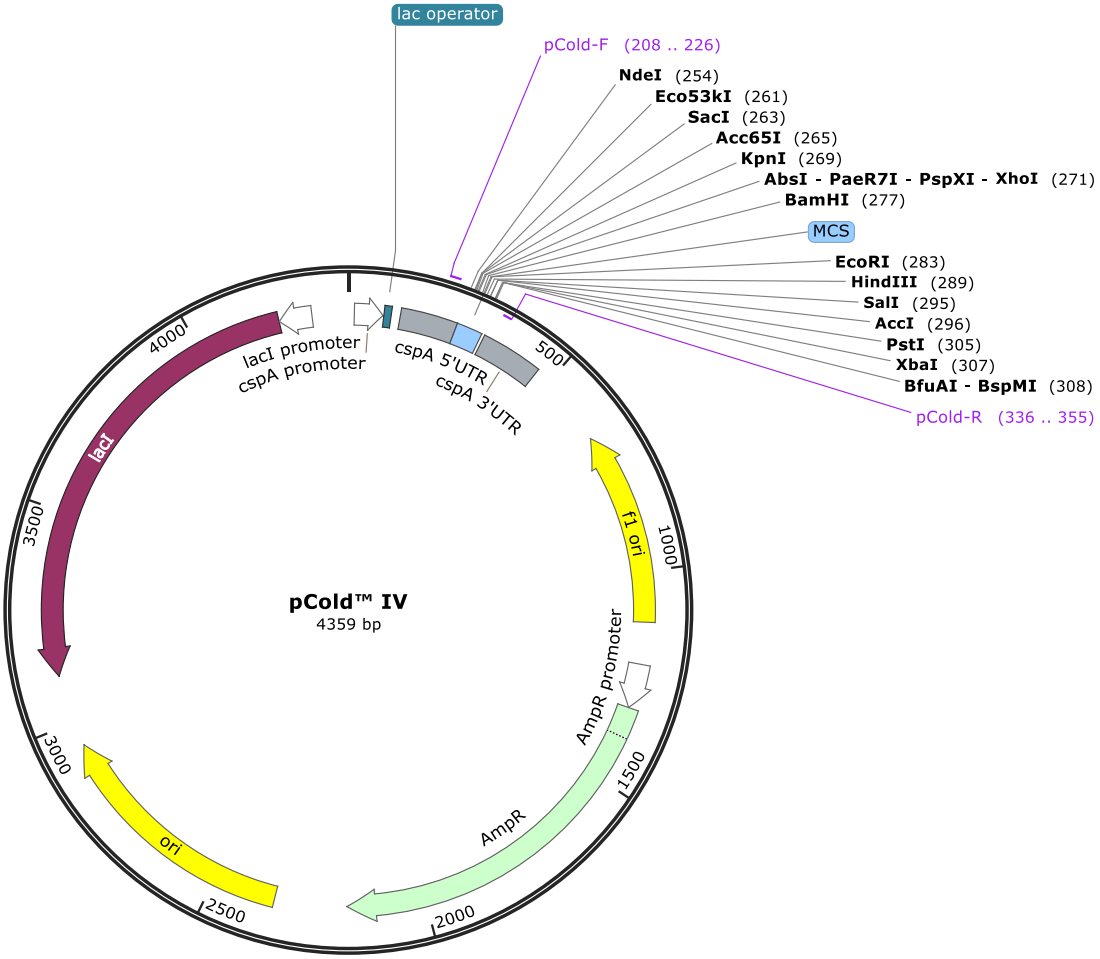

S 4: Vector map pColdIV: pColdIV has an ampicillin resistance gene, lac operator and cspA Promoter. Hemibodies were cloned into MCS together with a Thioredoxin-tag for better solubility and folding and a 3C Protease cleavage site. pColdIV was purchased from TaKaRa Bio (Cat: 3364)

7.3.2. pRSF-DUET

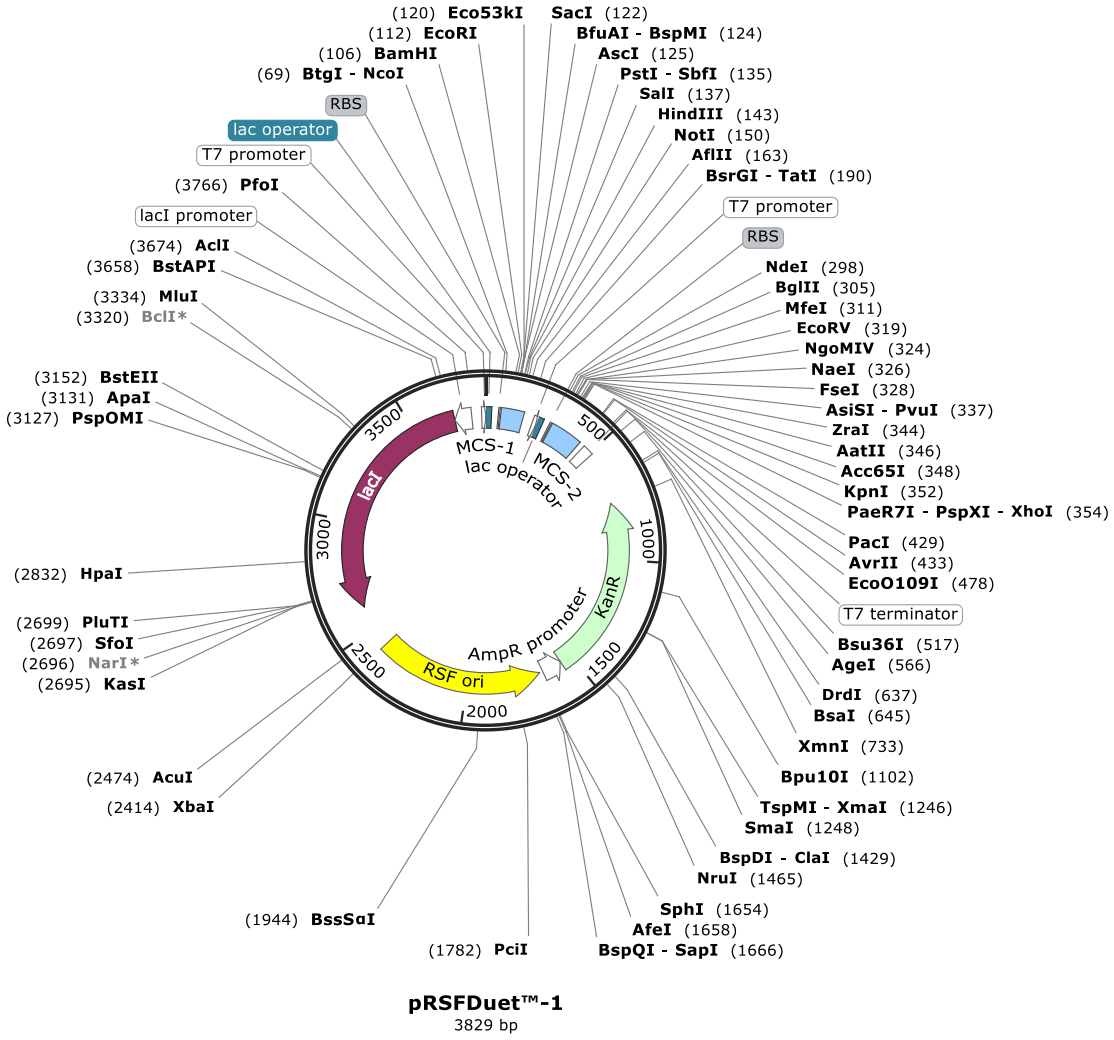

S 5: Vector map pRSFDUET: The plasmid contains two MCS, a T7-lac promotor and a kanamycin resistance gene. 3C-Protease was cloned into this vector for production of Hemibodies in Shuffle T7 cells.

7.3.3. pCET1019AS-hygro

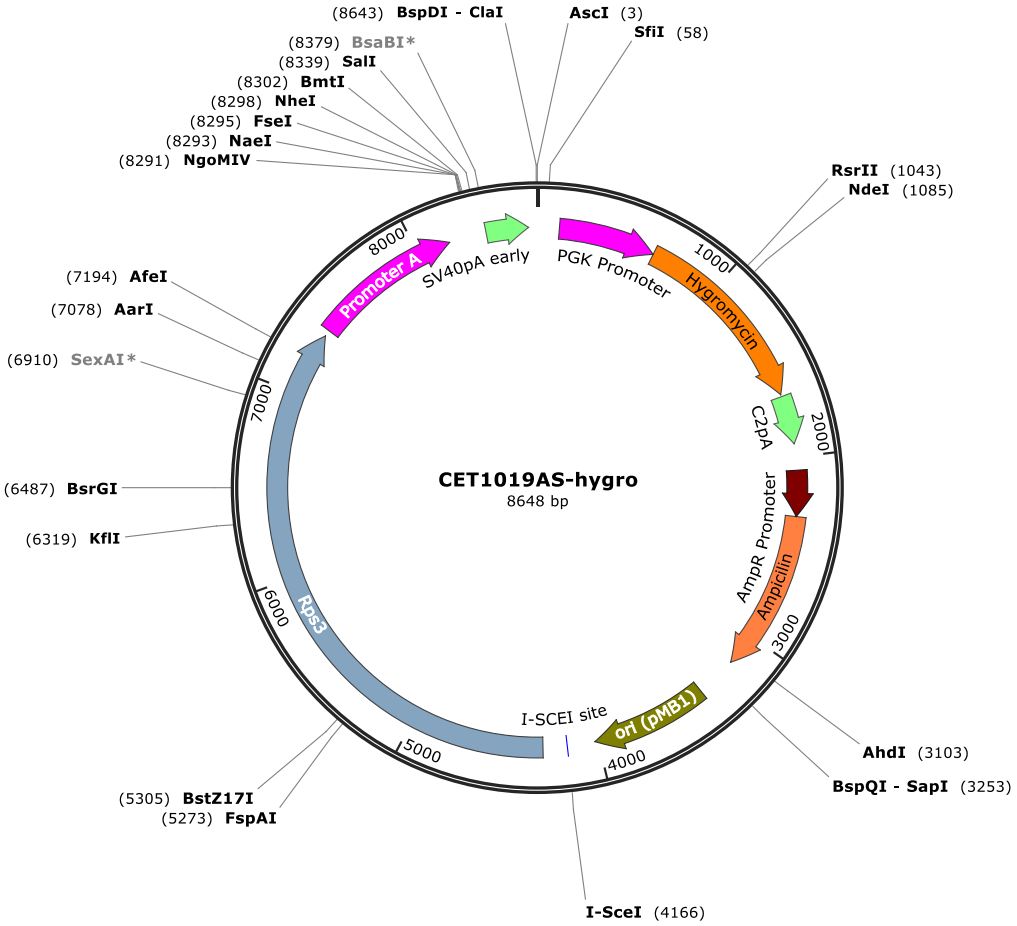

S 6: pCET1019AS-hygro: The vector is a mammalian expression plasmid containing the mouse Rps3 UCOE and a strong human cytomegalovirus (hCMV) immediate early promoter-enhancer element for stable integration into eukaryotic cells. For antibiotic selection a hygromycin resistance gene is included. The vector was used for stable CHO expression of Hemibodies. The vector was purchased from Merck (Cat: UC0E02)

7.3.4. pCET1019AS-puro

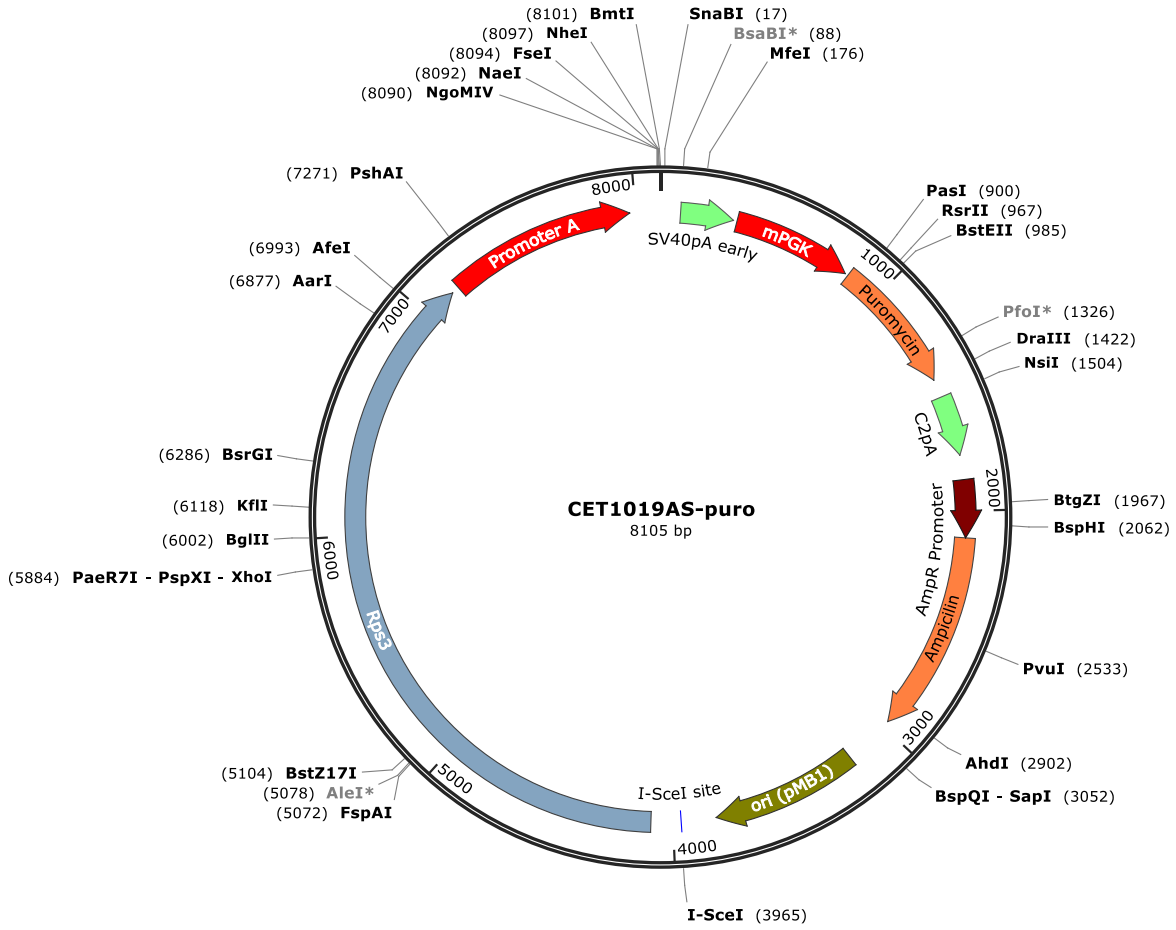

S 7: pCET1019AS-puro: Same vector as pCET1019AS-hygro (**Fehler! Verweisquelle konnte nicht gefunden werden.**). Instead of hygromycin, puromycin is incorporated into plasmid for antibiotic selection.

7.3.5. pCEP4

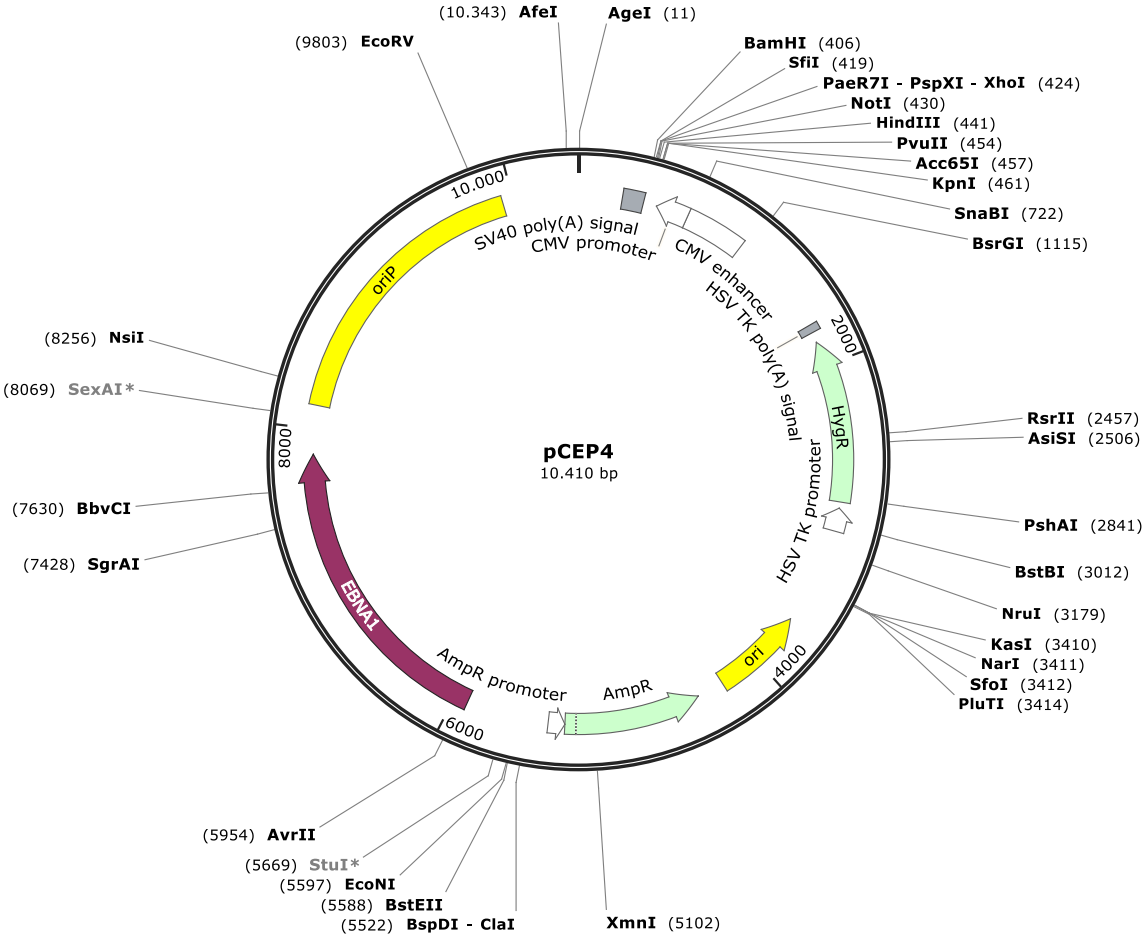

S 8: Vector map pCEP4: pCEP4 is an episomal mammalian expression vector. High level transcription is ensured by a strong CMV promoter. Via EBNA-1 gene extrachromosomal repilication is possible in human cells. For stable selection of transfected cells hygromycin B is incorporated into plasmid. The plasmid was used for transient expression of Hemibodies in ExpiHEK cells. It was purchased from Invitrogen (Cat: V044-50).

7.3.6. PB01

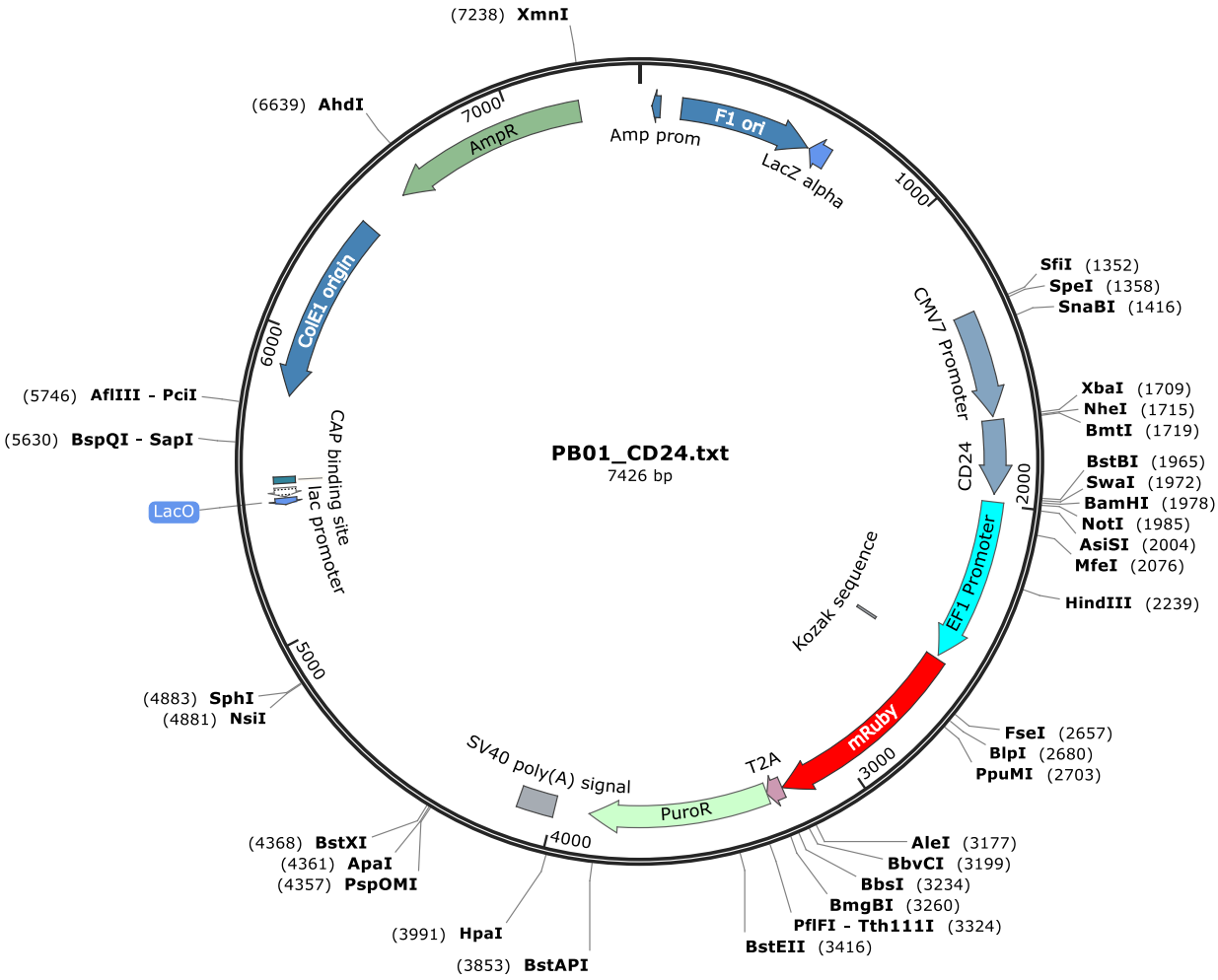

S 9: Vector map PB01: Leverage PiggyBac vector for making stable transgenic cell lines coexpressing mRuby. PB01_CD24 is shown as an example with CD24 cloned into the MCS. High expression of target antigens is accomplished by a CMV promoter. Stable cell line selection is possible due to puromycin resistance gene incorporated into the plasmid. The vector was originally purchased by System Biosciences.

7.3.7. PB02

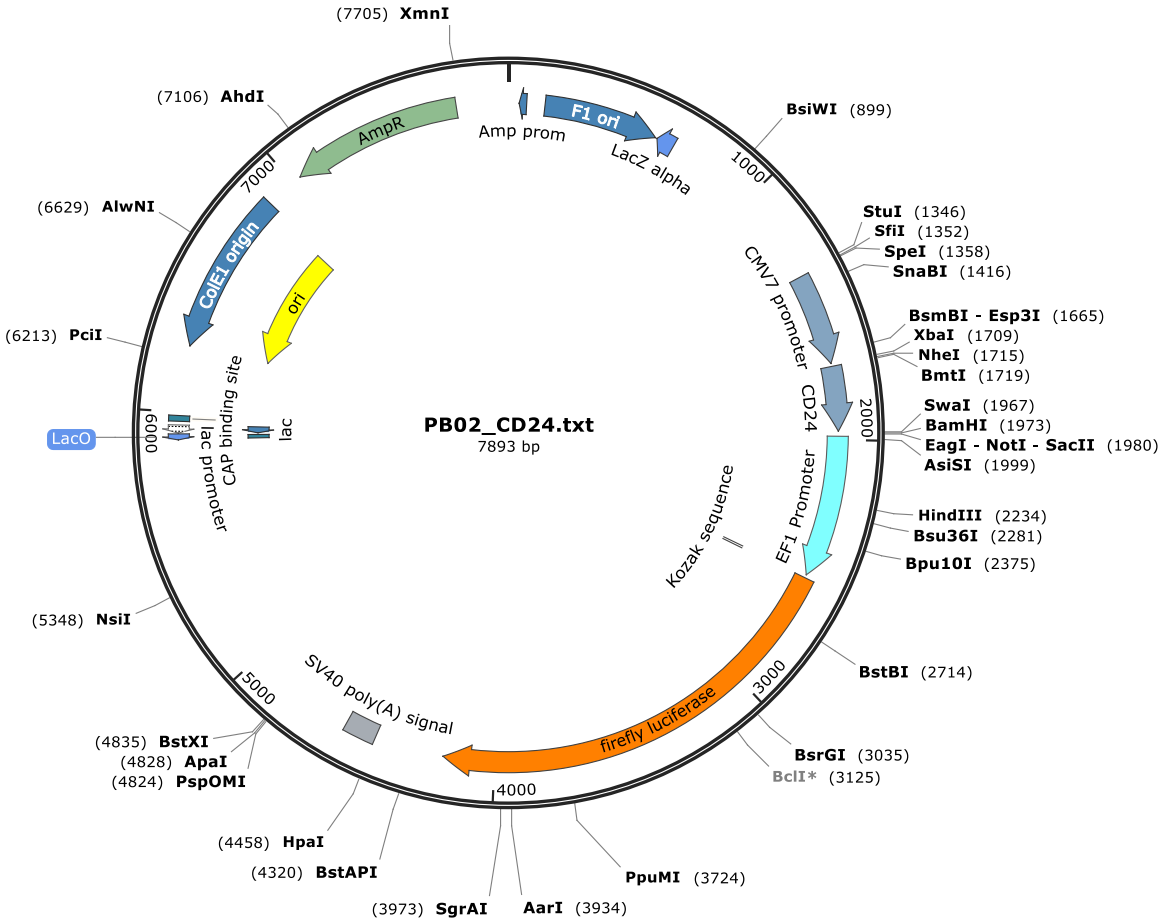

S 10: Vector map PB02: Same vector as PB01 (**Fehler! Verweisquelle konnte nicht gefunden werden.**). Instead of having mRuby and a puromycinR gene after the EF1 promoter, a firefly luciferase is incorporated into the plasmid. The vector was originally purchased by System Biosciences.

8. Acknowledgments

In this section I want to thank following persons.

First of all, my professor and first supervisor Prof. Dr. Gernot Stuhler for the chance to work in the Hemibody group on such an interesting topic and his support throughout the time. It was a great pleasure for me to be part of the team in the last four years. I also owe thanks to Dr. Hannes Neuweiler from the JMU for the willingness of appraisal of my thesis.

I also want to thank the post docs Boris Nowotny, Tim Schneyder and Toey for the great input they gave me, when I was stuck on the project. A special thanks to all the great people I was working with including the PhDs Marc-Dominic Bohn and Maria Geis, the lab staff Wen and Szn Yi for always helping me with FACS etc, or great meals in the lunch time. The great support of Thomas Renzing and Keali Rhöm was always keeping my back free in the lab.

Finally, I also want to thank my family for supporting me in my PhD time, especially my wife Alina for always being there for me, in good and in bad times, where nothing worked as expected.

Literaturverzeichnis

A. Yadav; N. Desai (2019): Cancer Stem Cells: Acquisition, Characteristics, Therapeutic Implications, Targeting Strategies and Future Prospects. In: *undefined*. Online verfügbar unter https://www.semanticscholar.org/paper/Cancer-Stem-Cells%3A-Acquisition%2C-Characteristics%2C-Yadav-Desai/c333ef2d03b1ca7f9b7ac42f6f888ec48f07a865.

Abramson, C. S.; Kersey, J. H.; LeBien, T. W. (1981): A monoclonal antibody (BA-1) reactive with cells of human B lymphocyte lineage. In: *Journal of immunology (Baltimore, Md. : 1950)* 126 (1), S. 83–88.

Ahmad, Zuhaida Asra; Yeap, Swee Keong; Ali, Abdul Manaf; Ho, Wan Yong; Alitheen, Noorjahan Banu Mohamed; Hamid, Muhajir (2012): scFv antibody: principles and clinical application. In: *Clinical & developmental immunology* 2012, S. 980250. DOI: 10.1155/2012/980250.

Ahmed, Syed Ijlal; Javed, Gohar; Laghari, Altaf Ali; Bareeqa, Syeda Beenish; Farrukh, Saba; Zahid, Shajeeah et al. (2018): CD133 Expression in Glioblastoma Multiforme: A Literature Review. In: *Cureus* 10 (10), e3439. DOI: 10.7759/cureus.3439.

Al-Hajj, Muhammad; Wicha, Max S.; Benito-Hernandez, Adalberto; Morrison, Sean J.; Clarke, Michael F. (2003): Prospective identification of tumorigenic breast cancer cells. In: *Proceedings of the National Academy of Sciences of the United States of America* 100 (7), S. 3983–3988. DOI: 10.1073/pnas.0530291100.

Another clinical trial of Amgen's BiTE therapy has been suspended - iNEWS (2021). Online verfügbar unter https://inf.news/en/science/3341323b744864702f6fe4fa53aa5199.html, zuletzt aktualisiert am 27.08.2021, zuletzt geprüft am 27.08.2021.

Bai, Rui; Shi, Zhong; Zhang, Jia-wei; Li, Dan; Zhu, Yong-liang; Zheng, Shu (2012): ST13, a proliferation regulator, inhibits growth and migration of colorectal cancer cell lines. In: *Journal of Zhejiang University. Science. B* 13 (11), S. 884–893. DOI: 10.1631/jzus.B1200037.

Banaszek, Agnes; Bumm, Thomas G. P.; Nowotny, Boris; Geis, Maria; Jacob, Kim; Wölfl, Matthias et al. (2019): On-target restoration of a split T cell-engaging antibody for precision immunotherapy. In: *Nat Commun* 10 (1), S. 5387. DOI: 10.1038/s41467-019-13196-0.

Bar, Eli E.; Chaudhry, Aneeka; Lin, Alex; Fan, Xing; Schreck, Karisa; Matsui, William et al. (2007): Cyclopamine-mediated hedgehog pathway inhibition depletes stem-like cancer cells in glioblastoma. In: *Stem cells (Dayton, Ohio)* 25 (10), S. 2524–2533. DOI: 10.1634/stemcells.2007-0166.

Barker, Nick; Ridgway, Rachel A.; van Es, Johan H.; van de Wetering, Marc; Begthel, Harry; van den Born, Maaike et al. (2009): Crypt stem cells as the cells-of-origin of intestinal cancer. In: *Nature* 457 (7229), S. 608–611. DOI: 10.1038/nature07602.

Beauchemin, Nicole; Arabzadeh, Azadeh (2013): Carcinoembryonic antigen-related cell adhesion molecules (CEACAMs) in cancer progression and metastasis. In: *Cancer metastasis reviews* 32 (3-4), S. 643–671. DOI: 10.1007/s10555-013-9444-6.

Beckmann, Anja; Hainz, Nadine; Tschernig, Thomas; Meier, Carola (2019): Facets of Communication: Gap Junction Ultrastructure and Function in Cancer Stem Cells and Tumor Cells. In: *Cancers* 11 (3). DOI: 10.3390/cancers11030288.

Bertolini, Giulia; Roz, Luca; Perego, Paola; Tortoreto, Monica; Fontanella, Enrico; Gatti, Laura et al. (2009): Highly tumorigenic lung cancer CD133+ cells display stem-like features and are spared by cisplatin treatment. In: *Proceedings of the National Academy of Sciences of the United States of America* 106 (38), S. 16281–16286. DOI: 10.1073/pnas.0905653106.

Bhatia, Vipul; Yadav, Anjali; Tiwari, Ritika; Nigam, Shivansh; Goel, Sakshi; Carskadon, Shannon et al. (2019): Epigenetic Silencing of miRNA-338-5p and miRNA-421 Drives SPINK1-Positive Prostate Cancer. In: *Clin Cancer Res* 25 (9), S. 2755–2768. DOI: 10.1158/1078-0432.CCR-18-3230.

Bircan, Sema; Kapucuoglu, Nilgun; Baspinar, Sirin; Inan, Gulsun; Candir, Ozden (2006): CD24 expression in ductal carcinoma in situ and invasive ductal carcinoma of breast: an immunohistochemistry-based pilot study. In: *Pathology, research and practice* 202 (8), S. 569–576. DOI: 10.1016/j.prp.2006.05.004.

Bisson, Isabelle; Prowse, David M. (2009): WNT signaling regulates self-renewal and differentiation of prostate cancer cells with stem cell characteristics. In: *Cell research* 19 (6), S. 683–697. DOI: 10.1038/cr.2009.43.

Bonnet, D.; Dick, J. E. (1997): Human acute myeloid leukemia is organized as a hierarchy that originates from a primitive hematopoietic cell. In: *Nature medicine* 3 (7), S. 730–737. DOI: 10.1038/nm0797-730.

Bornhorst, J. A.; Falke, J. J. (2000): Purification of proteins using polyhistidine affinity tags. In: *Methods in enzymology* 326, S. 245–254. DOI: 10.1016/s0076-6879(00)26058-8.

Bray, Freddie; Ferlay, Jacques; Soerjomataram, Isabelle; Siegel, Rebecca L.; Torre, Lindsey A.; Jemal, Ahmedin (2018): Global cancer statistics 2018: GLOBOCAN estimates of incidence and mortality worldwide for 36 cancers in 185 countries. In: *CA: a cancer journal for clinicians* 68 (6), S. 394–424. DOI: 10.3322/caac.21492.

Buache, E.; Etique, N.; Alpy, F.; Stoll, I.; Muckensturm, M.; Reina-San-Martin, B. et al. (2011): Deficiency in trefoil factor 1 (TFF1) increases tumorigenicity of human breast cancer cells and mammary tumor development in TFF1-knockout mice. In: *Oncogene* 30 (29), S. 3261–3273. DOI: 10.1038/onc.2011.41.

Canis, Martin; Lechner, Axel; Mack, Brigitte; Zengel, Pamela; Laubender, Rüdiger Paul; Koehler, Udo et al. (2013): CD133 induces tumour-initiating properties in HEK293 cells. In: *Tumor Biol.* 34 (1), S. 437–443. DOI: 10.1007/s13277-012-0568-z.

Cayrol, Romain; Wosik, Karolina; Berard, Jennifer L.; Dodelet-Devillers, Aurore; Ifergan, Igal; Kebir, Hania et al. (2008): Activated leukocyte cell adhesion molecule promotes leukocyte trafficking into the central nervous system. In: *Nature immunology* 9 (2), S. 137–145. DOI: 10.1038/ni1551.

Chaffer, Christine L.; Marjanovic, Nemanja D.; Lee, Tony; Bell, George; Kleer, Celina G.; Reinhardt, Ferenc et al. (2013): Poised chromatin at the ZEB1 promoter enables breast cancer cell plasticity and enhances tumorigenicity. In: *Cell* 154 (1), S. 61–74. DOI: 10.1016/j.cell.2013.06.005.

Chan, Carlos H. F.; Cook, Denise; Stanners, Clifford P. (2006): Increased colon tumor susceptibility in azoxymethane treated CEABAC transgenic mice. In: *Carcinogenesis* 27 (9), S. 1909–1916. DOI: 10.1093/carcin/bgl040.

Chen, Li-Sha; Wang, An-Xin; Dong, Bing; Pu, Ke-Feng; Yuan, Li-Hua; Zhu, Yi-Min (2012): A new prospect in cancer therapy: targeting cancer stem cells to eradicate cancer. In: *Chinese journal of cancer* 31 (12), S. 564–572. DOI: 10.5732/cjc.011.10444.

Chen, Yan-Jie; Luo, Shu-Neng; Dong, Ling; Liu, Tao-Tao; Shen, Xi-Zhong; Zhang, Ning-Ping; Liang, Li (2021): Interferon regulatory factor family influences tumor immunity and prognosis of patients with colorectal cancer. In: *Journal of translational medicine* 19 (1), S. 379. DOI: 10.1186/s12967-021-03054-3.

Chen, Zhong; Xu, Wen-Rong; Qian, Hui; Zhu, Wei; Bu, Xue-Feng; Wang, Sheng et al. (2009): Oct4, a novel marker for human gastric cancer. In: *Journal of surgical oncology* 99 (7), S. 414–419. DOI: 10.1002/jso.21270.

Choi, Dongho; Lee, Hyo-Won; Hur, Kyung-Yul; Kim, Jae-Joon; Park, Gyeong-Sin; Jang, Si-Hyong et al. (2009): Cancer stem cell markers CD133 and CD24 correlate with invasiveness and differentiation in colorectal adenocarcinoma. In: *World journal of gastroenterology* 15 (18), S. 2258–2264. DOI: 10.3748/wjg.15.2258.

Christian Schmees (2021): Isolation of PDMs. Online verfügbar unter https://www.nmi-tt.de/pharmaservices/immuno-oncology-services/.

Cioffi, Michele; D'Alterio, Crescenzo; Camerlingo, Rosalba; Tirino, Virginia; Consales, Claudia; Riccio, Anna et al. (2015): Identification of a distinct population of CD133(+)CXCR4(+) cancer stem cells in ovarian cancer. In: *Sci Rep* 5 (1), S. 10357. DOI: 10.1038/srep10357.

Cizelsky, Wiebke; Tata, Aleksandra; Kühl, Michael; Kühl, Susanne J. (2014): The Wnt/JNK signaling target gene alcam is required for embryonic kidney development. In: *Development* 141 (10), S. 2064–2074. DOI: 10.1242/dev.107938.

Cochrane, Catherine R.; Szczepny, Anette; Watkins, D. Neil; Cain, Jason E. (2015): Hedgehog Signaling in the Maintenance of Cancer Stem Cells. In: *Cancers* 7 (3), S. 1554–1585. DOI: 10.3390/cancers7030851.

Collins, Anne T.; Berry, Paul A.; Hyde, Catherine; Stower, Michael J.; Maitland, Norman J. (2005): Prospective identification of tumorigenic prostate cancer stem cells. In: *Cancer research* 65 (23), S. 10946–10951. DOI: 10.1158/0008-5472.CAN-05-2018.

Conaghan, Pj; Ashraf, Sq; Tytherleigh, Mg; Wilding, Jl; Tchilian, E.; Bicknell, D. et al. (2008): Targeted killing of colorectal cancer cell lines by a humanised IgG1 monoclonal antibody that binds to membrane-bound carcinoembryonic antigen. In: *British journal of cancer* 98 (7), S. 1217–1225. DOI: 10.1038/sj.bjc.6604289.

Cui, Hong-Yong; Wang, Shi-Jie; Song, Fei; Cheng, Xu; Nan, Gang; Zhao, Yu et al. (2021): CD147 receptor is essential for TFF3-mediated signaling regulating colorectal cancer progression. In: *Sig Transduct Target Ther* 6 (1), S. 268. DOI: 10.1038/s41392-021-00677-2.

Cytiva (2021): Quick fixes for retention time issues - Cytiva. Online verfügbar unter https://www.cytivalifesciences.com/en/us/solutions/protein-research/knowledge-center/protein-purification-methods/Chromatography-troubleshooting/quick-fixes-for-retention-time-issues, zuletzt aktualisiert am 12.10.2021, zuletzt geprüft am 12.10.2021.

Dave, Bhuvanesh; Granados-Principal, Sergio; Zhu, Rui; Benz, Stephen; Rabizadeh, Shahrooz; Soon-Shiong, Patrick et al. (2014): Targeting RPL39 and MLF2 reduces tumor initiation and metastasis in breast cancer by inhibiting nitric oxide synthase signaling. In: *Proceedings of the National Academy of Sciences of the United States of America* 111 (24), S. 8838–8843. DOI: 10.1073/pnas.1320769111.

Deonarain, Mahendra P.; Kousparou, Christina A.; Epenetos, Agamemnon A. (2009): Antibodies targeting cancer stem cells: a new paradigm in immunotherapy? In: *mAbs* 1 (1), S. 12–25. DOI: 10.4161/mabs.1.1.7347.

Devkota, Suzanne; Wang, Yunwei; Musch, Mark W.; Leone, Vanessa; Fehlner-Peach, Hannah; Nadimpalli, Anuradha et al. (2012): Dietary-fat-induced taurocholic acid promotes pathobiont expansion and colitis in Il10-/- mice. In: *Nature* 487 (7405), S. 104–108. DOI: 10.1038/nature11225.

Diekmann, Heike; Stuermer, Claudia A. O. (2009): Zebrafish neurolin-a and -b, orthologs of ALCAM, are involved in retinal ganglion cell differentiation and retinal axon pathfinding. In: *The Journal of comparative neurology* 513 (1), S. 38–50. DOI: 10.1002/cne.21928.

Einsele, Hermann; Borghaei, Hossein; Orlowski, Robert Z.; Subklewe, Marion; Roboz, Gail J.; Zugmaier, Gerhard et al. (2020): The BiTE (bispecific T-cell engager) platform: Development and future potential of a targeted immuno-oncology therapy across tumor types. In: *Cancer* 126 (14), S. 3192–3201. DOI: 10.1002/cncr.32909.

Espinosa-Sánchez, Asunción; Suárez-Martínez, Elisa; Sánchez-Díaz, Laura; Carnero, Amancio (2020): Therapeutic Targeting of Signaling Pathways Related to Cancer Stemness. In: *Frontiers in oncology* 10, S. 1533. DOI: 10.3389/fonc.2020.01533.

Espinoza, Ingrid; Agarwal, Sumit; Reddy, Amit; Shenoy, Veena; Subramony, Charulochana; Sakiyama, Marcelo et al. (2021): Expression of trefoil factor 3 is decreased in colorectal cancer. In: *Oncology reports* 45 (1), S. 254–264. DOI: 10.3892/or.2020.7829.

Fan, Xing; Khaki, Leila; Zhu, Thant S.; Soules, Mary E.; Talsma, Caroline E.; Gul, Naheed et al. (2010): NOTCH pathway blockade depletes CD133-positive glioblastoma cells and inhibits growth of tumor neurospheres and xenografts. In: *Stem cells (Dayton, Ohio)* 28 (1), S. 5–16. DOI: 10.1002/stem.254.

Fan, Xing; Matsui, William; Khaki, Leila; Stearns, Duncan; Chun, Jiong; Li, Yue-Ming; Eberhart, Charles G. (2006): Notch pathway inhibition depletes stem-like cells and blocks engraftment in embryonal brain tumors. In: *Cancer research* 66 (15), S. 7445–7452. DOI: 10.1158/0008-5472.CAN-06-0858.

Fanali, Caterina; Lucchetti, Donatella; Farina, Marisa; Corbi, Maddalena; Cufino, Valerio; Cittadini, Achille; Sgambato, Alessandro (2014): Cancer stem cells in colorectal cancer from pathogenesis to therapy: controversies and perspectives. In: *World journal of gastroenterology* 20 (4), S. 923–942. DOI: 10.3748/wjg.v20.i4.923.

Fang, Lishan; Cai, Junchao; Chen, Baixue; Wu, Shanshan; Li, Rong; Xu, Xiaonan et al. (2015): Aberrantly expressed miR-582-3p maintains lung cancer stem cell-like traits by activating Wnt/β-catenin signalling. In: *Nature communications* 6, S. 8640. DOI: 10.1038/ncomms9640.

Fang, Xianfeng; Zheng, Pan; Tang, Jie; Liu, Yang (2010a): CD24: from A to Z. In: *Cell Mol Immunol* 7 (2), S. 100–103. DOI: 10.1038/cmi.2009.119.

Fang, Xianfeng; Zheng, Pan; Tang, Jie; Liu, Yang (2010b): CD24: from A to Z. In: *Cell Mol Immunol* 7 (2), S. 100–103. DOI: 10.1038/cmi.2009.119.

Farid, Rola M.; Sammour, Sanaa Abd-Elmaged; Shehab ElDin, Zeinab Abdelkader; Salman, Manal Ibrahim; Omran, Tag Ibrahim (2019): Expression of CD133 and CD24 and their different phenotypes in urinary bladder carcinoma. In: *CMAR* 11, S. 4677–4690. DOI: 10.2147/CMAR.S198348.

Fedyanin, Mikhail; Anna, Popova; Elizaveta, Polyanskaya; Sergei, Tjulandin (2017): Role of Stem Cells in Colorectal Cancer Progression and Prognostic and Predictive Characteristics of Stem Cell Markers in Colorectal Cancer. In: *Current stem cell research & therapy* 12 (1), S. 19–30. DOI: 10.2174/1574888x11666160905092938.

Feng, Dongfeng; Peng, Gong; Li, Wei; Xu, Hongmei; Zhang, Tianqi; Wang, Nanya (2015): Identification and Characterization of Tumorigenic Liver Cancer Stem Cells by CD133 and CD24. In: *j biomater tissue eng* 5 (8), S. 635–646. DOI: 10.1166/jbt.2015.1363.

Francipane, Maria Giovanna; Alea, Mileidys Perez; Lombardo, Ylenia; Todaro, Matilde; Medema, J. P.; Stassi, Giorgio (2008): Crucial role of interleukin-4 in the survival of colon

cancer stem cells. In: *Cancer Res* 68 (11), S. 4022–4025. DOI: 10.1158/0008-5472.CAN-07-6874.

Fujiwara, Kenji; Ohuchida, Kenoki; Sada, Masafumi; Horioka, Kohei; Ulrich, Charles D.; Shindo, Koji et al. (2014): CD166/ALCAM expression is characteristic of tumorigenicity and invasive and migratory activities of pancreatic cancer cells. In: *PloS one* 9 (9), e107247. DOI: 10.1371/journal.pone.0107247.

Gao, Dan; Han, Yingjie; Yang, Yang; Herman, James G.; Linghu, Enqiang; Zhan, Qimin et al. (2017): Methylation of TMEM176A is an independent prognostic marker and is involved in human colorectal cancer development. In: *Epigenetics* 12 (7), S. 575–583. DOI: 10.1080/15592294.2017.1341027.

Geis, Maria; Nowotny, Boris; Bohn, Marc-Dominic; Kouhestani, Dina; Einsele, Hermann; Bumm, Thomas; Stuhler, Gernot (2021): Combinatorial targeting of multiple myeloma by complementing T cell engaging antibody fragments. In: *Commun Biol* 4 (1), S. 44. DOI: 10.1038/s42003-020-01558-0.

Gimferrer, Idoia; Calvo, Maria; Mittelbrunn, María; Farnós, Montse; Sarrias, Maria Rosa; Enrich, Carlos et al. (2004): Relevance of CD6-mediated interactions in T cell activation and proliferation. In: *Journal of immunology (Baltimore, Md. : 1950)* 173 (4), S. 2262–2270. DOI: 10.4049/jimmunol.173.4.2262.

Giordano, Marco; Cavallaro, Ugo (2020): Different Shades of L1CAM in the Pathophysiology of Cancer Stem Cells. In: *Journal of clinical medicine* 9 (5). DOI: 10.3390/jcm9051502.

Gisina, Alisa; Novikova, Svetlana; Kim, Yan; Sidorov, Dmitry; Bykasov, Stanislav; Volchenko, Nadezhda et al. (2021): CEACAM5 overexpression is a reliable characteristic of CD133-positive colorectal cancer stem cells. In: *Cancer biomarkers : section A of Disease markers*. DOI: 10.3233/CBM-203187.

Glumac, Paige M.; LeBeau, Aaron M. (2018): The role of CD133 in cancer: a concise review. In: *Clinical and Translational Medicine* 7 (1), S. 18. DOI: 10.1186/s40169-018-0198-1.

Gonzalez, R.; Griparic, L.; Vargas, V.; Burgee, K.; Santacruz, P.; Anderson, R. et al. (2009): A putative mesenchymal stem cells population isolated from adult human testes. In: *Biochemical and biophysical research communications* 385 (4), S. 570–575. DOI: 10.1016/j.bbrc.2009.05.103.

Gupta, Ruby; Sinha, Surajit; Paul, Rabindra N. (2018): The impact of microsatellite stability status in colorectal cancer. In: *Current problems in cancer* 42 (6), S. 548–559. DOI: 10.1016/j.currproblcancer.2018.06.010.

Guzman, M. L.; Neering, S. J.; Upchurch, D.; Grimes, B.; Howard, D. S.; Rizzieri, D. A. et al. (2001): Nuclear factor-kappaB is constitutively activated in primitive human acute myelogenous leukemia cells. In: *Blood* 98 (8), S. 2301–2307. DOI: 10.1182/blood.v98.8.2301.

Gzil, Arkadiusz; Zarębska, Izabela; Bursiewicz, Wiktor; Antosik, Paulina; Grzanka, Dariusz; Szylberg, Łukasz (2019): Markers of pancreatic cancer stem cells and their clinical and therapeutic implications. In: *Mol Biol Rep* 46 (6), S. 6629–6645. DOI: 10.1007/s11033-019-05058-1.

Hadjimichael, Christiana; Chanoumidou, Konstantina; Papadopoulou, Natalia; Arampatzi, Panagiota; Papamatheakis, Joseph; Kretsovali, Androniki (2015): Common stemness regulators of embryonic and cancer stem cells. In: *World journal of stem cells* 7 (9), S. 1150–1184. DOI: 10.4252/wjsc.v7.i9.1150.

Han, Sei-Myoung; Han, Sang-Hun; Coh, Ye-Rin; Jang, Goo; Chan Ra, Jeong; Kang, Sung-Keun et al. (2014): Enhanced proliferation and differentiation of Oct4- and Sox2-

overexpressing human adipose tissue mesenchymal stem cells. In: *Exp Mol Med* 46 (6), e101. DOI: 10.1038/emm.2014.28.

Hatano, Yuichiro; Fukuda, Shinya; Hisamatsu, Kenji; Hirata, Akihiro; Hara, Akira; Tomita, Hiroyuki (2017): Multifaceted Interpretation of Colon Cancer Stem Cells. In: *IJMS* 18 (7), S. 1446. DOI: 10.3390/ijms18071446.

Heidel, Florian H.; Bullinger, Lars; Feng, Zhaohui; Wang, Zhu; Neff, Tobias A.; Stein, Lauren et al. (2012): Genetic and pharmacologic inhibition of β-catenin targets imatinib-resistant leukemia stem cells in CML. In: *Cell stem cell* 10 (4), S. 412–424. DOI: 10.1016/j.stem.2012.02.017.

Hirata, Hirokazu; Murakami, Yoshinobu; Miyamoto, Yoshiaki; Tosaka, Mako; Inoue, Kayoko; Nagahashi, Ayako et al. (2006): ALCAM (CD166) is a surface marker for early murine cardiomyocytes. In: *Cells, tissues, organs* 184 (3-4), S. 172–180. DOI: 10.1159/000099624.

Honegger, Annemarie; Malebranche, Alain Daniel; Röthlisberger, Daniela; Plückthun, Andreas (2009): The influence of the framework core residues on the biophysical properties of immunoglobulin heavy chain variable domains. In: *Protein Eng Des Sel* 22 (3), S. 121–134. DOI: 10.1093/protein/gzn077.

Horst, David; Kriegl, Lydia; Engel, Jutta; Kirchner, Thomas; Jung, Andreas (2009a): Prognostic significance of the cancer stem cell markers CD133, CD44, and CD166 in colorectal cancer. In: *Cancer investigation* 27 (8), S. 844–850. DOI: 10.1080/07357900902744502.

Horst, David; Scheel, Silvio K.; Liebmann, Sibylle; Neumann, Jens; Maatz, Susanne; Kirchner, Thomas; Jung, Andreas (2009b): The cancer stem cell marker CD133 has high prognostic impact but unknown functional relevance for the metastasis of human colon cancer. In: *The Journal of pathology* 219 (4), S. 427–434. DOI: 10.1002/path.2597.

Hua, Jinlian; Yu, Haisheng; Dong, Wuzi; Yang, Chunrong; Gao, Zhimin; Lei, Anmin et al. (2009): Characterization of mesenchymal stem cells (MSCs) from human fetal lung: potential differentiation of germ cells. In: *Tissue & cell* 41 (6), S. 448–455. DOI: 10.1016/j.tice.2009.05.004.

Hummel, Horst-Dieter; Kufer, Peter; Grüllich, Carsten; Deschler-Baier, Barbara; Chatterjee, Manik; Goebeler, Maria-Elisabeth et al. (2019): Phase 1 study of pasotuxizumab (BAY 2010112), a PSMA-targeting Bispecific T cell Engager (BiTE) immunotherapy for metastatic castration-resistant prostate cancer (mCRPC). In: *JCO* 37 (15_suppl), S. 5034. DOI: 10.1200/JCO.2019.37.15_suppl.5034.

Imaizumi, Hideko; Ishibashi, Keiichiro; Takenoshita, Seiichi; Ishida, Hideyuki (2018): Aquaporin 1 expression is associated with response to adjuvant chemotherapy in stage II and III colorectal cancer. In: *Oncology letters* 15 (5), S. 6450–6456. DOI: 10.3892/ol.2018.8170.

Jacob, Juliane; Bellach, Joachim; Grützmann, Robert; Alldinger, Ingo; Pilarsky, Christian; Dietel, Manfred; Kristiansen, Glen (2004): Expression of CD24 in adenocarcinomas of the pancreas correlates with higher tumor grades. In: *Pancreatology : official journal of the International Association of Pancreatology (IAP) … [et al.]* 4 (5), S. 454–460. DOI: 10.1159/000079824.

Jagust, Petra; Alcalá, Sonia; Sainz Jr, Bruno; Heeschen, Christopher; Sancho, Patricia (2020): Glutathione metabolism is essential for self-renewal and chemoresistance of pancreatic cancer stem cells. In: *World journal of stem cells* 12 (11), S. 1410–1428. DOI: 10.4252/wjsc.v12.i11.1410.

Jassal, Bijay; Matthews, Lisa; Viteri, Guilherme; Gong, Chuqiao; Lorente, Pascual; Fabregat, Antonio et al. (2020): The reactome pathway knowledgebase. In: *Nucleic Acids Research* 48 (D1), D498-D503. DOI: 10.1093/nar/gkz1031.

Ji, Wei; Rivero, Francisco (2016): Atypical Rho GTPases of the RhoBTB Subfamily: Roles in Vesicle Trafficking and Tumorigenesis. In: *Cells* 5 (2). DOI: 10.3390/cells5020028.

Jia, Yunlu; Ying, Xiaogang; Zhou, Jichun; Chen, Yongxia; Luo, Xiao; Xie, Shudu et al. (2018): The novel KLF4/PLAC8 signaling pathway regulates lung cancer growth. In: *Cell death & disease* 9 (6), S. 603. DOI: 10.1038/s41419-018-0580-3.

Jiao, Jing; Hindoyan, Antreas; Wang, Shunyou; Tran, Linh M.; Goldstein, Andrew S.; Lawson, Devon et al. (2012): Identification of CD166 as a surface marker for enriching prostate stem/progenitor and cancer initiating cells. In: *PloS one* 7 (8), e42564. DOI: 10.1371/journal.pone.0042564.

Karaöz, Erdal; Doğan, Burcu Nur; Aksoy, Ayça; Gacar, Gülçin; Akyüz, Serap; Ayhan, Selda et al. (2010): Isolation and in vitro characterisation of dental pulp stem cells from natal teeth. In: *Histochemistry and cell biology* 133 (1), S. 95–112. DOI: 10.1007/s00418-009-0646-5.

Katoh, Masuko; Katoh, Masaru (2020): Precision medicine for human cancers with Notch signaling dysregulation (Review). In: *International journal of molecular medicine* 45 (2), S. 279–297. DOI: 10.3892/ijmm.2019.4418.

Kawasaki, Yoshihiro; Matsumura, Kosuke; Miyamoto, Masaya; Tsuji, Shinnosuke; Okuno, Masumi; Suda, Sakiko et al. (2015): REG4 is a transcriptional target of GATA6 and is essential for colorectal tumorigenesis. In: *Sci Rep* 5, S. 14291. DOI: 10.1038/srep14291.

Kay, R.; Takei, F.; Humphries, R. K. (1990): Expression cloning of a cDNA encoding M1/69-J11d heat-stable antigens. In: *Journal of immunology (Baltimore, Md. : 1950)* 145 (6), S. 1952–1959.

Ke, J.; Wu, X.; He, X.; Lian, L.; Zou, Y.; Wang, H. et al. (2012): A subpopulation of $CD24^+$ cells in colon cancer cell lines possess stem cell characteristics. In: *Neoplasma* 59 (3), S. 282–288. DOI: 10.4149/neo_2012_036.

Kemper, Kristel; Sprick, Martin R.; Bree, Martijn de; Scopelliti, Alessandro; Vermeulen, Louis; Hoek, Maarten et al. (2010): The AC133 epitope, but not the CD133 protein, is lost upon cancer stem cell differentiation. In: *Cancer Res* 70 (2), S. 719–729. DOI: 10.1158/0008-5472.CAN-09-1820.

Kim, Dae Kyoung; Ham, Min Hee; Lee, Seo Yul; Shin, Min Joo; Kim, Ye Eun; Song, Parkyong et al. (2020): CD166 promotes the cancer stem-like properties of primary epithelial ovarian cancer cells. In: *BMB Rep.* 53 (12), S. 622–627. DOI: 10.5483/BMB-Rep.2020.53.12.102.

Kim, Won-Tae; Ryu, Chun Jeih (2017): Cancer stem cell surface markers on normal stem cells. In: *BMB reports* 50 (6), S. 285–298. DOI: 10.5483/bmbrep.2017.50.6.039.

King, Judy A.; Tan, Fang; Mbeunkui, Flaubert; Chambers, Zachariah; Cantrell, Sarah; Chen, Hairu et al. (2010): Mechanisms of transcriptional regulation and prognostic significance of activated leukocyte cell adhesion molecule in cancer. In: *Mol Cancer* 9 (1), S. 266. DOI: 10.1186/1476-4598-9-266.

Kotelevets, Larissa; Chastre, Eric (2020): Rac1 Signaling: From Intestinal Homeostasis to Colorectal Cancer Metastasis. In: *Cancers* 12 (3). DOI: 10.3390/cancers12030665.

Kuespert, Katharina; Pils, Stefan; Hauck, Christof R. (2006): CEACAMs: their role in physiology and pathophysiology. In: *Current Opinion in Cell Biology* 18 (5), S. 565–571. DOI: 10.1016/j.ceb.2006.08.008.

Kwon, Mi Jeong; Han, Jinil; Seo, Ji Hyun; Song, Kyoung; Jeong, Hae Min; Choi, Jong-Sun et al. (2015): CD24 Overexpression Is Associated with Poor Prognosis in Luminal A and Triple-

Negative Breast Cancer. In: *PloS one* 10 (10), e0139112. DOI: 10.1371/journal.pone.0139112.

Lajoie, Marc J.; Boyken, Scott E.; Salter, Alexander I.; Bruffey, Jilliane; Rajan, Anusha; Langan, Robert A. et al. (2020): Designed protein logic to target cells with precise combinations of surface antigens. In: *Science (New York, N.Y.)* 369 (6511), S. 1637–1643. DOI: 10.1126/science.aba6527.

Laux, Holger; Romand, Sandrine; Nuciforo, Sandro; Farady, Christopher J.; Tapparel, Joel; Buechmann-Moeller, Stine et al. (2018): Degradation of recombinant proteins by Chinese hamster ovary host cell proteases is prevented by matriptase-1 knockout. In: *Biotechnology and Bioengineering* 115 (10), S. 2530–2540. DOI: 10.1002/bit.26731.

Le, Tri; Phan, Tan; Pham, Minh; Tran, Dat; Lam, Loc; Nguyen, Tung et al. (2020): BBrowser: Making single-cell data easily accessible. In: *bioRxiv*, 2020.12.11.414136. DOI: 10.1101/2020.12.11.414136.

Lee, Hae-Ock; Hong, Yourae; Etlioglu, Hakki Emre; Cho, Yong Beom; Pomella, Valentina; van den Bosch, Ben et al. (2020): Lineage-dependent gene expression programs influence the immune landscape of colorectal cancer. In: *Nat Genet* 52 (6), S. 594–603. DOI: 10.1038/s41588-020-0636-z.

Leggett, Barbara; Whitehall, Vicki (2010): Role of the serrated pathway in colorectal cancer pathogenesis. In: *Gastroenterology* 138 (6), S. 2088–2100. DOI: 10.1053/j.gastro.2009.12.066.

Levin, Trevor G.; Powell, Anne E.; Davies, Paige S.; Silk, Alain D.; Dismuke, Adria D.; Anderson, Eric C. et al. (2010): Characterization of the intestinal cancer stem cell marker CD166 in the human and mouse gastrointestinal tract. In: *Gastroenterology* 139 (6), 2072-2082.e5. DOI: 10.1053/j.gastro.2010.08.053.

Li, Chenwei; Heidt, David G.; Dalerba, Piero; Burant, Charles F.; Zhang, Lanjing; Adsay, Volkan et al. (2007): Identification of pancreatic cancer stem cells. In: *Cancer research* 67 (3), S. 1030–1037. DOI: 10.1158/0008-5472.CAN-06-2030.

Li, Cunxi; Ma, Haiting; Wang, Yang; Cao, Zheng; Graves-Deal, Ramona; Powell, Anne E. et al. (2014): Excess PLAC8 promotes an unconventional ERK2-dependent EMT in colon cancer. In: *J Clin Invest* 124 (5), S. 2172–2187. DOI: 10.1172/JCI71103.

Lin, Kezhi; Zou, Ruanmin; Lin, Feng; Zheng, Shuang; Shen, Xian; Xue, Xiangyang (2014): Expression and effect of CXCL14 in colorectal carcinoma. In: *Molecular medicine reports* 10 (3), S. 1561–1568. DOI: 10.3892/mmr.2014.2343.

Lin, Tsung-Chieh (2021): Functional Roles of SPINK1 in Cancers. In: *IJMS* 22 (8). DOI: 10.3390/ijms22083814.

Lindhofer, H.; Schoberth, A.; Pelster, D.; Hess, J.; Herold, J.; Jäger, M. (2009): Elimination of cancer stem cells (CD133+/EpCAM+) from malignant ascites by the trifunctional antibody catumaxomab: Results from a pivotal phase II/III study. In: *JCO* 27 (15_suppl), S. 3014. DOI: 10.1200/jco.2009.27.15_suppl.3014.

Lingwood, Daniel; Simons, Kai (2010): Lipid rafts as a membrane-organizing principle. In: *Science (New York, N.Y.)* 327 (5961), S. 46–50. DOI: 10.1126/science.1174621.

Liu, Allan Yi; Cai, Yao; Mao, Yubin; Lin, Yancheng; Zheng, Hong; Wu, Tiantian et al. (2014): Twist2 promotes self-renewal of liver cancer stem-like cells by regulating CD24. In: *Carcinogenesis* 35 (3), S. 537–545. DOI: 10.1093/carcin/bgt364.

Liu, Feng; Akiyama, Yasuto; Tai, Sachiko; Maruyama, Kouji; Kawaguchi, Yoshihiro; Muramatsu, Kouji; Yamaguchi, Ken (2008): Changes in the expression of CD106, osteogenic

genes, and transcription factors involved in the osteogenic differentiation of human bone marrow mesenchymal stem cells. In: *Journal of bone and mineral metabolism* 26 (4), S. 312–320. DOI: 10.1007/s00774-007-0842-0.

Liu, Gentao; Yuan, Xiangpeng; Zeng, Zhaohui; Tunici, Patrizia; Ng, Hiushan; Abdulkadir, Iman R. et al. (2006): Analysis of gene expression and chemoresistance of CD133+ cancer stem cells in glioblastoma. In: *Molecular cancer* 5, S. 67. DOI: 10.1186/1476-4598-5-67.

Majores, Michael; Schindler, Anne; Fuchs, Angela; Stein, Johannes; Heukamp, Lukas; Altevogt, Peter; Kristiansen, Glen (2015): Membranous CD24 expression as detected by the monoclonal antibody SWA11 is a prognostic marker in non-small cell lung cancer patients. In: *BMC clinical pathology* 15, S. 19. DOI: 10.1186/s12907-015-0019-z.

Mak, Anthony B.; Nixon, Allison M. L.; Kittanakom, Saranya; Stewart, Jocelyn M.; Chen, Ginny I.; Curak, Jasna et al. (2012): Regulation of CD133 by HDAC6 promotes β-catenin signaling to suppress cancer cell differentiation. In: *Cell reports* 2 (4), S. 951–963. DOI: 10.1016/j.celrep.2012.09.016.

Malanchi, Ilaria; Peinado, Hector; Kassen, Deepika; Hussenet, Thomas; Metzger, Daniel; Chambon, Pierre et al. (2008): Cutaneous cancer stem cell maintenance is dependent on beta-catenin signalling. In: *Nature* 452 (7187), S. 650–653. DOI: 10.1038/nature06835.

Mărgaritescu, Claudiu; Pirici, Daniel; Cherciu, Irina; Bărbălan, Alexandru; Cârtână, Tatiana; Săftoiu, Adrian (2014): CD133/CD166/Ki-67 triple immunofluorescence assessment for putative cancer stem cells in colon carcinoma. In: *Journal of gastrointestinal and liver diseases : JGLD* 23 (2), S. 161–170. Online verfügbar unter https://pubmed.ncbi.nlm.nih.gov/24949608/.

Maria Geis (2019): Identifizierung von Zielmolekülen und Herstellung zweigeteilter trivalenter T-Zell-aktivierender Antikörperderivate zur immuntherapeutischen Behandlung von Multiplen Myelom. Würzburg.

Muraro, Manuele Giuseppe; Mele, Valentina; Däster, Silvio; Han, Junyi; Heberer, Michael; Cesare Spagnoli, Giulio; Iezzi, Giandomenica (2012): CD133+, CD166+CD44+, and CD24+CD44+ phenotypes fail to reliably identify cell populations with cancer stem cell functional features in established human colorectal cancer cell lines. In: *Stem cells translational medicine* 1 (8), S. 592–603. DOI: 10.5966/sctm.2012-0003.

Ni, Yang-Hong; Zhao, Xia; Wang, Wei (2020): CD24, A Review of its Role in Tumor Diagnosis, Progression and Therapy. In: *Current gene therapy* 20 (2), S. 109–126. DOI: 10.2174/1566523220666200623170738.

Nowell, P. C. (1976): The clonal evolution of tumor cell populations. In: *Science (New York, N.Y.)* 194 (4260), S. 23–28. DOI: 10.1126/science.959840.

O'Brien, Catherine A.; Pollett, Aaron; Gallinger, Steven; Dick, John E. (2007): A human colon cancer cell capable of initiating tumour growth in immunodeficient mice. In: *Nature* 445 (7123), S. 106–110. DOI: 10.1038/nature05372.

O'Brien, Michael J.; Yang, Shi; Mack, Charline; Xu, Huihong; Huang, Christopher S.; Mulcahy, Elizabeth et al. (2006): Comparison of microsatellite instability, CpG island methylation phenotype, BRAF and KRAS status in serrated polyps and traditional adenomas indicates separate pathways to distinct colorectal carcinoma end points. In: *The American journal of surgical pathology* 30 (12), S. 1491–1501. DOI: 10.1097/01.pas.0000213313.36306.85.

Ohneda, O.; Ohneda, K.; Arai, F.; Lee, J.; Miyamoto, T.; Fukushima, Y. et al. (2001): ALCAM (CD166): its role in hematopoietic and endothelial development. In: *Blood* 98 (7), S. 2134–2142. DOI: 10.1182/blood.v98.7.2134.

Pádua, Diana; Figueira, Paula; Ribeiro, Inês; Almeida, Raquel; Mesquita, Patrícia (2020): The Relevance of Transcription Factors in Gastric and Colorectal Cancer Stem Cells Identification and Eradication. In: *Frontiers in cell and developmental biology* 8, S. 442. DOI: 10.3389/fcell.2020.00442.

Palma, Fatima Domenica Elisa de; D'Argenio, Valeria; Pol, Jonathan; Kroemer, Guido; Maiuri, Maria Chiara; Salvatore, Francesco (2019): The Molecular Hallmarks of the Serrated Pathway in Colorectal Cancer. In: *Cancers* 11 (7). DOI: 10.3390/cancers11071017.

Pan, Yunzhi; Ma, Sai; Cao, Kaiyue; Zhou, Sufang; Zhao, Aiqin; Li, Ming et al. (2018): Therapeutic approaches targeting cancer stem cells. In: *Journal of cancer research and therapeutics* 14 (7), S. 1469–1475. DOI: 10.4103/jcrt.JCRT_976_17.

Park, Heae Surng; Kim, Byung Chang; Yeo, Hyun Yang; Kim, Kyung-Hee; Yoo, Byong Chul; Park, Ji Won; Chang, Hee Jin (2018): Deleted in malignant brain tumor 1 is a novel prognostic marker in colorectal cancer. In: *Oncology reports* 39 (5), S. 2279–2287. DOI: 10.3892/or.2018.6287.

Pino, Maria S.; Chung, Daniel C. (2010): The chromosomal instability pathway in colon cancer. In: *Gastroenterology* 138 (6), S. 2059–2072. DOI: 10.1053/j.gastro.2009.12.065.

Pirruccello, S. J.; LeBien, T. W. (1986): The human B cell-associated antigen CD24 is a single chain sialoglycoprotein. In: *Journal of immunology (Baltimore, Md. : 1950)* 136 (10), S. 3779–3784.

Powell, Emily; Shao, Jiansu; Picon, Hector M.; Bristow, Christopher; Ge, Zhongqi; Peoples, Michael et al. (2018): A functional genomic screen in vivo identifies CEACAM5 as a clinically relevant driver of breast cancer metastasis. In: *npj Breast Cancer* 4 (1), S. 9. DOI: 10.1038/s41523-018-0062-x.

Prat-Vidal, C.; Roura, S.; Farré, J.; Gálvez, C.; Llach, A.; Molina, C. E. et al. (2007): Umbilical cord blood-derived stem cells spontaneously express cardiomyogenic traits. In: *Transplantation proceedings* 39 (7), S. 2434–2437. DOI: 10.1016/j.transproceed.2007.06.016.

Prieur, Alexandre; Cappellini, Monica; Habif, Guillaume; Lefranc, Marie-Paule; Mazard, Thibault; Morency, Eric et al. (2017): Targeting the Wnt Pathway and Cancer Stem Cells with Anti-progastrin Humanized Antibodies as a Potential Treatment for K-RAS-Mutated Colorectal Cancer. In: *Clinical cancer research : an official journal of the American Association for Cancer Research* 23 (17), S. 5267–5280. DOI: 10.1158/1078-0432.CCR-17-0533.

Przystal, Justyna M.; Becker, Hannes; Canjuga, Denis; Tsiami, Foteini; Anderle, Nicole; Keller, Anna-Lena et al. (2021): Targeting CSF1R Alone or in Combination with PD1 in Experimental Glioma. In: *Cancers* 13 (10). DOI: 10.3390/cancers13102400.

PubMed Central (PMC) (2021): Cytokine release syndrome. Online verfügbar unter https://www.ncbi.nlm.nih.gov/pmc/articles/PMC6003181/, zuletzt aktualisiert am 13.10.2021, zuletzt geprüft am 13.10.2021.

Rappa, Germana; Mercapide, Javier; Anzanello, Fabio; Le, Thuc T.; Johlfs, Mary G.; Fiscus, Ronald R. et al. (2013): Wnt interaction and extracellular release of prominin-1/CD133 in human malignant melanoma cells. In: *Experimental cell research* 319 (6), S. 810–819. DOI: 10.1016/j.yexcr.2013.01.003.

Rau, Alexander; Lieb, Wolfgang S.; Seifert, Oliver; Honer, Jonas; Birnstock, Dennis; Richter, Fabian et al. (2020): Inhibition of Tumor Cell Growth and Cancer Stem Cell Expansion by a Bispecific Antibody Targeting EGFR and HER3. In: *Molecular cancer therapeutics* 19 (7), S. 1474–1485. DOI: 10.1158/1535-7163.MCT-19-1095.

Revitope (2021): Revitope Oncology Inc. - Powered for Precision. Online verfügbar unter https://www.revitope.com/, zuletzt aktualisiert am 10.08.2021, zuletzt geprüft am 13.10.2021.

Reynolds, Neil A.; Wagstaff, Antona J. (2004): Cetuximab: in the treatment of metastatic colorectal cancer. In: *Drugs* 64 (1), 109-18; discussion 119-121. DOI: 10.2165/00003495-200464010-00007.

Ricci-Vitiani, Lucia; Lombardi, Dario G.; Pilozzi, Emanuela; Biffoni, Mauro; Todaro, Matilde; Peschle, Cesare; Maria, Ruggero de (2007): Identification and expansion of human colon-cancer-initiating cells. In: *Nature* 445 (7123), S. 111–115. DOI: 10.1038/nature05384.

Rinkenbaugh, Amanda L.; Baldwin, Albert S. (2016): The NF-κB Pathway and Cancer Stem Cells. In: *Cells* 5 (2). DOI: 10.3390/cells5020016.

Sagiv, Eyal; Memeo, Lorenzo; Karin, Adi; Kazanov, Diana; Jacob-Hirsch, Jasmin; Mansukhani, Mahesh et al. (2006): CD24 is a new oncogene, early at the multistep process of colorectal cancer carcinogenesis. In: *Gastroenterology* 131 (2), S. 630–639. DOI: 10.1053/j.gastro.2006.04.028.

Sahlberg, Sara Häggblad; Spiegelberg, Diana; Glimelius, Bengt; Stenerlöw, Bo; Nestor, Marika (2014): Evaluation of cancer stem cell markers CD133, CD44, CD24: association with AKT isoforms and radiation resistance in colon cancer cells. In: *PloS one* 9 (4), e94621. DOI: 10.1371/journal.pone.0094621.

Santaliz-Ruiz, Luis E., IV; Xie, Xiujie; Old, Matthew; Teknos, Theodoros N.; Pan, Quintin (2014): Emerging role of nanog in tumorigenesis and cancer stem cells. In: *International journal of cancer* 135 (12), S. 2741–2748. DOI: 10.1002/ijc.28690.

Sari, Ita Novita; Yang, Ying-Gui; Phi, Lan Thi Hanh; Kim, Hyungjoo; Baek, Moo Jun; Jeong, Dongjun; Kwon, Hyog Young (2016): Interferon-induced transmembrane protein 1 (IFITM1) is required for the progression of colorectal cancer. In: *Oncotarget* 7 (52), S. 86039–86050. DOI: 10.18632/oncotarget.13325.

Sarkar, Abby; Hochedlinger, Konrad (2013): The sox family of transcription factors: versatile regulators of stem and progenitor cell fate. In: *Cell stem cell* 12 (1), S. 15–30. DOI: 10.1016/j.stem.2012.12.007.

Saunders, Kevin O. (2019): Conceptual Approaches to Modulating Antibody Effector Functions and Circulation Half-Life. In: *Front. Immunol.* 10, S. 1296. DOI: 10.3389/fimmu.2019.01296.

Schmidt, Marcus; Hellwig, Birte; Hammad, Seddik; Othman, Amnah; Lohr, Miriam; Chen, Zonglin et al. (2012): A comprehensive analysis of human gene expression profiles identifies stromal immunoglobulin κ C as a compatible prognostic marker in human solid tumors. In: *Clin Cancer Res* 18 (9), S. 2695–2703. DOI: 10.1158/1078-0432.CCR-11-2210.

Schwitalla, Sarah; Fingerle, Alexander A.; Cammareri, Patrizia; Nebelsiek, Tim; Göktuna, Serkan I.; Ziegler, Paul K. et al. (2013): Intestinal tumorigenesis initiated by dedifferentiation and acquisition of stem-cell-like properties. In: *Cell* 152 (1-2), S. 25–38. DOI: 10.1016/j.cell.2012.12.012.

Shmelkov, Sergey V.; Butler, Jason M.; Hooper, Andrea T.; Hormigo, Adilia; Kushner, Jared; Milde, Till et al. (2008): CD133 expression is not restricted to stem cells, and both CD133+ and CD133- metastatic colon cancer cells initiate tumors. In: *J Clin Invest* 118 (6), S. 2111–2120. DOI: 10.1172/JCI34401.

Simon, Karen (2016): Colorectal cancer development and advances in screening. In: *Clinical interventions in aging* 11, S. 967–976. DOI: 10.2147/CIA.S109285.

Singh, Sheila K.; Clarke, Ian D.; Terasaki, Mizuhiko; Bonn, Victoria E.; Hawkins, Cynthia; Squire, Jeremy; Dirks, Peter B. (2003): Identification of a cancer stem cell in human brain tumors. In: *Cancer research* 63 (18), S. 5821–5828.

Sjöberg, Elin; Augsten, Martin; Bergh, Jonas; Jirström, Karin; Östman, Arne (2016): Expression of the chemokine CXCL14 in the tumour stroma is an independent marker of survival in breast cancer. In: *British journal of cancer* 114 (10), S. 1117–1124. DOI: 10.1038/bjc.2016.104.

Sninsky, Jared A.; Bishnupuri, Kumar S.; González, Iván; Trikalinos, Nikolaos A.; Chen, Ling; Dieckgraefe, Brian K. (2021): Reg4 and its downstream transcriptional activator CD44ICD in stage II and III colorectal cancer. In: *Oncotarget* 12 (4), S. 278–291. DOI: 10.18632/oncotarget.27896.

Sonkar, Kanchan; Ayyappan, Vinay; Tressler, Caitlin M.; Adelaja, Oluwatobi; Cai, Ruoqing; Cheng, Menglin; Glunde, Kristine (2019): Focus on the glycerophosphocholine pathway in choline phospholipid metabolism of cancer. In: *NMR in biomedicine* 32 (10), e4112. DOI: 10.1002/nbm.4112.

Spiess, Christoph; Zhai, Qianting; Carter, Paul J. (2015): Alternative molecular formats and therapeutic applications for bispecific antibodies. In: *Molecular Immunology* 67 (2 Pt A), S. 95–106. DOI: 10.1016/j.molimm.2015.01.003.

Springer, T.; Galfrè, G.; Secher, D. S.; Milstein, C. (1978): Monoclonal xenogeneic antibodies to murine cell surface antigens: identification of novel leukocyte differentiation antigens. In: *European journal of immunology* 8 (8), S. 539–551. DOI: 10.1002/eji.1830080802.

Stangeland, Biljana; Mughal, Awais A.; Grieg, Zanina; Sandberg, Cecilie Jonsgar; Joel, Mrinal; Nygård, Ståle et al. (2015): Combined expressional analysis, bioinformatics and targeted proteomics identify new potential therapeutic targets in glioblastoma stem cells. In: *Oncotarget* 6 (28), S. 26192–26215. DOI: 10.18632/oncotarget.4613.

Sung, Hyuna; Ferlay, Jacques; Siegel, Rebecca L.; Laversanne, Mathieu; Soerjomataram, Isabelle; Jemal, Ahmedin; Bray, Freddie (2021): Global cancer statistics 2020: GLOBOCAN estimates of incidence and mortality worldwide for 36 cancers in 185 countries. In: *CA: a cancer journal for clinicians*. DOI: 10.3322/caac.21660.

Suzuki, T.; Kiyokawa, N.; Taguchi, T.; Sekino, T.; Katagiri, Y. U.; Fujimoto, J. (2001): CD24 induces apoptosis in human B cells via the glycolipid-enriched membrane domains/rafts-mediated signaling system. In: *Journal of immunology (Baltimore, Md. : 1950)* 166 (9), S. 5567–5577. DOI: 10.4049/jimmunol.166.9.5567.

Tachezy, Michael; Zander, Hilke; Wolters-Eisfeld, Gerrit; Müller, Julia; Wicklein, Daniel; Gebauer, Florian et al. (2014): Activated leukocyte cell adhesion molecule (CD166): an "inert" cancer stem cell marker for non-small cell lung cancer? In: *Stem cells (Dayton, Ohio)* 32 (6), S. 1429–1436. DOI: 10.1002/stem.1665.

Tai, Mei-Hui; Chang, Chia-Cheng; Kiupel, Matti; Webster, Joshua D.; Olson, L. Karl; Trosko, James E. (2005): Oct4 expression in adult human stem cells: evidence in support of the stem cell theory of carcinogenesis. In: *Carcinogenesis* 26 (2), S. 495–502. DOI: 10.1093/carcin/bgh321.

Takeda, Koki; Mizushima, Tsunekazu; Yokoyama, Yuhki; Hirose, Haruka; Wu, Xin; Qian, Yamin et al. (2018): Sox2 is associated with cancer stem-like properties in colorectal cancer. In: *Sci Rep* 8 (1), S. 17639. DOI: 10.1038/s41598-018-36251-0.

Talebi, Ardeshir; Kianersi, Kianoosh; Beiraghdar, Mozhdeh (2015): Comparison of gene expression of SOX2 and OCT4 in normal tissue, polyps, and colon adenocarcinoma using

immunohistochemical staining. In: *Advanced biomedical research* 4, S. 234. DOI: 10.4103/2277-9175.167958.

Tchoupa, Arnaud Kengmo; Schuhmacher, Tamara; Hauck, Christof R. (2014): Signaling by epithelial members of the CEACAM family - mucosal docking sites for pathogenic bacteria. In: *Cell Commun Signal* 12 (1), S. 27. DOI: 10.1186/1478-811X-12-27.

Terzić, Janos; Grivennikov, Sergei; Karin, Eliad; Karin, Michael (2010): Inflammation and colon cancer. In: *Gastroenterology* 138 (6), 2101-2114.e5. DOI: 10.1053/j.gastro.2010.01.058.

Thompson, John A.; Eades-Perner, Anne-Marie; Ditter, Margarethe; Muller, William J.; Zimmermann, Wolfgang (1997): Expression of transgenic carcinoembryonic antigen (CEA) in tumor-prone mice: An animal model for CEA-directed tumor immunotherapy. In: *Int. J. Cancer* 72 (1), S. 197–202. DOI: 10.1002/(SICI)1097-0215(19970703)72:1<197::AID-IJC28>3.0.CO;2-F.

Tiwari, Ritika; Manzar, Nishat; Bhatia, Vipul; Yadav, Anjali; Nengroo, Mushtaq A.; Datta, Dipak et al. (2020): Androgen deprivation upregulates SPINK1 expression and potentiates cellular plasticity in prostate cancer. In: *Nat Commun* 11 (1), S. 384. DOI: 10.1038/s41467-019-14184-0.

Unverdorben, Felix; Richter, Fabian; Hutt, Meike; Seifert, Oliver; Malinge, Pauline; Fischer, Nicolas; Kontermann, Roland E. (2016): Pharmacokinetic properties of IgG and various Fc fusion proteins in mice. In: *mAbs* 8 (1), S. 120–128. DOI: 10.1080/19420862.2015.1113360.

Vander Griend, Donald J.; Karthaus, Wouter L.; Dalrymple, Susan; Meeker, Alan; DeMarzo, Angelo M.; Isaacs, John T. (2008): The role of CD133 in normal human prostate stem cells and malignant cancer-initiating cells. In: *Cancer Res* 68 (23), S. 9703–9711. DOI: 10.1158/0008-5472.CAN-08-3084.

Vazzana, N.; Riondino, S.; Toto, V.; Guadagni, F.; Roselli, M.; Davi, G.; Ferroni, P. (2012): Obesity-driven inflammation and colorectal cancer. In: *Current medicinal chemistry* 19 (34), S. 5837–5853. DOI: 10.2174/092986712804143349.

Vermeulen, Louis; Sousa E Melo, Felipe de; van der Heijden, Maartje; Cameron, Kate; Jong, Joan H. de; Borovski, Tijana et al. (2010): Wnt activity defines colon cancer stem cells and is regulated by the microenvironment. In: *Nat Cell Biol* 12 (5), S. 468–476. DOI: 10.1038/ncb2048.

Vogelstein, B.; Fearon, E. R.; Hamilton, S. R.; Kern, S. E.; Preisinger, A. C.; Leppert, M. et al. (1988): Genetic alterations during colorectal-tumor development. In: *The New England journal of medicine* 319 (9), S. 525–532. DOI: 10.1056/NEJM198809013190901.

Wang, Jian-Zhang; Yang, Shou-Xing; Ye, Fangpeng; Xia, Xuan-Ping; Shao, Xiao-Xiao; Xia, Sheng-Long et al. (2018): Hypoxia-induced Rab11-family interacting protein 4 expression promotes migration and invasion of colon cancer and correlates with poor prognosis. In: *Molecular medicine reports* 17 (3), S. 3797–3806. DOI: 10.3892/mmr.2017.8283.

Wang, Ying; Zhang, You; Herman, James G.; Linghu, Enqiang; Guo, Mingzhou (2017): Epigenetic silencing of TMEM176A promotes esophageal squamous cell cancer development. In: *Oncotarget* 8 (41), S. 70035–70048. DOI: 10.18632/oncotarget.19550.

Wang, Zhiwei; Li, Yiwei; Banerjee, Sanjeev; Sarkar, Fazlul H. (2009): Emerging role of Notch in stem cells and cancer. In: *Cancer letters* 279 (1), S. 8–12. DOI: 10.1016/j.canlet.2008.09.030.

Wei, Fang; Zhang, Tong; Deng, Shu-Chou; Wei, Jian-Chang; Yang, Ping; Wang, Qiang et al. (2019): PD-L1 promotes colorectal cancer stem cell expansion by activating HMGA1-

dependent signaling pathways. In: *Cancer letters* 450, S. 1–13. DOI: 10.1016/j.canlet.2019.02.022.

Weichert, W.; Knösel, T.; Bellach, J.; Dietel, M.; Kristiansen, G. (2004): ALCAM/CD166 is overexpressed in colorectal carcinoma and correlates with shortened patient survival. In: *Journal of clinical pathology* 57 (11), S. 1160–1164. DOI: 10.1136/jcp.2004.016238.

Wu, Jun-I; Wang, Lu-Hai (2019): Emerging roles of gap junction proteins connexins in cancer metastasis, chemoresistance and clinical application. In: *Journal of biomedical science* 26 (1), S. 8. DOI: 10.1186/s12929-019-0497-x.

Wuebben, Erin L.; Rizzino, Angie (2017): The dark side of SOX2: cancer - a comprehensive overview. In: *Oncotarget* 8 (27), S. 44917–44943. DOI: 10.18632/oncotarget.16570.

Xia, Yan; Zhang, Yin-Li; Yu, Chao; Chang, Ting; Fan, Heng-Yu (2014): YAP/TEAD co-activator regulated pluripotency and chemoresistance in ovarian cancer initiated cells. In: *PloS one* 9 (11), e109575. DOI: 10.1371/journal.pone.0109575.

Xiao, Wei; Gao, Zhiyong; Duan, Yixing; Yuan, Wuxiong; Ke, Yang (2017a): Notch signaling plays a crucial role in cancer stem-like cells maintaining stemness and mediating chemotaxis in renal cell carcinoma. In: *Journal of experimental & clinical cancer research : CR* 36 (1), S. 41. DOI: 10.1186/s13046-017-0507-3.

Xiao, Yang; Yurievich, Usenko Alexander; Yosypovych, Smorzhevskyi Valentyn (2017b): Long noncoding RNA XIST is a prognostic factor in colorectal cancer and inhibits 5-fluorouracil-induced cell cytotoxicity through promoting thymidylate synthase expression. In: *Oncotarget* 8 (47), S. 83171–83182. DOI: 10.18632/oncotarget.20487.

Xie, Yuan-Hong; Chen, Ying-Xuan; Fang, Jing-Yuan (2020): Comprehensive review of targeted therapy for colorectal cancer. In: *Sig Transduct Target Ther* 5 (1), S. 22. DOI: 10.1038/s41392-020-0116-z.

Yamagishi, Hidetsugu; Kuroda, Hajime; Imai, Yasuo; Hiraishi, Hideyuki (2016): Molecular pathogenesis of sporadic colorectal cancers. In: *Chinese journal of cancer* 35, S. 4. DOI: 10.1186/s40880-015-0066-y.

Yamaguchi, Junpei; Yokoyama, Yukihiro; Kokuryo, Toshio; Ebata, Tomoki; Enomoto, Atsushi; Nagino, Masato (2018): Trefoil factor 1 inhibits epithelial-mesenchymal transition of pancreatic intraepithelial neoplasm. In: *J Clin Invest* 128 (8), S. 3619–3629. DOI: 10.1172/JCI97755.

Yan, Ming; Yang, Xihu; Wang, Lizhen; Clark, David; Zuo, Hui; Ye, Dongxia et al. (2013): Plasma membrane proteomics of tumor spheres identify CD166 as a novel marker for cancer stem-like cells in head and neck squamous cell carcinoma. In: *Molecular & cellular proteomics : MCP* 12 (11), S. 3271–3284. DOI: 10.1074/mcp.M112.025460.

Yan, Xiaofei; Zhao, Jian; Zhang, Rui (2017): Interleukin-37 mediates the antitumor activity in colon cancer through β-catenin suppression. In: *Oncotarget* 8 (30), S. 49064–49075. DOI: 10.18632/oncotarget.17093.

Yeung, Trevor M.; Gandhi, Shaan C.; Wilding, Jennifer L.; Muschel, Ruth; Bodmer, Walter F. (2010): Cancer stem cells from colorectal cancer-derived cell lines. In: *Proceedings of the National Academy of Sciences of the United States of America* 107 (8), S. 3722–3727. DOI: 10.1073/pnas.0915135107.

Yusufu, Aikeremu; Shayimu, Paerhati; Tuerdi, Rousidan; Fang, Cheng; Wang, Fei; Wang, Haijiang (2019): TFF3 and TFF1 expression levels are elevated in colorectal cancer and promote the malignant behavior of colon cancer by activating the EMT process. In: *International journal of oncology* 55 (4), S. 789–804. DOI: 10.3892/ijo.2019.4854.

Zakaria, Norashikin; Mohd Yusoff, Narazah; Zakaria, Zubaidah; Widera, Darius; Yahaya, Badrul Hisham (2018): Inhibition of NF-κB Signaling Reduces the Stemness Characteristics of Lung Cancer Stem Cells. In: *Front. Oncol.* 8, S. 166. DOI: 10.3389/fonc.2018.00166.

Zhang, Jian; Shi, ZhenFeng; Huang, JinXing; Zou, XiaoGuang (2016): CSTB Downregulation Promotes Cell Proliferation and Migration and Suppresses Apoptosis in Gastric Cancer SGC-7901 Cell Line. In: *Oncology research* 24 (6), S. 487–494. DOI: 10.3727/096504016X14685034103752.

Zhang, Rui; Zhang, Fan; Sun, Zeguo; Liu, Pengpeng; Zhang, Xiao; Ye, Yingnan et al. (2019): LINE-1 Retrotransposition Promotes the Development and Progression of Lung Squamous Cell Carcinoma by Disrupting the Tumor-Suppressor Gene FGGY. In: *Cancer Res* 79 (17), S. 4453–4465. DOI: 10.1158/0008-5472.CAN-19-0076.

Zhu, Guangwei; Cheng, Zhibin; Huang, Yongjian; Zheng, Wei; Yang, Shugang; Lin, Chunlin; Ye, Jianxin (2019): TRAF6 promotes the progression and growth of colorectal cancer through nuclear shuttle regulation NF-kB/c-jun signaling pathway. In: *Life sciences* 235, S. 116831. DOI: 10.1016/j.lfs.2019.116831.

Eidesstattliche Erklärung

Hiermit erkläre ich an Eides statt, die Dissertation: „**Eliminierung von Krebsstammzellen des kolorektalen Karzinoms mithilfe von Hemibodies**“, eigenständig, d. h. insbesondere selbständig und ohne Hilfe eines kommerziellen Promotionsberaters, angefertigt und keine anderen, als die von mir angegebenen Quellen und Hilfsmittel verwendet zu haben.

Ich erkläre außerdem, dass die Dissertation weder in gleicher noch in ähnlicher Form bereits in einem anderen Prüfungsverfahren vorgelegen hat.

Weiterhin erkläre ich, dass bei allen Abbildungen und Texten, bei denen die Verwertungsrechte (Copyright) nicht bei mir liegen, diese von den Rechtsinhabern eingeholt wurden und die Textstellen bzw. Abbildungen entsprechend den rechtlichen Vorgaben gekennzeichnet sind sowie bei Abbildungen, die dem Internet entnommen wurden, der entsprechende Hypertextlink angegeben wurde.

Affidavit

I hereby declare that my thesis entitled: „ **Targeting Colorectal Cancer Stem Cells with Hemibodies**” is the result of my own work. I did not receive any help or support from commercial consultants. All sources and / or materials applied are listed and specified in the thesis.

Furthermore I verify that the thesis has not been submitted as part of another examination process neither in identical nor in similar form.

Besides I declare that if I do not hold the copyright for figures and paragraphs, I obtained it from the rights holder and that paragraphs and figures have been marked according to law or for figures taken from the internet the hyperlink has been added accordingly.

Würzburg, den_____

_____

Signature PhD-student